CERN 77-10
Intersecting Storage
Rings Division
6 June 1977

ORGANISATION EUROPÉENNE POUR LA RECHERCHE NUCLÉAIRE
CERN EUROPEAN ORGANIZATION FOR NUCLEAR RESEARCH

SELECTION OF FORMULAE CONCERNING PROTON STORAGE RINGS

G. Guignard

GENEVA
1977

CERN - Service d'information scientifique - RD/237 - 1500 - juin 1977

Abstract

This compilation of formulae concerning proton storage rings covers bunched beams as well as coasting beams. Some formulae are common to both storage rings and proton synchrotrons. Where meaningful, the application of a particular formula to the CERN Intersecting Storage Rings (ISR) is given.

FOREWORD

This report is divided into independent chapters, each of which treats a specific subject. Each chapter is preceded by a list of symbol definitions applicable to that chapter and, where necessary, further definitions are given in the text accompanying a formula. The symbols which are common throughout are listed separately at the beginning. Thus, to establish a symbol's meaning, the reader must first consult the text with the formula, secondly the list at the beginning of the chapter and, if necessary, the list at the beginning of the report.

A short list of basic references, in which the reader can find most of the formulae, is given at the beginning of each chapter. Some formulae, however, have been derived specifically for this report and no references exist for them.

The values of some commonly used constants and of parameters related to the energy and to the working conditions in the CERN storage rings are given in Tables 1 to 10.

The author would welcome any comments or corrections concerning the formulae presented in this report which readers may wish to make.

CONTENTS

LIST OF FREQUENTLY USED SYMBOLS AND THEIR MEANINGS

x	horizontal transverse coordinate	[m]
z	vertical transverse coordinate	[m]
y	general transverse coordinate, either horizontal or vertical	[m]
$y' = dy/ds$	derivative of the general transverse coordinate	[rad]
s	distance along beam axis	[m]
R	average machine radius	[m]
$\theta = s/R$	azimuthal angle	[rad]
t	time	[s]
I	beam current	[A]
e	electronic charge	[As]
c	velocity of the light	[ms^{-1}]
β	ratio of particle velocity to that of light	
γ	ratio of total energy of particle to its rest energy	
$\eta = \frac{1}{\gamma^2} - \frac{1}{\gamma_t^2}$	revolution frequency spread per unit of momentum spread, γ_t being the value of γ at the transition energy where η changes its sign	
p	particle momentum	[GeV/c]
B_x, B_z	transverse components of the magnetic induction	[T]
B_θ	azimuthal component of the magnetic induction	[T]
$B\rho$	magnetic rigidity	[Tm]
β_y	transverse betatron amplitude function [m] in plane (y,s). A second index I ($\beta_{y,I}$) indicates that the amplitude function is taken at one intersection of storage rings	
Q_y	number of betatron oscillations per revolution in transverse plane (y,s)	
r_e	classical electron radius	[m]
r_p	classical proton radius	[m]

The definitions of x, z, s, θ are summarized in Fig. 1. A prime denotes differentiation with respect to s. The sign $\hat{}$ or - on top of a variable indicates its maximum or average value , respectively. The notation $|Z|$ stands for the modulus of Z if Z is complex, and the absolute value of Z if Z is real. The values of some physical constants such as e and c are given in Table 1.

The MKSA unit system is used throughout this report except for the rest energy [eV], the momentum of a particle [eV/c] and the vacuum pressure [Torr]. These three exceptions are retained to respect common usage.

The following abbreviations are used:

- w.r.t. for with respect to ;
- r.m.s. for root mean square ;
- ISR for Intersecting Storage Rings at CERN ;
- SFM for Split Field Magnet, installed in intersection 4 of the ISR.

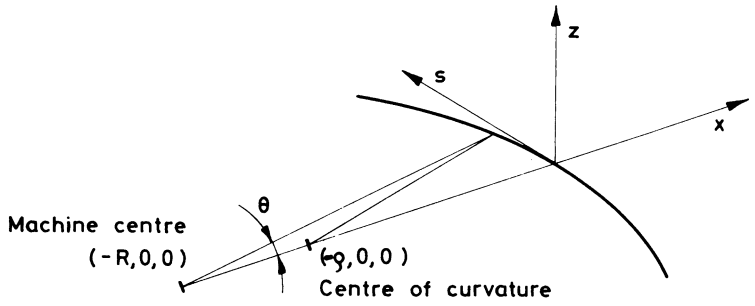

Fig. 1 Coordinate system

1. FORMULAE IN CONNECTION WITH THE TRANSVERSE PHASE SPACE[1,2,3)]

Symbols frequently used in this chapter

α_y Twiss parameter

μ_y phase of the betatron oscillation

E_y transverse emittance [m rad]

d distance along beam axis from the entrance of a given element [m]

y horizontal or vertical transverse amplitude of the betatron oscillation of a particle [m]

y' amplitude derivative or betatron oscillation angle [rad]

y_p transverse position of the phase ellipse centre associated with a momentum deviation [m].

1.1 Definitions of the basic beam parameters

The transverse parameters, in which we are interested, are the betatron amplitude function β_y [m], the Twiss parameter α_y, the phase μ_y, the momentum compaction $\alpha_{p,y}$ [m] and the number of betatron oscillations per revolution Q_y. For each transverse plane, these functions are defined by the following relations:

$$y(s) = \sqrt{\beta_y(s)\, E_y}\left[a \cos \mu_y(s) + b \sin \mu_y(s)\right]$$

$$\alpha_y(s) = -\frac{1}{2}\beta_y'(s)$$

$$\mu_y(s) = \int_o^s \frac{ds}{\beta_y(s)}$$

$$\alpha_{p,y}(s) = \frac{y_p(s)}{\Delta p/p}$$

$$Q_y = \frac{1}{2\pi}\int_o^{\ell} \frac{ds}{\beta_y(s)} = \frac{\mu_y(2\pi R)}{2\pi} \quad .$$

E_y is given explicitly in Section 1.4.

The first relation defines the β_y function, where a, b are dimensionless constants depending on the initial conditions. ℓ is the machine circumference.

It is worth noting that the average value of the horizontal momentum compaction is directly related to γ_t by

$$\bar{\alpha}_{p,x} = \frac{R}{\gamma_t^2} \quad .$$

Two other parameters associated with Q_y are often used:

$$Q'_y = \left.\frac{\partial Q_y}{\partial(\Delta p/p)}\right|_{\Delta p/p=0} ,$$

$$Q''_y = \frac{1}{2}\left.\frac{\partial^2 Q_y}{\partial^2(\Delta p/p)}\right|_{\Delta p/p=0} ,$$

Q'/Q often being called the chromaticity.

Note the special meaning of the prime, which is here a derivative with respect to $\Delta p/p$, and the unusual factor 2 in the definition of Q''.

For the ISR: the values of all these parameters can be obtained from the computer program AGS[4].

The value of R can be found in Table 2. Table 3 gives $\bar{\beta}_y$, $\beta_{z,I}$ and $\bar{\alpha}_{p,x}$ for the standard ISR working conditions. Table 4 gives Q_y at centre line and $\bar{x}$ = 40 mm as well as Q'_y for the presently existing working lines.

1.2 Matrix formalism for betatron oscillations

Let us consider a given element of the machine. It can be characterized by a 2×2 matrix M(d), which is defined as follows:

$$\begin{pmatrix} y(d) \\ y'(d) \end{pmatrix} = M(d) \begin{pmatrix} y_1 \\ y'_1 \end{pmatrix} \qquad d \le \ell ,$$

where ℓ is the length of the machine element [m].

Since d is the longitudinal distance [m] from the entrance of the element, y_1 and y'_1 are the amplitude of the oscillation and its derivative at the entrance to the element.

Let us consider four particular forms of matrix M(d).

i) Straight section:

$$M(d) = \begin{pmatrix} 1 & d \\ 0 & 1 \end{pmatrix} .$$

ii) Gradient sector magnet:

$$M(d) = \begin{pmatrix} \mathrm{cf}(\sqrt{K}\,d) & \frac{1}{\sqrt{K}}\,\mathrm{sf}(\sqrt{K}\,d) \\ \mathrm{sign}\ \sqrt{K}\,\mathrm{sf}(\sqrt{K}\,d) & \mathrm{cf}(\sqrt{K}\,d) \end{pmatrix} ,$$

where the significance of the symbols depends on the plane of the gradient sector magnet.

In the focusing plane, the following meanings are valid:

$$\mathrm{sf} = \sin, \qquad \mathrm{cf} = \cos, \qquad \mathrm{sign} = -1 .$$

In the defocusing plane, the meanings are:

$$\mathrm{sf} = \mathrm{sh}, \qquad \mathrm{cf} = \mathrm{ch}, \qquad \mathrm{sign} = 1 .$$

The parameter K $[m^{-2}]$ can be expressed as follows:

$$K = \frac{|n| + \text{sign}}{\rho^2} \quad \text{in the bending plane,}$$

$$K = \frac{|n|}{\rho^2} = \frac{|G|}{B\rho} \quad \text{in the plane perpendicular to the bending.}$$

G is the sector magnet gradient $[Tm^{-1}]$,
ρ is the bending radius [m] .

By convention, F-units are focusing in the horizontal plane while D-units are defocusing.

iii) Quadrupole lens:

The matrix M(d) given in ii) is valid, with

$$\frac{1}{\rho} = 0 ,$$

$$K = \frac{|G|}{B\rho} ,$$

in both planes.

iv) Edge effect of a gradient magnet:

For a gradient magnet with a linear fringe field, the matrix M in the bending plane will be

$$M = \begin{pmatrix} 1 & 0 \\ \frac{\tan \varepsilon}{\rho} & 1 \end{pmatrix} ,$$

and in the other transverse plane

$$M = \begin{pmatrix} 1 & 0 \\ \frac{1}{\rho}\left[\frac{b}{6\rho \cos \varepsilon} - \tan \varepsilon\right] & 1 \end{pmatrix} .$$

ε is the angle between the magnet edge and the perpendicular to the beam direction. ε is taken as positive for both edges of a rectangular magnet (Fig. 2).

b is the length of the fringe field region [m] (Fig. 2).

ρ is the bending radius [m] .

For the ISR: the values of ρ, n/ρ and $B\rho$ are given in Tables 2 and 5.

Since the gradient magnets of the ISR are rectangular, their matrix M is a product of three matrices: one matrix of type ii) for the central part and two matrices of type iv) for the two edges, with ε taken as being equal to half of the bending angle. Assuming b/ρ small, M becomes

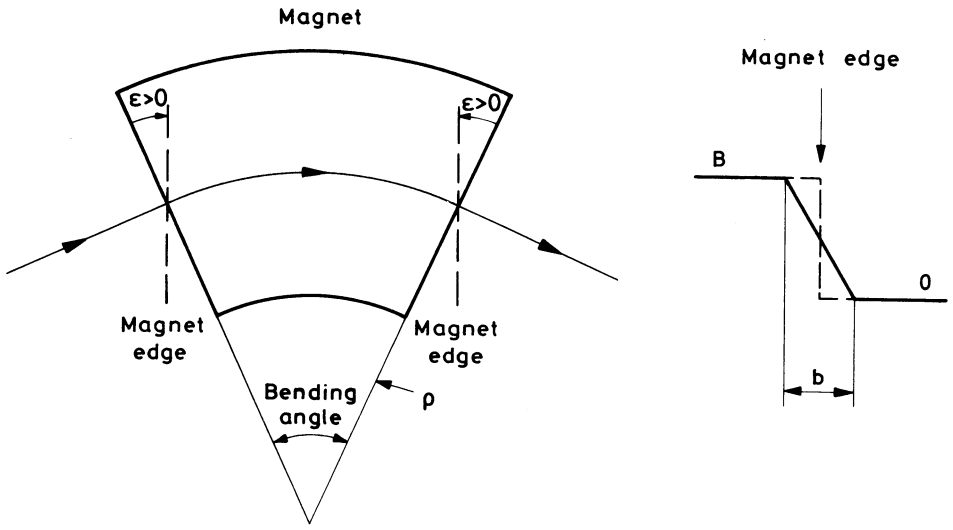

Fig. 2 Field boundaries for magnets

$$M(d) = \begin{pmatrix} \mathrm{cf}(\sqrt{K}\,d) \pm \dfrac{\tan\varepsilon}{\rho\sqrt{K}}\,\mathrm{sf}(\sqrt{K}\,d) & \dfrac{1}{\sqrt{K}}\,\mathrm{sf}(\sqrt{K}\,d) \\ \left[\mathrm{sign}\sqrt{K} + \dfrac{\tan^2\varepsilon}{\sqrt{K}\,\rho^2}\right]\mathrm{sf}(\sqrt{K}\,d) \pm \dfrac{2\tan\varepsilon}{\rho}\,\mathrm{cf}(\sqrt{K}\,d) & \mathrm{cf}(\sqrt{K}\,d) \pm \dfrac{\tan\varepsilon}{\rho\sqrt{K}}\,\mathrm{sf}(\sqrt{K}\,d) \end{pmatrix}$$

The parameter definitions are given above and the signs + and - correspond to the bending plane and to the plane perpendicular to the bending, respectively.

1.3 Interpolation of the transverse parameters through any element

Computer programs like AGS[4] give the values of α_y, β_y, μ_y at a discrete number of points. It can be useful to have formulae giving the values of the parameters at any point inside the element, knowing their values $\alpha_{y,1}$, $\beta_{y,1}$ [m], $\mu_{y,1}$ at the entrance.

$$\alpha_y(d) = -m_{11}m_{21}\beta_{y,1} - m_{12}m_{22}\frac{1+\alpha_{y,1}^2}{\beta_{y,1}} + (m_{11}m_{22} + m_{12}m_{21})\,\alpha_{y,1} ,$$

$$\beta_y(d) = m_{11}^2\beta_{y,1} + m_{12}^2\frac{1+\alpha_{y,1}^2}{\beta_{y,1}} - 2m_{11}m_{12}\alpha_{y,1} ,$$

$$\mu_y(d) = \mu_{y,1} + \mathrm{arctg}\,\frac{m_{12}}{m_{11}\beta_{y,1} - m_{12}\alpha_{y,1}} .$$

The coefficients m_{ij} (functions of d) are the elements of the matrix M(d) defined in Section 1.2.

From these general formulae, two special cases can be deduced:

i) Interpolation in a straight section:

$$\alpha_y(d) = \alpha_{y,1} - d\,\frac{1+\alpha_{y,1}^2}{\beta_{y,1}} \quad ,$$

$$\beta_y(d) = \beta_{y,1} - 2d\alpha_{y,1} + d^2\,\frac{1+\alpha_{y,1}^2}{\beta_{y,1}} \quad ,$$

$$\mu_y(d) = \mu_{y,1} + \operatorname{arctg}\frac{d}{\beta_{y,1} - d\alpha_{y,1}} \quad .$$

ii) Interpolation in a gradient sector magnet:

$$\alpha_y(d) = \alpha_{y,1}\,cf(2\sqrt{K}\,d) - \left[\frac{1+\alpha_{y,1}^2}{\sqrt{K}\,\beta_{y,1}} + \operatorname{sign}\sqrt{K}\,\beta_{y,1}\right]\frac{1}{2}\,sf(2\sqrt{K}\,d) \quad ,$$

$$\beta_y(d) = \beta_{y,1}\,cf^2(\sqrt{K}\,d) - \frac{\alpha_{y,1}}{\sqrt{K}}\,sf(2\sqrt{K}\,d) + \frac{1+\alpha_{y,1}^2}{K\,\beta_{y,1}}\,sf^2(\sqrt{K}\,d) \quad ,$$

$$\mu_y(d) = \mu_{y,1} + \operatorname{arctg}\frac{sf(\sqrt{K}\,d)}{\sqrt{K}\,\beta_{y,1}\,cf(\sqrt{K}\,d) - \alpha_{y,1}\,sf(\sqrt{K}\,d)} \quad ,$$

where the definitions of sf, cf, sign and K are explicitly given in Section 1.2.

1.4 Transverse emittance

Let us consider one particle of constant energy making an infinite number of turns. All the positions taken by this particle in a transverse phase plane (y, y') at one given point of the machine circumference define an ellipse (Fig. 3) with the following equation:

$$E_y = \frac{\pi}{\beta_y}\left[y^2 + (\beta_y y' + \alpha_y y)^2\right] \quad .$$

The emittance E_y is the ellipse area and the factor π has to be included in the numerical value of E_y.

1.5 Normalized transverse emittance

The emittance E_y is an invariant if the energy of the particle does not change. With an energy change, the invariant becomes the normalized transverse emittance ε_y [m rad]

$$\varepsilon_y = E_y\,\beta\gamma \quad .$$

For the ISR: Typical values of ε_y are given in Table 2. These values correspond to ellipses containing 86.466 % of the particles assuming a gaussian distribution (see also Section 1.6).

1.6 Beam size in the transverse plane

$$\hat{y} = \sqrt{\frac{\beta_y E_y}{\pi}} \quad .$$

The beam size will be $2\hat{y}$.

For a gaussian particle density, the relation $\hat{y} = 2\sigma_y$ is used, where σ_y is the standard deviation [m].

For zero divergence ($y' = 0$), the maximum value of y will be

$$y_0 = \sqrt{\frac{\beta_y}{(1 + \alpha_y^2)} \frac{E_y}{\pi}} \quad .$$

The definitions of y_0 and $\hat{y}$ are summarized in Fig. 3.

1.7 Angular divergence of a beam

$$\hat{y}' = \sqrt{\frac{(1 + \alpha_y^2) E_y}{\beta_y \pi}} \quad .$$

The total divergence [rad] will be $2\hat{y}'$.

At the pulse centre ($y = 0$), the maximum angular divergence will be

$$y_0' = \sqrt{\frac{E_y}{\pi \beta_y}} \quad .$$

The definitions of y_0' and $\hat{y}'$ are summarized in Fig. 3.

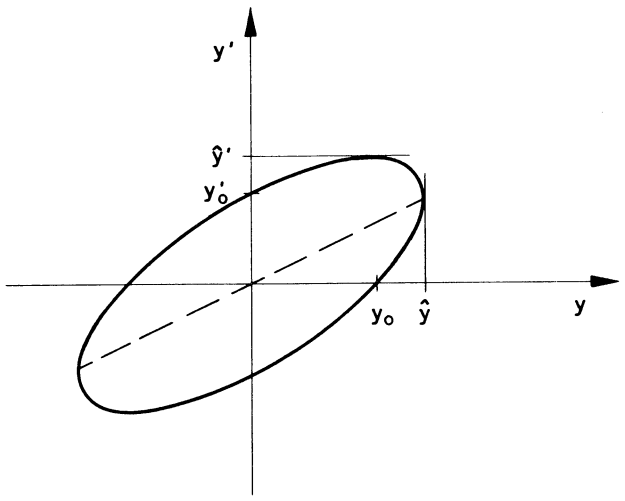

Fig. 3 A two-dimensional beam phase ellipse

2. FORMULAE IN CONNECTION WITH THE MAGNETIC FIELD[1,2,3,5,6]

Symbols frequently used in this chapter

s_1 longitudinal position of one given magnetic element [m]

ℓ circumference of the machine [m]

$\mu_y(s)$ phase of the betatron oscillation (defined in Section 1.1) in plane (y,s).

2.1 Magnetic rigidity

The general relation is

$$B\rho = \frac{p}{e} .$$

For p in GeV/c and $B\rho$ in Tm, this relation simply becomes

$$B\rho = \frac{10^9}{c} p = 3.335641\ p ,$$

ρ being the bending radius [m].

Note: [T] = [Vsm^{-2}].

For the ISR: Table 2 gives the bending radius and Table 5 gives the magnetic rigidity [Tm] for the standard ISR energies.

2.2 Orbit deformation associated with dipole fields

$$y(s) = \frac{\text{sign}\ \sqrt{\beta_y(s)}}{2 \sin \pi Q_y} \int_0^{\ell} \sqrt{\beta_y(s_1)}\ \frac{\Delta B(s_1)}{B\rho} \cos\left[Q_y \pi - \left|\mu_y(s) - \mu_y(s_1)\right|\right] ds_1 ,$$

$y(s)$ is the orbit amplitude at the position s of the circumference [m] ,

ΔB is the dipole field [T] orthogonal to the y-axis and to the s-axis,

sign is +1 for the vertical plane and -1 for the horizontal plane,

$B\rho$ is the magnetic rigidity [Tm] (see Section 2.1).

For dipoles or sections of dipoles which are short compared to the betatron oscillation wavelength, the integral on ds_1 can be replaced by a summation.

Since the functions $y(s)$ and $\Delta B(s)$ are periodic with the machine circumference, it is possible to develop them in Fourier's series. Using the phase μ_y (Section 1.1) instead of the coordinate s, the expression for the orbit becomes

$$y(\mu_y) = \sqrt{\beta_y(\mu_y)} \sum_{p=-\infty}^{\infty} \frac{Q_y^2}{Q_y^2 - p^2} C_p \exp\left[ip \frac{\mu_y}{Q_y}\right] ,$$

with

$$C_p = \frac{1}{2\pi Q_y} \int_0^{2\pi Q_y} \beta_y^{3/2}(\mu_y) \frac{\Delta B(\mu_y)}{B\rho} \exp\left[-ip \frac{\mu_y}{Q_y}\right] d\mu_y .$$

p is an integer, and ΔB and $B\rho$ are defined above.

Assuming there is a correction system able to compensate exactly the harmonics n to m of the amplitude function y(s), the average gain in the ratio of the extreme amplitudes after and before correction will be for distributed dipole fields:

$$g(Q_y, n, m) = 1 - \frac{\sum_{p=n}^{m} \frac{1}{|Q_y^2 - p^2|}}{\sum_{p=1}^{\infty} \frac{1}{|Q_y^2 - p^2|}} \quad .$$

n, m, p are integers and $g = \bar{\hat{y}}_{corr} / \bar{\hat{y}}$.

The infinite sum can be calculated analytically using[7)]

$$\sum_{p=1}^{\infty} \frac{1}{p^2 - Q_y^2} = \frac{\pi}{2Q_y} \left(\frac{1}{\pi Q_y} - \operatorname{cotg} \pi Q_y \right) .$$

2.3 Tune shifts, amplitude beating and horizontal momentum compaction changes associated with quadrupole fields

$$\Delta Q_y = \frac{1}{4\pi} \int_0^{\ell} \beta_y(s_1) \frac{G(s_1)}{B\rho} \, ds_1 \ ,$$

$$\frac{\Delta \beta_y}{\beta_y}(s) = \frac{1}{2 \sin 2\pi Q_y} \int_0^{\ell} \beta_y(s_1) \frac{G(s_1)}{B\rho} \cos \left[2 \left(Q_y \pi - |\mu_y(s) - \mu_y(s_1)| \right) \right] ds_1 \ ,$$

$$\Delta \alpha_{p,x}(s) = - \frac{\sqrt{\beta_x(s)}}{2 \sin \pi Q_x} \int_0^{\ell} \sqrt{\beta_x(s_1)} \frac{G(s_1)}{B\rho} \alpha_{p,x}(s_1) \cos \left[Q_x \pi - |\mu_x(s) - \mu_x(s_1)| \right] ds_1 \ .$$

G is the quadrupole gradient $[Tm^{-1}]$,
$\alpha_{p,x}$ is the horizontal momentum compaction at the quadrupole [m] (see Section 1.1),
$B\rho$ is the magnetic rigidity [Tm] (see Section 2.1).

For a short quadrupole, the note mentioned in Section 2.2 equally applies.

2.4 Vertical momentum compaction associated with skew quadrupole fields

The vertical momentum compaction [m] is the ratio of the vertical shift in position to the momentum change. Its mathematical definition is given in Section 1.1.

$$\alpha_{p,z}(s) = \frac{\sqrt{\beta_z(s)}}{2 \sin \pi Q_z} \int_0^{\ell} \sqrt{\beta_z(s_1)} \frac{G_s(s_1)}{B\rho} \alpha_{p,x}(s_1) \cos \left[\pi Q_z - |\mu_z(s) - \mu_z(s_1)| \right] ds_1 \ .$$

$G_s = dB_x/dx$ is the skew gradient $[Tm^{-1}]$,
$B\rho$ is the magnetic rigidity [Tm] (see Section 2.1),
$\alpha_{p,x}(s_1)$ is the horizontal momentum compaction at the skew quadrupole [m] (see Section 1.1).

For a short skew quadrupole, the note mentioned in Section 2.2 equally applies.

The vertical momentum compaction excited by a skew quadrupole manifests itself as a median plane tilt, which is given by

$$\chi = \operatorname{arctg} \frac{\alpha_{p,z}}{\alpha_{p,x}} ,$$

χ being the median plane tilt [rad].

2.5 Multipole analysis of a two-dimensional magnetic field

In cartesian coordinates, the two-dimensional magnetic field in a magnet gap can be derived from a complex potential P [Tm]:

$$P = V + iU = \sum_{N=1}^{\infty} \frac{1}{N!} B^{(N-1)} w^N ,$$

where:

$$w = x + iz ,$$

$$B^{(N-1)} = B_z^{(N-1)} + i B_x^{(N-1)} = \frac{\partial^{(N-1)} B_z}{\partial x^{(N-1)}}\bigg|_{x=z=0} + i \frac{\partial^{(N-1)} B_x}{\partial x^{(N-1)}}\bigg|_{x=z=0} .$$

N is an integer associated with the 2N-pole term.

The field components are then given by:

$$B_x = - \frac{\partial V}{\partial z} = \operatorname{Im} \left(\frac{\partial P}{\partial w} \right) ,$$

$$B_z = \frac{\partial V}{\partial x} = \operatorname{Re} \left(\frac{\partial P}{\partial w} \right) .$$

In cylindrical coordinates, the complex potential P can be written:

$$P = \sum_{N=1}^{\infty} \frac{1}{N!} B^{(N-1)} r^N e^{iN\phi} ,$$

r is the distance from the origin [m],
ϕ is the angle between the x-axis and the radius vector [rad].

The real component of P becomes

$$V = \sum_{N=1}^{\infty} \frac{r^N}{N!} \left[B_z^{(N-1)} \cos N\phi - B_x^{(N-1)} \sin N\phi \right],$$

and the field components are given by

$$B_r = \frac{\partial V}{\partial r} ,$$

$$B_\phi = - \frac{1}{r} \frac{\partial V}{\partial \phi} .$$

Note that the derivatives can be calculated from

$$B_x^{(N-1)} = -\frac{N!}{\pi r^N}\int_0^{2\pi} V \sin N\phi \, d\phi \ ,$$

$$B_z^{(N-1)} = \frac{N!}{\pi r^N}\int_0^{2\pi} V \cos N\phi \, d\phi \ .$$

3. FORMULAE IN CONNECTION WITH THE LONGITUDINAL PHASE SPACE[2,3]

Symbols frequently used in this chapter

V	cavity voltage [V]
Φ_s	phase of the synchronous particle
Φ	phase of a particle
h	harmonic of the radio-frequency system: $\Delta\Phi = -h\Delta\theta$
M	number of bunches
ℓ	total bunch length [m]
E_o	rest energy of proton (Table 1) [eV]
m_o	rest mass of proton [eV/c^2]

3.1 Acceleration rate

The rate of energy increase for the synchronous particle is given by:

$$\frac{d(B\rho)}{dt} = \frac{V \sin \Phi_s}{2\pi R} \ .$$

The phase of the synchronous particle is often replaced by

$$\Gamma = \sin \Phi_s \ .$$

Using the relation in Section 2.1 for p in GeV/c and Bρ in Tm, the rate of momentum increase can be written:

$$\frac{dp}{dt} = k\frac{V\Gamma}{R} \ ,$$

where:

$$k = \frac{c}{2\pi 10^9} = 0.0477135 \ [ms^{-1}].$$

For the ISR: R and V are given in Table 2.

3.2 Motion of a nonsynchronous particle

The momentum increase of a nonsynchronous particle differs from the one of the synchronous particle and the former particle will oscillate around the latter in agreement with

$$\frac{d}{dt}\left(\frac{R^2\ \gamma\ E_o}{\eta\ c^2\ h}\ \frac{d\Phi}{dt}\right) + \frac{eV}{2\pi}\ (\sin\Phi - \sin\Phi_s) = 0\ .$$

The values of R, γ and η have to be taken for the synchronous particle. When these parameters are constant or slowly varying, the motion equation becomes

$$\frac{d^2\Phi}{dt^2} + \frac{4\pi^2\ f_p^2}{\cos\Phi_s}\ (\sin\Phi - \sin\Phi_s) = 0\ .$$

This equation and its first integral also give the variation of the momentum for the nonsynchronous particle, since

$$\frac{\Delta p}{p} = -\frac{1}{2\pi\ f_{rev}\ h\ \eta}\frac{d\Phi}{dt} = -\frac{\sqrt{2}\ f_p}{f_{rev}\ h\ \eta}\sqrt{\frac{\cos\Phi - \cos\Phi_i + (\Phi - \Phi_i)\sin\Phi_s}{\cos\Phi_s}}$$

f_p is the phase oscillation frequency (Section 3.3) $[s^{-1}]$
f_{rev} is the revolution frequency (Section 3.3) $[s^{-1}]$
Φ_i is one of the two extreme stable phases where $d\phi_i/dt = 0$ (Section 3.6).

For the ISR: R and h are given in Table 2, while γ is given for the ISR standard energies in Table 5. The η-values given in Table 6 correspond to the currently used working lines. For other lines, η can be calculated starting from γ_t given in Table 3. Note that all these figures are only strictly valid on the central orbit.

3.3 Revolution frequency and phase oscillation frequency

The revolution frequency $[s^{-1}]$ of the particles is

$$f_{rev} = \frac{\beta c}{2\pi R}\ .$$

In the case of small phase oscillation amplitudes around the stable phase Φ_s, the oscillation frequency $[s^{-1}]$ is exactly given by

$$f_p = \frac{k}{R}\sqrt{\frac{eV\ h\ \eta}{\gamma\ E_o}\cos\Phi_s}\ ,$$

where:

$k = \frac{c}{(2\pi)^{3/2}} = 1.90349 \times 10^7\ [ms^{-1}]$, and

$\cos\Phi_s = \sqrt{1 - \Gamma^2}$, γ and η being taken for the synchronous particle.

For the ISR: the values of E_o, R, V, h, β, γ and η can be found in Tables 1, 2, 5 and 6. The value of the revolution frequency for light, f_{rev}^{ℓ} ($\beta = 1$), is given in Table 2.

3.4 Revolution frequency spread and stability condition

The frequency spread is related to the momentum spread

$$\frac{\Delta f_{rev}}{f_{rev}} = \eta \frac{\Delta p}{p} ,$$

where:

$$\eta = \frac{1}{\gamma^2} - \frac{1}{\gamma_{tr}^2} = \frac{1}{\gamma^2} - \frac{\bar{\alpha}_{p,x}}{R} ,$$

f_{rev} is defined in Section 3.3.

Looking at the motion equation in Section 3.2, it is clear that the motion is stable and that the RF buckets can exist only if f_p^2 is positive, which is equivalent to

$$\eta \cos \Phi_s > 0 .$$

For the ISR: the values of η for different conditions are given in Table 6. Since η is always negative, the stability criterion implies that

$$\frac{\pi}{2} < \Phi_s < \pi .$$

3.5 Moving bucket area

The moving bucket area (Fig. 4) is given in the coordinates $c\Delta p/E_o = \Delta p/m_o c$ and Φ, by the following relation:

$$A = k \, \alpha(\Gamma) \sqrt{\frac{eV \gamma}{h|\eta|E_o}} ,$$

where:

$$k = \frac{16}{\sqrt{2\pi}} = 6.38308 ,$$

$\alpha(\Gamma)$ is the factor between the moving and stationary bucket areas (Table 7).

For the ISR: the harmonic h and the voltage V are given in Table 2 and the values of γ are given in Table 5 for the ISR standard energies. Table 6 gives the values of η for different conditions.

3.6 Separatrix equation and extreme stable phases of a bucket

For stable motion (Section 3.4), the particles must remain inside the bucket. The limit of the bucket in the phase plane ($\Delta p/m_o c$, Φ) is called the separatrix (Fig. 4) and is given by the equation

$$\frac{1}{8\pi^2} \left(\frac{d\Phi}{dt}\right)^2 - \frac{f_p^2}{\cos \Phi_s} (\cos \Phi + \Phi \sin \Phi_s) = - \frac{f_p^2}{\cos \Phi_s} (\cos \Phi_1 + \Phi_1 \sin \Phi_s)$$

keeping in mind that (Section 3.2)

$$\frac{\Delta p}{m_o c} = - \frac{\beta \gamma}{2\pi f_{rev} h \eta} \frac{d\Phi}{dt} ,$$

f_{rev} is the revolution frequency (Section 3.3) $[s^{-1}]$,
f_p is the phase oscillation frequency (Section 3.3) $[s^{-1}]$,
Φ_1 is one of the extreme phases which can be reached by a stable particle.

The two extreme phases Φ_1 and Φ_2 are given by (Fig. 4)

$$\Phi_1 = \pi - \Phi_s ,$$

$$\Phi_2 \sin \Phi_s + \cos \Phi_2 = \Phi_1 \sin \Phi_s - \cos \Phi_s .$$

$\Phi_1 - \Phi_2$ is the total phase spread of the bucket. It is equal to $2\Delta\Phi$ in Section 3.9 only if the bunch fills the bucket, since by definition the bunch is the part of the bucket full of particles.

3.7 Momentum spread in the bucket

The extreme momenta which can be reached by a stable particle (Fig. 4) are given by

$$\frac{\Delta p}{p} = \pm \frac{1}{\beta} \sqrt{\frac{eV}{h \eta \gamma E_o}} \sqrt{\frac{2}{\pi} \cos \Phi_s - (1 - \frac{2}{\pi} \Phi_s) \sin \Phi_s} .$$

Using the definition of $\alpha_{p,x}$ given in Section 1.1, the momentum spread of the bucket can give its horizontal width.

For the ISR: E_o, h, β, γ, η are given in Tables 1, 2, 5 and 6.

It should be kept in mind that the stability criterion (Section 3.4) implies that in this machine

$$\frac{\pi}{2} < \Phi_s < \pi .$$

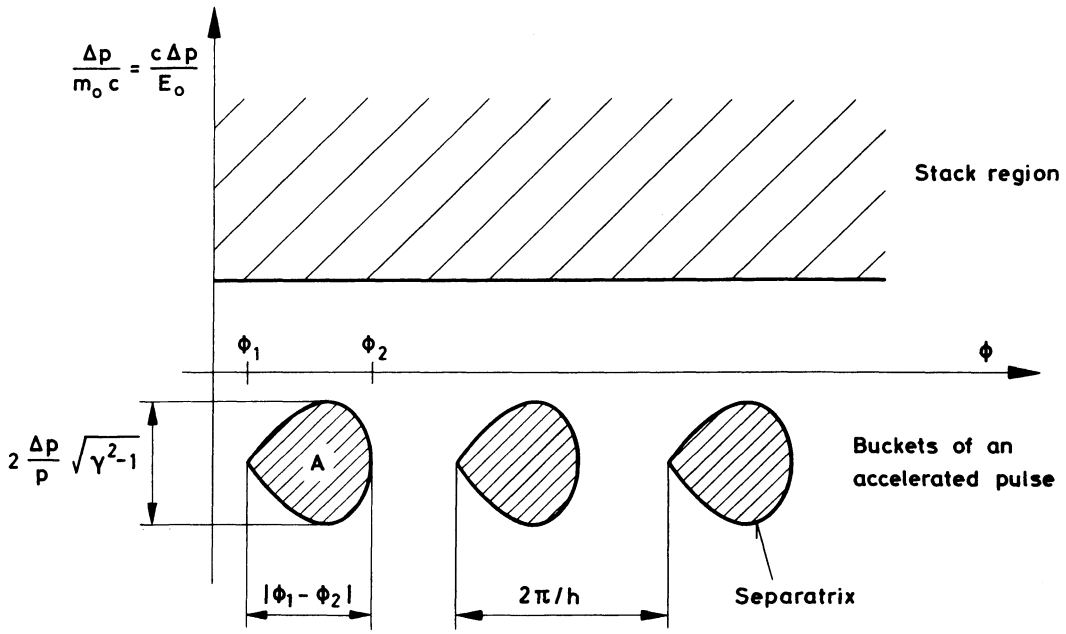

Fig. 4 Longitudinal phase space

3.8 Time needed for an adiabatic change of bucket parameters

When stacking in the momentum space of proton storage rings, it is necessary to reduce the bucket area when the pulse arrives close to the stacked beam, in order to avoid perturbing the stack. The necessary time [s] for adiabatic change of bucket parameters is:

$$T = \frac{1 + \eta_{ad}}{4\pi(1 - \eta_{ad})} \left(\frac{1}{f_{p,2}} - \frac{1}{f_{p,1}} \right) .$$

$f_{p,1}$ is the phase oscillation frequency (Section 3.3) associated with the initial bucket [s^{-1}],

$f_{p,2}$ is the phase oscillation frequency (Section 3.3) associated with the final bucket [s^{-1}],

η_{ad} is the phase-space efficiency of the process, defined as follows:

$$\eta_{ad} = \frac{1 - \varepsilon_p}{1 + \varepsilon_p} ,$$

ε_p being the theoretical adiabaticity.

For the ISR: the bucket area is reduced by diminishing the cavity voltage at the end of the accelerating cycle. In this case, the formula for T [s] becomes:

$$T = \left[\sqrt{\frac{V_1}{V_2}} - 1 \right] \frac{1}{800\varepsilon} .$$

ε is the adiabaticity coefficient as set in the ISR and is related to ε_p by

$$\varepsilon = \varepsilon_p \frac{f_{p,1}}{63.66} .$$

Typical values for ε are: 0.015/0.05.

V_1 is the initial accelerating voltage [V],

V_2 is the final accelerating voltage [V].

3.9 Debunching time

In the absence of radio-frequency fields, the beam debunches. By definition, the time in which the front of the bunch reaches the tail of the next bunch, for rectangular bunches, is the debunching time t_{db} [s]:

$$t_{db} = \frac{\pi - \Delta\phi}{2\pi f_{rev} h|\eta|\Delta p/p} .$$

f_{rev} is the revolution frequency (Section 3.3) [s^{-1}],

$2\Delta\phi$ is the total phase spread of the bunch,

$2\Delta p$ is the total momentum spread of the bunch [GeV/c].

For the ISR: the values of h and f_{rev}^{ℓ} are given in Table 2. The standard ISR values of η are given in Table 6.

3.10 Azimuthal current distribution inside one bunch

For a given number N of charges in a bunched beam and a given number M of bunches, the azimuthal current distribution inside a single bunch can be written as follows for rectangular, parabolic and triangular bunches successively:

$$\left.\begin{aligned} I_\theta &= I_o \\ I_\theta &= \frac{3}{2} I_o \left[1 - \left(\frac{2R}{\ell}\right)^2 \theta^2\right] \\ I_\theta &= 2 I_o \left[1 + \text{sign}\ \frac{2R}{\ell}\,\theta\right] \end{aligned}\right\} \quad \text{for } -\frac{\ell}{2R} \le \theta \le \frac{\ell}{2R} \ ,$$

sign is + 1 for $\theta < 0$ and - 1 for $\theta \ge 0$.

The expression for I_o is

$$I_o = \frac{Ne\beta c}{M\,\ell} \ ,$$

N being the total number of charges.

For gaussian bunches, the current distribution inside a bunch is given by

$$I_\theta = \frac{Ne\beta c}{\sqrt{2\pi}\,\sigma_s\,M} \exp\left[-\frac{R^2\theta^2}{2\sigma_s^2}\right]$$

σ_s is the r.m.s. value of the coordinate s for a gaussian bunch [m].

In this case, a standard definition of the bunch length may be $\ell = 4\sigma_s$.

For the ISR: the values of R and β are given in Tables 2 and 5, respectively. The bunch length is of the order of 7 m and the bunches are approximately parabolic.

3.11 Average current for a circulating beam

The average current I is

$$I = k\frac{N\beta}{R} \ ,$$

where:

$k = \frac{ec}{2\pi} = 7.64462 \times 10^{-12}$ [Am],

N is the total number of charges in the circulating beam.

This formula is valid either for a bunched beam or for a coasting beam.

For the ISR: the values of R and β are given in Tables 2 and 5, respectively.

3.12 Bunching factor

By definition, the bunching factor is the ratio of the average current I [A] in the circulating beam to the peak current $\hat{I}$ [A] inside a bunch. This factor can be calculated from the formulae in Sections 3.10 and 3.11 and will depend on the shape of the bunches

$$B_f = \frac{I}{\hat{I}} = \frac{M\,\ell}{S\,2\pi\,R} \quad .$$

The total length ℓ of the bunches is taken as 4 times the r.m.s. value for a gaussian shape, as mentioned in Section 3.10.

S is a shape factor taking the following values:

S = 1	for rectangular bunches
S = 1.5	for parabolic bunches
S = 1.6	for gaussian bunches
S = 2	for triangular bunches.

For the ISR: the bunches are approximately parabolic, so that S = 1.5. The bunch length is of the order of 7 m.

3.13 Relative amplitudes of the bunch harmonics

The relative amplitudes of the bunch harmonics q are defined as follows:

$$I_\theta = \hat{I} \sum_q c_q\, e^{iq\theta} \quad , \qquad q = \text{integer} \ ,$$

I_θ is the azimuthal current distribution of a bunched beam (Section 3.10) [A],
$\hat{I}$ is the peak current inside a bunch (Section 3.10) [A].

The expressions for c_q depend upon the current distribution inside a single pulse. If the bunches are (Section 3.10)

i) rectangular

$$c_q = D\,\frac{1}{\pi q}\,\sin\frac{q\ell}{2R} \quad ,$$

ii) parabolic

$$c_q = D\,\frac{4R}{\pi\, q^2\, \ell}\left[\frac{2R}{q\ell}\,\sin\frac{q\ell}{2R} - \cos\frac{q\ell}{2R}\right] ,$$

iii) gaussian

$$c_q = D\,\frac{\sigma_s}{\sqrt{2\pi}\,R}\,\exp\left[-\frac{q^2\,\sigma_s^2}{2R^2}\right] ,$$

iv) triangular

$$c_q = D\,\frac{2R}{\pi\, q^2\, \ell}\left[1 - \cos\frac{q\ell}{2R}\right] ,$$

where D is the following series development:

$$D = \sum_{k=0}^{M-1} \exp\left[-\,i\,q\,k\,\frac{2\pi}{h}\right] , \qquad k = \text{integer} \ .$$

If the bunch harmonic number q is a multiple of h, D becomes equal to the number of bunches M. If, furthermore, the number of bunches is equal to h, D is zero for all bunch harmonics which are not a multiple of h.

For the ISR: the values of h and R are given in Table 2. The bunch length is given in Section 3.10. The bunches are approximately parabolic, so that formula ii) above applies. Since M is smaller or equal to 20, none of the harmonic amplitudes c_q is zero.

4. FORMULAE IN CONNECTION WITH THE VACUUM CONDITIONS[8,9,10,11]

Symbols frequently used in this chapter

L	half distance between two vacuum pumps [m]
S	half-lumped pumping speed $[m^3 s^{-1}]$
c_m	molecular conductance per unit length of the vacuum pipe $[m^4 s^{-1}]$
σ_+	ionization cross-section of the gas $[m^2]$
η_d	net desorption factor, i.e. the number of molecules desorbed per incident ion minus the sticking probability of the ion, which is normally equal to 1
n	molecular density of the gas $[m^{-3}]$
P	pressure of the gas [Torr]
g	gas desorption per tube length, independent of gas density $[m^{-1} s^{-1}]$
A	cross-sectional area of the vacuum tube $[m^2]$

4.1 Relation between pressure and gas density

The molecular density n $[m^{-3}]$ of a gas at pressure P [Torr] is given by

$$n = k \frac{P}{T} ,$$

where:

$$k = N_m \frac{T_{st}}{P_{st} V_m} = 9.65118 \times 10^{24} \; [m^{-3} \text{ K Torr}^{-1}],$$

N_m is the number of molecules per mole (Table 1),
T_{st} is the standard temperature (Table 1) [K],
P_{st} is the standard pressure (Table 1) [Torr],
V_m is the molar volume of an ideal gas under standard conditions (Table 1) $[m^3]$,
T is the temperature of the gas [K] .

The atomic density n_a $[m^{-3}]$ is obtained by multiplying the molecular density n by the number of atoms N_a in a molecule.

For the ISR: using T = 300 K, this relation becomes

$$n = 3.21706 \times 10^{22} \; P .$$

4.2 Gas desorption coefficient and molecular conductance

The gas desorption per tube length g $[m^{-1}s^{-1}]$ is defined by

$$g = p_r \, q \, .$$

p_r is the perimeter of the vacuum chamber [m],
q is the specific gas desorption $[m^{-2}s^{-1}]$.

The specific molecular conductance c_m $[m^4 s^{-1}]$ is

for a long tube of circular section:

$$c_m = 97 \, \pi \sqrt{\frac{T}{M}} \, r^3 \quad ,$$

for a long tube of elliptical section:

$$c_m = 97 \, \pi \sqrt{\frac{T}{M}} \, a \, b^2 \quad ,$$

for a long tube of rectangular section:

$$c_m = 92.6 \, \pi \sqrt{\frac{T}{M}} \, a^2 \, b \; Y(\delta = a/b) \quad ,$$

where:

$$Y(\delta) = \frac{1}{\delta} \ln \left(\delta + \sqrt{\delta^2 + 1}\right) + \ln \left(\frac{1 + \sqrt{\delta^2 + 1}}{\delta}\right) + \frac{1}{3\delta^2} \left[1 + \delta^3 - (1 + \delta^2)^{3/2}\right] .$$

T is the absolute temperature of the gas [K],
M is the molecular mass (Table 8),
r is the radius of a circular tube [m]
a is the half-major axis of an elliptical tube or the half-major side of a rectangular tube [m],
b is the half-minor axis of an elliptical tube or the half-minor side of a rectangular tube [m].

For the ISR: some typical values of the perimeter p_r and of the specific conductance c_m for nitrogen molecules at 300 K are summarized in Section 4.3 for different regions of the machine circumference.

For the ISR residual gas composition, the total specific gas desorption q is 4×10^{10} $m^{-2}s^{-1}$. This value is essentially the H_2 contribution to the specific desorption, since the value of q for N_2 or CO is of the order of 1 % of the total value.

4.3 Equilibrium pressure without a particle beam

The geometric model used is a periodic structure with constant specific molecular conductance c_m and regularly spaced pumps (at distance 2L), all having the same pumping speed 2S. The model assumes, furthermore, that the gas desorption coefficient g is constant. In this model, the longitudinal coordinate s has its origin at the mid-point between two pumps.

$$n_o(s) = g\left(\frac{L}{S} + \frac{L^2 - s^2}{2c_m}\right) .$$

g and c_m are explicitly given in Section 4.2.

The equilibrium molecular density n_o is that density existing in the vacuum pipe before stacking a beam. The corresponding equilibrium pressure P_o can be deduced from the relation given in Section 4.1.

For the ISR: it is shown in Section 4.2 that g depends on the perimeter p_r of the vacuum chamber and that c_m depends on the gas. Some values of p_r, of c_m for the nitrogen at 300 K and of the distance 2L are given in the following table for different regions of the ISR machine:

	2L [m]	p_r [m]	$c_m(N_2)$ [$m^4 s^{-1}$]
Elliptical chamber 0.05 × 0.16 m^2	5 2.5	0.355	0.05
Round chamber 0.16 m diameter	10 4	0.503	0.51
Experimental region I2 0.15 m diameter	8 4	0.471	0.42
Special chamber in injection septum magnet 0.04 × 0.16 m^2	8 1.6	0.343	0.03

The value of the pumping speed for one half the combined station ion pump and sublimation pump is S = 0.5 $m^3 s^{-1}$

4.4 Dynamic pressure behaviour in the presence of a beam

The particle beam induces gas desorption via bombardment of the chamber walls by ions created in the residual gas. Neglecting the surface effects, the corresponding dynamic change in the molecular density n [m^{-3}] is given by

$$n(s,t) = \sum_{\nu=1}^{\infty} \cos \lambda_\nu s \left[\frac{C_\nu}{F_\nu} + \left(B_\nu - \frac{C_\nu}{F_\nu}\right) \exp\left(-\frac{F_\nu t}{A}\right)\right] ,$$

where:

$$C_\nu = \left(\frac{2g}{a_\nu^2 \lambda_\nu}\right) \sin L\lambda_\nu ,$$

$$F_\nu = c_m \lambda_\nu^2 - \sigma_+ \eta_d \frac{I}{e} ,$$

$$a_\nu^2 = L + \frac{\sin 2\lambda_\nu L}{2\lambda_\nu} ,$$

and λ_ν are the roots of the transcendental equation $\lambda_\nu \tan \lambda_\nu L = \frac{S}{c_m}$.

The initial gas distribution n(s,0) gives for the Fourier's coefficients B :

$$B_\nu = \frac{1}{a_\nu^2} \int_{-L}^{L} n(s,0) \cos \lambda_\nu s \, ds \quad .$$

The geometric model used is identical to the model given in Section 4.3 and η_d is also assumed to be constant.

The relation between the density n and the pressure P is given in Section 4.1. The coefficients g and c_m are given explicitly in Section 4.2.

For the ISR: the latest values of the ionization cross-section at 26 GeV/c are given in Table 8. The total value of q is given in Section 4.2. The present values of L, S and c_m for N_2 at 300 K are given in Section 4.3.

4.5 Equilibrium pressure in the presence of a beam

A finite equilibrium pressure can only exist for negative exponents in the expression given in Section 4.4. The stability condition in the presence of a beam is thus given by $F_1 > 0$, i.e.

$$\eta_d I < (\eta_d I)_{\text{critical}} = \frac{e\, c_m}{\sigma_+} \lambda_1^2 \quad .$$

λ_1 is the first root of the transcendental equation given in Section 4.4.

When this condition is fulfilled, the equilibrium density is given by

$$n(s, t \to \infty) = \sum_{\nu=1}^{\infty} \frac{C_\nu}{F_\nu} \cos \lambda_\nu s \quad ,$$

where C_ν and F_ν are given in Section 4.4.

Taking the first term $\nu = 1$ of this series expansion, an approximate pressure bump equation valid for the equilibrium can be written. This yields the relationship between the starting pressure P_o [Torr] given in Section 4.3 and the pressure in the presence of a beam P_∞ [Torr] :

$$P_\infty = \frac{P_o}{1 - \frac{\sigma_+ \eta_d I}{e\, c_m \lambda_1^2}} \quad ,$$

in which appears the so-called effective pumping speed S_{eff} [$m^2 s^{-1}$]

$$S_{eff} = c_m \lambda_1^2 = \frac{g}{P_o} \quad .$$

The last relationship between the equilibrium pressures with and without beam can be generalized for a system with 2 gas components. The pressures $P_{\infty,1}$ and $P_{\infty,2}$ are related to the starting pressures $P_{o,1}$ and $P_{o,2}$ by

$$P_{\infty,i} = \frac{P_{o,j}\,\frac{b_{ij}}{S_{eff,i}} + P_{o,i}\left(1 - \frac{b_{jj}}{S_{eff,j}}\right)}{\left(1 - \frac{b_{ii}}{S_{eff,i}}\right)\left(1 - \frac{b_{jj}}{S_{eff,j}}\right) - \frac{b_{ij}\,b_{ji}}{S_{eff,i}\,S_{eff,j}}}$$

with:

$i = 1, 2$; $j = 1, 2$ and $i \neq j$.

The coefficients b_{ij} are defined by

$$b_{ij} = \frac{\sigma_{+,j}}{e}\,\eta_{d,ij}\,I \qquad i,j = 1, 2 .$$

$\sigma_{+,j}$ is the ionization cross-section of the gas number j $[m^2]$,
$\eta_{d,ij}$ gives the desorption yield of gas i by an ion of gas j.

For the ISR: the following approximate values of S_{eff} can be used for estimating the values of η_d in an elliptical chamber (0.05×0.16 m^2):

$$S_{eff,H_2} \cong 0.028 \quad m^2 s^{-1}$$
$$S_{eff,CO} \cong 0.0075 \quad m^2 s^{-1} ,$$

η_d being given by the relation (see above)

$$\eta_d = \frac{e\,S_{eff}}{\sigma_+\,I}\left(1 - \frac{P_o}{P_\infty}\right) .$$

P_o and P_∞ are measured and σ_+ is given in Table 8.

4.6 Pressure decay when dumping the beam

When the beam is dumped, the pressure decreases again. The starting decay rate is simply related to the equilibrium pressure in the presence of the beam P_∞ by

$$\dot{P}_d = -\frac{\sigma_+\,\eta_d\,I}{e\,A}\,P_\infty .$$

$\dot{P}_d$ is the decay rate of the pressure just after dumping the beam [Torr s^{-1}] .

4.7 Clearing current associated with electron production

The ionization of the residual gas produces electrons, which give rise to a clearing current. In addition to this, the ions produced may sputter metal atoms from the vacuum chamber walls, which further increase the clearing current seen by collecting electrodes. The global effect is

$$I_{cl} = I^o_{cl}\left(1 + \frac{\delta I \Sigma_+}{\frac{\pi}{2}\,\bar{v}\,s_t\,re - \Delta I \Sigma_+}\right) ,$$

where:

$I^o_{cl} = \sigma_{+,N_2}\, n_+ d\, I$,

I_{cl} is the total clearing current seen on the collecting electrodes [A] ,

I^o_{cl} is the clearing current due to primary electrons only [A] ,

δ and Δ are the sputtering coefficients for the residual gas and for the sputtered atoms, respectively,

$\bar{v}$ is the mean velocity of the sputtered atoms [m s^{-1}],

s_t is the sticking probability of the sputtered atoms,

Σ_+ is the ionization cross-section of the sputtered atoms [m^2] ,

σ_{+,N_2} is the ionization cross-section of the nitrogen gas [m^2] ,

d is the length over which electrons are cleared [m] ,

r is the radius of the vacuum tube [m] ,

n_+ is the equivalent density of nitrogen gas for ionization [m^{-3}] .

The molecular density n_+ is related to the N_2 equivalent ionization pressure P_+ [Torr] by (Section 4.1)

$$n_+ = k \frac{P_+}{T} .$$

k is given explicitly in Section 4.1,

T is the absolute temperature of the residual gas [K] .

The pressure P_+ is the pressure of nitrogen giving the same ionization current as the actual residual gas. For a mixture of different gases, the expression of P_+ is

$$P_+ = \frac{1}{\sigma_{+,N_2}} \sum_i \left(P_i \sum_j \sigma_{+,j} \right) .$$

i is numbering the gases of the mixture,

j is numbering the atoms in a molecule of the ith gas. If there are m identical atoms B in a molecule, the summation on j should contain every one and can be replaced by $m\sigma_{+,B}$,

P_i is the pressure of the ith gas [Torr] ,

$\sigma_{+,j}$ is the ionization cross-section for protons on the jth atom [m^2].

Since the denominator in the expression for I_{cl} may vanish at some given current I, the clearing current and the density of sputtered atoms will tend to infinity. This critical beam current is given by

$$I_{critical} = \frac{\pi \bar{v} s_t re}{2\Delta\Sigma} .$$

For the ISR: using the value of σ_{+,N_2} given in Table 8 and T = 300 K, the clearing current due to primary electrons is

$$I^o_{cl} = 2.63799\, P_+ d\, I .$$

For the typical ISR residual gas composition, P_+ is calculated from the above mentioned formula, so that:

$$P_+ = 0.64\, P_g ,$$

P_g being the gauge pressure [Torr] .

4.8 Beam neutralization factor

Electrons produced by ionization of the residual gas (Section 4.7) become trapped in the potential well of the particle beam and as a result the beam becomes partly neutralized. If ρ_c is the total charge density in the beam and ρ_p the density of the protons alone, the definition of the neutralization factor η_e is

$$\rho_c = \rho_p (1 - \eta_e) .$$

5. FORMULAE IN CONNECTION WITH LUMINOSITY[12,13,14,15]

Symbols frequently used in this chapter

L luminosity $[m^{-2}s^{-1}]$

L_o luminosity for centred beams $[m^{-2}s^{-1}]$

h_{eff} effective height associated with two vertically centred beams colliding vertically at zero angle [m]

w_{eff} effective width associated with two horizontally centred beams colliding horizontally at zero angle [m]

$\sigma_{1,2}$ r.m.s. value for the vertical densities of particles in beams 1 and 2 [m]

$\tau_{1,2}$ r.m.s. value for the horizontal densities of particles in beams 1 and 2 [m]

ψ horizontal colliding angle [rad]

5.1 Effective sizes of thin beams

For horizontal and vertical Gaussian distributions with r.m.s. values $\tau_{1,2}$ and $\sigma_{1,2}$, the effective sizes are

$$w_{eff} = \sqrt{2\pi}\sqrt{\tau_1^2 + \tau_2^2}$$

$$h_{eff} = \sqrt{2\pi}\sqrt{\sigma_1^2 + \sigma_2^2} .$$

These relations apply to the case of Gaussian beams colliding at zero angle horizontally and vertically, respectively.

The values of $\sigma_{1,2}$ and $\tau_{1,2}$ have to be taken for $\beta_{z,I}$ and $\beta_{x,I}$, respectively (see Section 1.6).

Note: $2\sqrt{\pi} = 3.544908$, $\sqrt{2\pi} = 2.506628$.

5.2 Horizontal standard deviation of a stacked beam

When the beam is stacked in the longitudinal phase space (Fig. 4), its shape is approximately rectangular in the variable x. For a rectangular horizontal distribution with Gaussian tails, the standard deviations $\tau_{1,2}$ are given by

$$\tau_{1,2} = \frac{1}{2\sqrt{3}} \sqrt{\frac{w_{1,2}^3 + 3\sqrt{2\pi}\ \delta_{1,2}\ w_{1,2}^2 + 2\delta_{1,2}^2\ w_{1,2} + 12\sqrt{2\pi}\ \delta_{1,2}^3}{w_{1,2} + \sqrt{2\pi}\ \delta_{1,2}}} ,$$

$w_{1,2}$ is the total width of the rectangular part of the distribution [m] ,
$\delta_{1,2}$ is the r.m.s. value of the Gaussian tails of the distribution [m] .

Note : $2\sqrt{3} = 3.464102$, $\sqrt{2\pi} = 2.506628$.

5.3 General definition of the luminosity

By definition, the luminosity is the time-averaged integral over the interaction volume Ω of the number of reactions per unit time and unit volume

$$L = \frac{1}{\sigma_r\ \tau_{rev}} \int_0^{\tau_{rev}} \int_{\Omega} \frac{d^2N}{d\Omega dt}\ dt d\Omega ,$$

τ_{rev} is the revolution time of the particles [s] (see Section 3.3),
σ_r is the total cross-section of the reaction [m^2],
Ω is the interaction volume where the two beams collide [m^3], $d\Omega = ds\ dx\ dz$.

The number of reactions per unit time and unit volume satisfies the following relation associated with the Lorentz transformation of the variables:

$$\frac{1}{\sigma_r} \frac{d^2N}{d\Omega dt} = \rho_1(x,z,s,t)\ \rho_2(x,z,s,t)\ c\ E(\beta_1,\beta_2,\psi) ,$$

where the relavistic factor E is given by

$$E(\beta_1,\beta_2,\psi) = \sqrt{\beta_1^2 + \beta_2^2 + 2\beta_1\beta_2 \cos\psi - \beta_1^2\beta_2^2 \sin^2\psi} .$$

When $\beta_1 = \beta_2$, this factor becomes

$$E(\beta,\psi) = 2\beta \cos\frac{\psi}{2} \sqrt{1 - \beta^2 \sin^2\frac{\psi}{2}} .$$

$\rho_{1,2}(x,z,s,t)$ are the particle densities per unit volume, which can also depend explicitly on time as, for instance, in the case of a bunched beam.
The indices 1 and 2 are associated with beam 1 and beam 2.

Some specific applications of this general formula are given in Sections 5.4 to 5.7.

Note : $L\ [\mu b^{-1}s^{-1}] = 10^{-34}\ L\ [m^{-2}s^{-1}]$.

5.4 Luminosity for two coasting beams with a non-zero colliding angle

Assuming a vertical Gaussian distribution of the particles and a horizontal colliding angle, the luminosity for two coasting beams is given by

$$L = E(\beta_1,\beta_2,\psi) \frac{I_1\ I_2}{e^2\ c\ \beta_1\beta_2\ h_{eff} \sin\psi} \exp\left[-\frac{1}{2}\frac{z^2}{\sigma_1^2 + \sigma_2^2}\right] ,$$

z is the vertical beam separation [m] .
The indices 1 and 2 are associated with beam 1 and beam 2.

The effective height h_{eff} is defined in Section 5.1 and is assumed not to vary over the interaction length. The relativistic coefficient $E(\beta_1,\beta_2,\psi)$ is given in Section 5.3.

With the assumption that $\beta_1 = \beta_2 = 1$, the expression for L simplifies to

$$L = k \frac{I_1 I_2}{h_{eff} \operatorname{tg} (\psi/2)} \exp\left[-\frac{1}{2}\frac{z^2}{\sigma_1^2 + \sigma_2^2}\right],$$

where:

$$k = \frac{1}{e^2 c} = 1.299427\ 10^{29}\ [A^{-2}m^{-1}s^{-1}].$$

This formula is also valid for a vertical colliding angle and a horizontal Gaussian distribution provided that the vertical variable z, h_{eff} and $\sigma_{1,2}$ are replaced by their horizontal equivalents x, w_{eff} and $\tau_{1,2}$, respectively.

This formula applies directly to the case where one of the two beams is bunched, if the interaction length is small compared with the bunch length and if the average current (Section 3.11) of the bunched beam is used.

For the ISR: the different values of ψ associated with the SFM are given in Table 10. For the nominal value of $\psi = 14.773^{o}$ and for $\beta_1 = \beta_2 = 1$, L reduces to

$$L = 1.0024\ 10^{30} \frac{I_1 I_2}{h_{eff}} \exp\left[-\frac{1}{2}\frac{z^2}{\sigma_1^2 + \sigma_2^2}\right].$$

5.5 Luminosity for two bunched beams with a non-zero colliding angle

Assuming transverse Gaussian distributions for the particles, a finite horizontal colliding angle and a bunch length which is large compared to the interaction length, the luminosity for two bunched beams is given by

$$L = E(\beta_1,\beta_2,\psi) \frac{2\pi R}{M\ell} S' \frac{I_1 I_2}{e^2 c\ \beta_1\beta_2\ h_{eff} \sin\psi} \exp\left[-\frac{1}{2}\frac{z^2}{\sigma_1^2 + \sigma_2^2}\right],$$

z is the vertical beam separation [m] ,
M is the number of bunches in the two beams,
ℓ is the full bunch length [m] .
The indices 1 and 2 are associated with beam 1 and beam 2.

The effective height h_{eff} is defined in Section 5.1 and is assumed not to vary over the interaction length. The relativistic coefficient $E(\beta_1,\beta_2,\psi)$ is given in Section 5.3.

S' is a shape factor depending on the form of the bunches (Section 3.10):

S' = 1 for rectangular bunches,
S' = 1.2 for parabolic bunches,
S' = 1.234 for Gaussian bunches,
S' = 1.333 for triangular bunches.

In the case of Gaussian bunches, the bunch length has been taken as 4 times the r.m.s. value (Section 3.10). These values of S' are true if the bunches of each beam are synchronous.

As in Section 5.4, this expression for L simplifies when $\beta_1 = \beta_2 = 1$ and remains valid for a vertical colliding angle provided that the vertical variables z, h_{eff} and $\sigma_{1,2}$ are replaced by their horizontal equivalents x, w_{eff} and $\tau_{1,2}$.

5.6 Luminosity for two coasting beams with zero colliding angle

Assuming horizontal and vertical Gaussian distributions of the particles, it is possible to calculate the luminosity for two coasting beams with zero colliding angle when the interaction length is given. Since the interaction length can be arbitrarily large, it may be important in this specific case to take into account the variations of the beam sizes over this length:

$$L = L_o \exp\left\{-\frac{1}{2}\left[\frac{z^2}{\sigma_1^2 + \sigma_2^2} + \frac{x^2}{\tau_1^2 + \tau_2^2}\right]\right\} ,$$

where:

$$L_o = (\beta_1 + \beta_2)\,\frac{I_1\, I_2}{e^2 c\, \beta_1\beta_2\, h_{eff}\, w_{eff}}\, 2\beta_{z,I}\, F\left[\operatorname{arctg}\frac{d}{2\beta_{z,I}}\,,\ \sqrt{1-\left(\frac{\beta_{z,I}}{\beta_{x,I}}\right)^2}\right]$$

$$\text{for } \beta_{x,I} \geqslant \beta_{z,I} ,$$

$$L_o = (\beta_1 + \beta_2)\,\frac{I_1\, I_2}{e^2 c\, \beta_1\beta_2\, h_{eff}\, w_{eff}}\, 2\beta_{x,I}\, F\left[\operatorname{arctg}\frac{d}{2\beta_{x,I}}\,,\ \sqrt{1-\left(\frac{\beta_{x,I}}{\beta_{z,I}}\right)^2}\right]$$

$$\text{for } \beta_{x,I} \leqslant \beta_{z,I} ,$$

$F(\phi,k)$ being the elliptic integral of the first kind[7,16].

x is the horizontal beam separation [m] ,
z is the vertical beam separation [m] ,
d is the interaction length [m] .
The indices 1 and 2 are associated with beam 1 and beam 2. $\beta_{x,I}$ and $\beta_{z,I}$ are the minima of the betatron amplitude functions, which are assumed to be at the centre of the interaction region. The effective sizes h_{eff} and w_{eff} defined in Section 5.1 are taken at these minima, and the size variation is quadratic.

If the beam sizes do not vary over the interaction length, L_o simplifies to

$$L_o = (\beta_1 + \beta_2)\,\frac{I_1\, I_2\, d}{e^2 c\, \beta_1\beta_2\, h_{eff}\, w_{eff}} .$$

The above formula directly applies to the case where one of the two beams is bunched provided the average current (Section 3.11) of the bunched beam is used.

5.7 Luminosity for two bunched beams with zero colliding angle

Assuming horizontal and vertical Gaussian distributions of the particles, the luminosity for two bunched beams with zero colliding angle is given by

$$L = (\beta_1 + \beta_2)\,\frac{\pi R}{M}\,\frac{I_1\, I_2}{e^2 c\, \beta_1\beta_2\, h_{eff}\, w_{eff}}\, \exp\left\{-\frac{1}{2}\left[\frac{z^2}{\sigma_1^2 + \sigma_2^2} + \frac{x^2}{\tau_1^2 + \tau_2^2}\right]\right\} ,$$

x is the horizontal beam separation [m] ,
z is the vertical beam separation [m] ,
M is the number of bunches.
The indices 1 and 2 are associated with beam 1 and beam 2. The effective sizes h_{eff} and w_{eff} are defined in Section 5.1 and are assumed not to vary over the interaction length, which is equal to the bunch length.

Compared with the case described in Section 5.5, this expression for L is not depending on the bunch shape and is only valid if the bunches of each beam are synchronous.

5.8 Beam-beam rate at one intersection

$$B = \sigma_m L$$

B is the beam-beam rate $[s^{-1}]$,
σ_m is the monitor constant at this intersection $[m^2]$.

5.9 Measurement of the effective sizes of the beam

For two beams colliding at a large horizontal angle, the only relevant beam size is the height as shown in Sections 5.4 and 5.5. On the contrary for colinear beams, both the height and the width are important (Sections 5.6 and 5.7). In both situations, however, the same method can be used for measuring the effective sizes of the beam, which are defined in Section 5.1. For Gaussian distributions, the effective sizes are given by integrating the beam-beam rate w.r.t. the beam separation:

$$h_{eff} = \frac{1}{\hat{B}(z=0)} \int_{-\infty}^{\infty} B(z)\, dz \ ,$$

$$w_{eff} = \frac{1}{\hat{B}(x=0)} \int_{-\infty}^{\infty} B(x)\, dx \ ,$$

$\hat{B}(z=0)$ is the maximum beam-beam rate appearing in z = 0 $[s^{-1}]$,
$\hat{B}(x=0)$ is the maximum beam-beam rate appearing in x = 0 $[s^{-1}]$,
B(x) is the beam-beam rate as a function of the horizontal beam separation x $[s^{-1}]$,
B(z) is the beam-beam rate as a function of the vertical beam separation z $[s^{-1}]$.

For the ISR: this method of measurement of h_{eff} is commonly used. In addition to this, there is a beam profile monitor using a sodium curtain. Measuring the full widths D_1 and D_2 [m] with this monitor at the half-maxima of the vertical beam profiles for beams 1 and 2, the effective height can be estimated from

$$h_{eff} = \sqrt{2\pi}\ \sqrt{0.191\ (D_1^2 + D_2^2) - 1.1\ 10^{-6}}\ \sqrt{\frac{\beta_{z,I}}{\beta_{z,m}}} \ .$$

The constant $1.1\ 10^{-6}$ comes from an experimental estimation of the instrument's resolution (valid for h_{eff}, D_1 and D_2 in m). $\beta_{z,m}$ is the value of β_z at the monitor position. If only one beam is measured (D_m), it is necessary to assume that both beams have roughly the same height $D_1 = D_2 = D_m$ in the above formula.

5.10 Luminosity loss due to orbit distortions for a non-zero colliding angle

Orbit distortions can appear as median plane tilts and longitudinal slopes at the intersections. If the horizontal colliding angle is different from zero, both these mechanisms reduce the luminosity for vertically aligned beams as follows:

$$\frac{\Delta L}{L} = -5.0 \frac{1}{h_{eff}^2} \left[(\tau_1 \chi_1)^2 + (\tau_2 \chi_2)^2\right],$$

$$\frac{\Delta L}{L} = -4.1 \frac{(\tau_1^2 + \tau_2^2) \cos^2 (\psi/2)}{h_{eff}^2 \sin^2 \psi} (\Phi_1 - \Phi_2)^2 ,$$

$\Delta L/L$ is the luminosity loss,

$\chi_{1,2}$ are the horizontal median plane tilts for beams 1 and 2 [rad] ,

$\Phi_{1,2}$ are the longitudinal slopes in the plane (z,s) for beams 1 and 2 [rad] ,

$\tau_{1,2}$ are given explicitly in Section 5.2 for a stacked beam [m] ,

h_{eff} is given explicitly in Section 5.1 [m] .

These formulae are still valid for a vertical colliding angle, vertical median plane tilts and longitudinal slopes in the plane (x,s) if $\tau_{1,2}$ and h_{eff} are replaced by $\sigma_{1,2}$ and w_{eff}, respectively.

For the ISR: possible values for ψ are given in Table 10.

5.11 Luminosity loss due to orbit distortions for a zero colliding angle

From the two effects mentioned in Section 5.10, only the second is important for a zero colliding angle, since the beam is generally circular in such an intersection ($\alpha_{p,x} = 0$). For vertically aligned beams, the reduction of luminosity will be

$$\frac{\Delta L}{L} = -2.6\ 10^{-3} \frac{d^2}{h_{eff}^2} (\Phi_1 - \Phi_2)^2,$$

d is the interaction length [m] ,

$\Phi_{1,2}$ are the longitudinal slopes in the plane (z,s) for beams 1 and 2 [rad] .

This formula gives the luminosity loss for longitudinal slopes in the plane (x,s) provided that h_{eff} is replaced by w_{eff}.

6. FORMULAE IN CONNECTION WITH CURRENT LOSS RATE AND STORED ENERGY[17]

6.1 Current loss due to the total luminosity

The current loss in s^{-1} is given by

$$\frac{1}{I}\frac{dI}{dt} = k\frac{\beta\, L\, N\, \sigma_{pp}}{R\, I} ,$$

with

$$k = \frac{ec}{2\pi} = 7.6446\ 10^{-12}\ [Am] ,$$

N is the number of intersections,
L is the luminosity $[\ m^{-2}s^{-1}]$,
σ_{pp} is the total proton-proton cross-section $[m^2]$.

In practical cases, the current loss is very often given in ppm min^{-1} so that the formula becomes

$$\frac{1}{I}\frac{dI}{dt} = 4.5868\ 10^{-4}\frac{\beta\, L\, N\, \sigma_{pp}}{R\, I} .$$

For the ISR: using R, N and σ_{pp} given in Table 2, the current loss is, in s^{-1},

$$\frac{1}{I}\frac{dI}{dt} = 1.6673\ \ 10^{-42}\frac{\beta\, L}{I} ,$$

and, in ppm min^{-1},

$$\frac{1}{I}\frac{dI}{dt} = 10^{-34}\frac{\beta\, L}{I} .$$

6.2 Current loss due to the nuclear scattering on the residual gas

The current loss in s^{-1} is given by

$$\frac{1}{I}\frac{dI}{dt} = c\, n_{NS}\, \sigma_{n,N} ,$$

$\sigma_{n,N}$ is the total nuclear cross-section for protons on nitrogen $[m^2]$,
n_{NS} is the equivalent density of nitrogen atoms for nuclear scattering $[m^{-3}]$.

The atom density n_{NS} is related to the N_2 equivalent nuclear scattering pressure P_{NS} [Torr] by (see Section 4.1)

$$n_{NS} = k\, N_a \frac{P_{NS}}{T} ,$$

where:

$$k\, N_a = 1.93024\ 10^{25}\ [m^{-3}\ K\ Torr^{-1}],$$

k is explicitly given in Section 4.1,
N_a is the number of atoms in the N_2 molecules, i.e. $N_a = 2$,
T is the temperature of the residual gas [K] .

The pressure P_{NS} is the pressure of nitrogen giving the same beam losses due to nuclear scattering as the actual residual gas.

For a mixture of different gases, the expression of P_{NS} is

$$P_{NS} = \frac{1}{2\sigma_{n,N}} \sum_i \left(P_i \sum_j \sigma_{n,j} \right) ,$$

i is numbering the gases in the mixture,

j is numbering the atoms in a molecule of the i^{th} gas. If there are m identical atoms B in a molecule, the summation on j should include all of them and can be replaced by $m\sigma_{n,B}$,

P_i is the pressure of the i^{th} gas [Torr] ,

$\sigma_{n,j}$ is the total nuclear cross-section for protons on the i^{th} atom [m^2] .

For the ISR: using $\sigma_{n,N}$ given in Table 9 and T = 300 K, the current loss is, in s^{-1},

$$\frac{1}{I}\frac{dI}{dt} = 7.3298\ 10^2\ P_{NS} ,$$

and, in ppm min^{-1},

$$\frac{1}{I}\frac{dI}{dt} = 4.3979\ 10^{10}\ P_{NS} .$$

The values of $\sigma_{n,j}$ at the ISR energies are given in Table 9 for different atoms. P_{NS} is computed by the ISR control computer according to the above formula. For the ISR residual-gas composition, P_{NS} is given by

$$P_{NS} = 0.37\ P_g ,$$

P_g being the gauge pressure [Torr] .

6.3 Stored energy in the beam

The total energy stored in a particle beam is given by

$$E_s = 10^4 \frac{I\ cp}{f_{rev}\ \beta} ,$$

f_{rev} is the revolution frequency [s^{-1}] (Section 3.3),

E_s is the stored energy [J] .

For the ISR: β is given in Table 5 for the standard energies and the value of the revolution frequency f_{rev}^{ℓ} for particles travelling at the speed of light is given in Table 2.

7. FORMULAE IN CONNECTION WITH BEAM BLOW-UP BY SCATTERING AND BEAM DAMPING BY STOCHASTIC COOLING[17,18,19,20,21,22]

Symbols frequently used in this chapter

σ_y r.m.s. value of the radial or vertical beam dimension [m]

w stack width [m]

E_y transverse emittance as defined in Section 1.4 [m rad]

$\bar{\alpha}_{p,x}$ average value of the horizontal momentum compaction as defined in Section 1.1 [m]

E_o rest energy of proton [GeV]

E_e rest energy of electron [GeV]

7.1 Multiple scattering effect on transverse beam dimensions

The rate of fractional r.m.s. beam dimension increase $[s^{-1}]$ due to multiple scattering in the residual gas is given by

$$\frac{1}{\sigma_y}\frac{d\sigma_y}{dt} = k\frac{\bar{\beta}_y}{p^2 E_y} n_{MS} ,$$

where:

$$k = 4\pi^2\left(\frac{E_e}{c}\right)^2 r_e^2 \, c \, G_N = 1.08543\ 10^{-23}\ [(GeV/c)^2\ m^3 s^{-1}],$$

and

$$\sigma_y = \frac{1}{2}\sqrt{\frac{E_y \beta_y}{\pi}} .$$

G_N is the absolute gas factor for the nitrogen atom (Table 1). This factor is given for any atom j by

$$G_j = Z_j^2 \ln\left[\frac{3.836\ 10^4}{(A_j Z_j)^{1/3}}\right] ,$$

Z_j is the charge of the atom j (Z = 7 for N),
A_j is the atomic number of the atom j (A = 14 for N),
n_{MS} is the equivalent density of nitrogen atoms for multiple scattering $[m^{-3}]$.

The atom density n_{MS} is related to the N_2 equivalent multiple scattering pressure P_{MS} [Torr] by (see Section 4.1)

$$n_{MS} = k N_a \frac{P_{MS}}{T} ,$$

where:

$$k N_a = 1.93024\ 10^{25}\ [m^{-3}\ K\ Torr^{-1}] ,$$

k is explicitly given in Section 4.1,
N_a is the number of atoms in the N_2 molecules, i.e. $N_a = 2$,
T is the temperature of the residual gas [K] .

The pressure P_{MS} is the pressure of nitrogen giving the same multiple scattering effect as the actual residual gas. For a mixture of different gases, the expression of P_{MS} is

$$P_{MS} = \frac{1}{2G_N} \sum_i \left(P_i \sum_j G_j \right) ,$$

i is numbering the gases in the mixture,

j is numbering the atoms in a molecule of the i^{th} gas. If there are m identical atoms B in a molecule, the summation on j should include all of them and can be replaced by mG_B,

P_i is the pressure of the i^{th} gas [Torr] ,

G_j is the absolute gas factor for the j^{th} atom. The values of G_j are given in Table 1 for different atoms.

Particle losses on an aperture limit can be calculated knowing the rate of change of the standard deviations of the particle distributions and knowing the form of these distributions. Frequently, a Gaussian distribution is chosen for the vertical plane and a rectangular distribution with Gaussian tails is chosen for the horizontal plane.

Note : For two vertically centred beams with the same Gaussian vertical distribution and colliding vertically at zero angle, the effective height is related to the emittance by

$$h_{eff} = \sqrt{E_z \, \beta_{z,I}} \quad .$$

For the ISR: using the relation between n_{MS} and P_{MS} with T = 300 K, the rate of fractional standard deviation increase $[s^{-1}]$ is

$$\frac{1}{\sigma_y} \frac{d\sigma_y}{dt} = 0.698380 \frac{\bar{\beta}_y}{p^2 \, E_y} P_{MS} \quad .$$

Table 2 gives the normalized emittance values. The values of $\bar{\beta}_y$ are given for different working conditions in Table 3. P_{MS} is calculated by the ISR control computer according to the above formula. For the ISR residual-gas composition, P_{MS} is given by

$$P_{MS} = 0.20 \, P_g ,$$

P_g being the gauge pressure [Torr] .

7.2 Intra-beam scattering effect on vertical beam dimension

This formula, giving the rate of vertical dimension change, takes into account the angular distribution of collision momenta inside a wide and uniform stack[18]:

$$\frac{1}{\sigma_z} \frac{d\sigma_z}{dt} = k \frac{I\beta \sqrt{\bar{\beta}_x \bar{\beta}_z}}{w p^5 \, E_z^{3/2} \sqrt{E_x}} F_1 \left(\frac{\sigma_{p,z}}{\sigma_{p,x}} , \frac{\sigma_{p,s}}{\sigma_{p,x}} \right) \ell nC \quad ,$$

where:

$$k = \frac{4\pi^2}{e} r_p^2 \left(\frac{E_o}{c} \right)^5 = 4.2201 \; 10^{-16} \; [(GeV/c)^5 \; m^2 \; A^{-1} \; s^{-1}].$$

The rate of fractional standard deviation change is given in s^{-1}.

The parameters appearing in the function F_1 and the variable C are defined as follows:

$$\frac{\sigma_{p,z}}{\sigma_{p,x}} = \frac{\bar{\sigma}_z \bar{\beta}_x}{\bar{\sigma}_x \bar{\beta}_z} = \sqrt{\frac{\bar{\beta}_x E_z}{\bar{\beta}_z E_x}}$$

$$\frac{\sigma_{p,s}}{\sigma_{p,x}} = \frac{\bar{\beta}_x}{\gamma\, \bar{\alpha}_{p,x}} \quad \text{valid for } w >> \bar{\sigma}_x$$

$$C = k_1 \frac{E_z^{3/2} p^2}{\sqrt{\bar{\beta}_z}} ,$$

with

$$\sigma_y = \frac{1}{2} \sqrt{\frac{E_y \beta_y}{\pi}} \quad \text{(see also Section 1.6)},$$

and

$$k_1 = \frac{1.36}{8\pi^{3/2} E_o^2 r_p} = 2.2597\ 10^{16} \quad [\mathrm{GeV}^{-2}\ \mathrm{m}^{-1}] .$$

The function F_1 is given in Fig. 5.

This formula contains the assumption that E_x changes only slowly with time, that the current losses remain small and that the rate of the vertical dimension change does not exceed ~0.15 h^{-1}.

The note in Section 7.1 concerning the effective height also applies here.

For the ISR: the values of $\bar{\beta}_y$ and $\bar{\alpha}_{p,x}$ are given in Table 3. The relativistic parameters are given for standard energies in Table 5 and the normalized emittance is given in Table 2.

7.3 Intra-beam scattering effect on transverse beam dimensions and momentum spread

The theory referred to in this section[19] takes into account the energy spread within the beam and the linear part of the dependence of the scattering angle on the coordinates of the betatron oscillations. It then gives not only the vertical dimension change but also the horizontal blow-up and the increase in momentum spread $[s^{-1}]$:

$$\frac{1}{\sigma_z} \frac{d\sigma_z}{dt} = \frac{A}{2} F_2(a,b,c)$$

$$\frac{1}{\sigma_x} \frac{d\sigma_x}{dt} = \frac{A}{2} \left[F_2\left(\frac{1}{i}, \frac{1}{b}, k\right) + \frac{1}{\sqrt{1 + \frac{E_x \bar{\beta}_x}{w^2}}} F_2\left(i, \frac{1}{a}, j\right) \right]$$

$$\frac{1}{\Delta p/p} \frac{d(\Delta p/p)}{dt} = nA\, F_2\left(i, \frac{1}{a}, j\right) \left[1 - \frac{1}{\sqrt{1 + \frac{E_x \bar{\beta}_x}{w^2}}} \right] ,$$

n is equal to $\frac{1}{2}$ and 1 for bunched and unbunched beams, respectively.

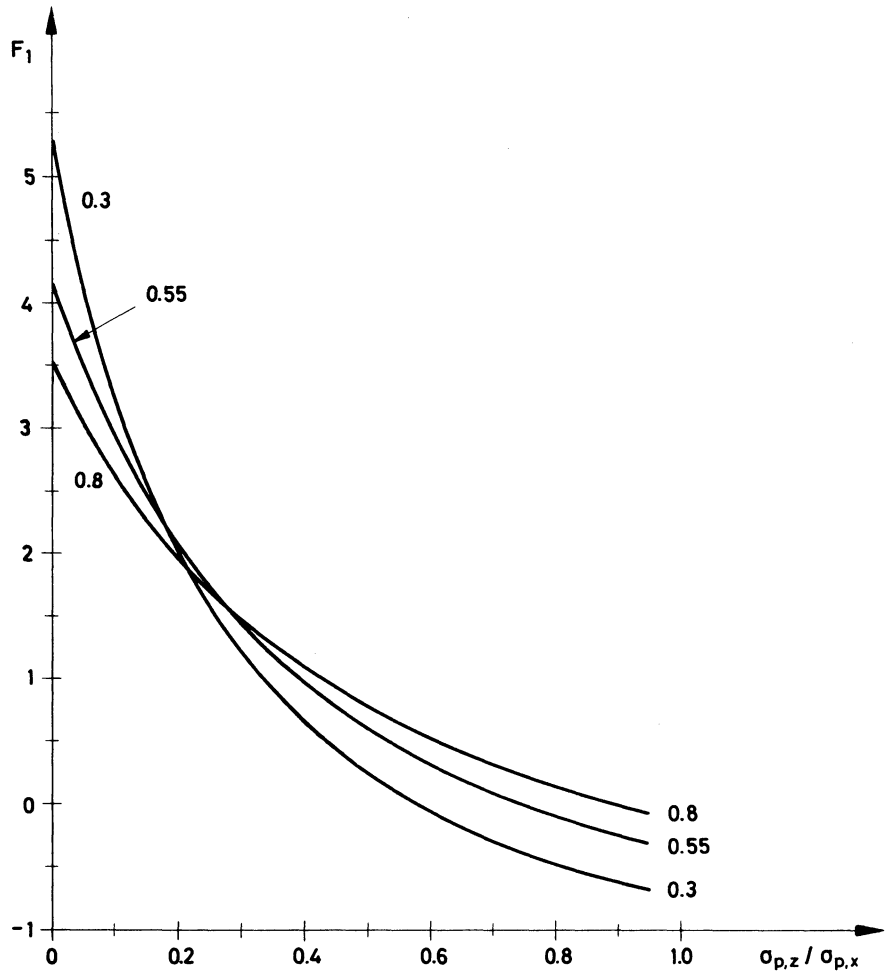

$F_1 \left(\frac{\sigma_{p,z}}{\sigma_{p,x}} , \frac{\sigma_{p,s}}{\sigma_{p,x}} \right)$ as a function of $\frac{\sigma_{p,z}}{\sigma_{p,x}}$ with $\frac{\sigma_{p,s}}{\sigma_{p,x}}$ as parameter

Fig. 5 Function F_1 for estimating the intra-beam scattering effect (formula in Section 7.2)

The parameters a, b, c, i, j and k appearing in the function F_2 and the variable A are defined as follows:

$$a = \frac{\gamma \sqrt{E_z}\, \bar{\alpha}_{p,x} \sqrt{E_x \bar{\beta}_x + w^2}}{w \sqrt{E_x \bar{\beta}_x \bar{\beta}_z}} ,$$

$$b = \sqrt{\frac{\bar{\beta}_x E_z}{\bar{\beta}_z E_x}} ,$$

$$c = \frac{k_1\, p\, E_z^{3/4}}{E_o\, \bar{\beta}_z^{1/4}} ,$$

$$i = \frac{w\,\bar{\beta}_x}{\gamma\ \bar{\alpha}_{p,x}\sqrt{E_x\bar{\beta}_x + w^2}}$$

$$j = k_1 \frac{\beta w\sqrt{E_x\bar{\beta}_x}}{\bar{\alpha}_{p,x}\sqrt{E_x\bar{\beta}_x + w^2}} (E_z\bar{\beta}_z)^{1/4} ,$$

$$k = \frac{k_1}{E_o} p \sqrt{\frac{E_x}{\bar{\beta}_x}} (E_z\bar{\beta}_z)^{1/4} ,$$

$$A = k_2 \frac{I\,\bar{\alpha}_{p,x}}{p^4\, w\, E_x E_z} ,$$

where:

$$k_1 = \frac{1}{\sqrt{2r_p}\,\pi^{3/4}} = 2.41886\ 10^8\ [m^{-1/2}] ,$$

$$k_2 = \frac{2\pi}{e} r_p^2\, E_o^4 = 7.15851\ 10^{-17}\ [m^2\ GeV^4\ A^{-1}\ s^{-1}] .$$

The function $F_2(a,b,c)$ cannot be evaluated analytically and it is necessary to use the computer calculated curves in Figs. 6 and 7. To reduce the range of numerical values for F_2, one can use the following relations:

$$F_2(a,b,c) = F_2(b,a,c)$$

$$F_2(a,b,c) + \frac{1}{a^2} F_2\left(\frac{1}{a}, \frac{b}{a}, \frac{c}{a}\right) + \frac{1}{b^2} F_2\left(\frac{1}{b}, \frac{a}{b}, \frac{c}{b}\right) = 0 .$$

The formula in Section 7.3 for the vertical dimension is not directly comparable in its algebraic form with the preceeding formula in Section 7.2, because the functions F_1 and F_2 are not defined in the same way. Nevertheless, we can say that both these formulae (7.2 and 7.3) agree within ~15 % for the vertical dimension change.

The note in Section 7.1 concerning the effective height also applies here.

It should be noted that there is a mistake of a factor of 2 in the reference paper[19] and this is the reason why we have taken the factor A/2 instead of A in the formulae of Section 7.3. The two first relations give the rate of change of the standard deviations as in Section 7.1 and the third one gives the momentum spread increase. Therefore, it is possible to calculate the losses of particles in a limited aperture provided the distributions are known.

For the ISR: the values of $\bar{\beta}_y$, $\beta_{z,I}$ and $\bar{\alpha}_{p,x}$ are given in Table 3. The relativistic parameters are given for standard energies in Table 5 and the emittance is given in Table 2.

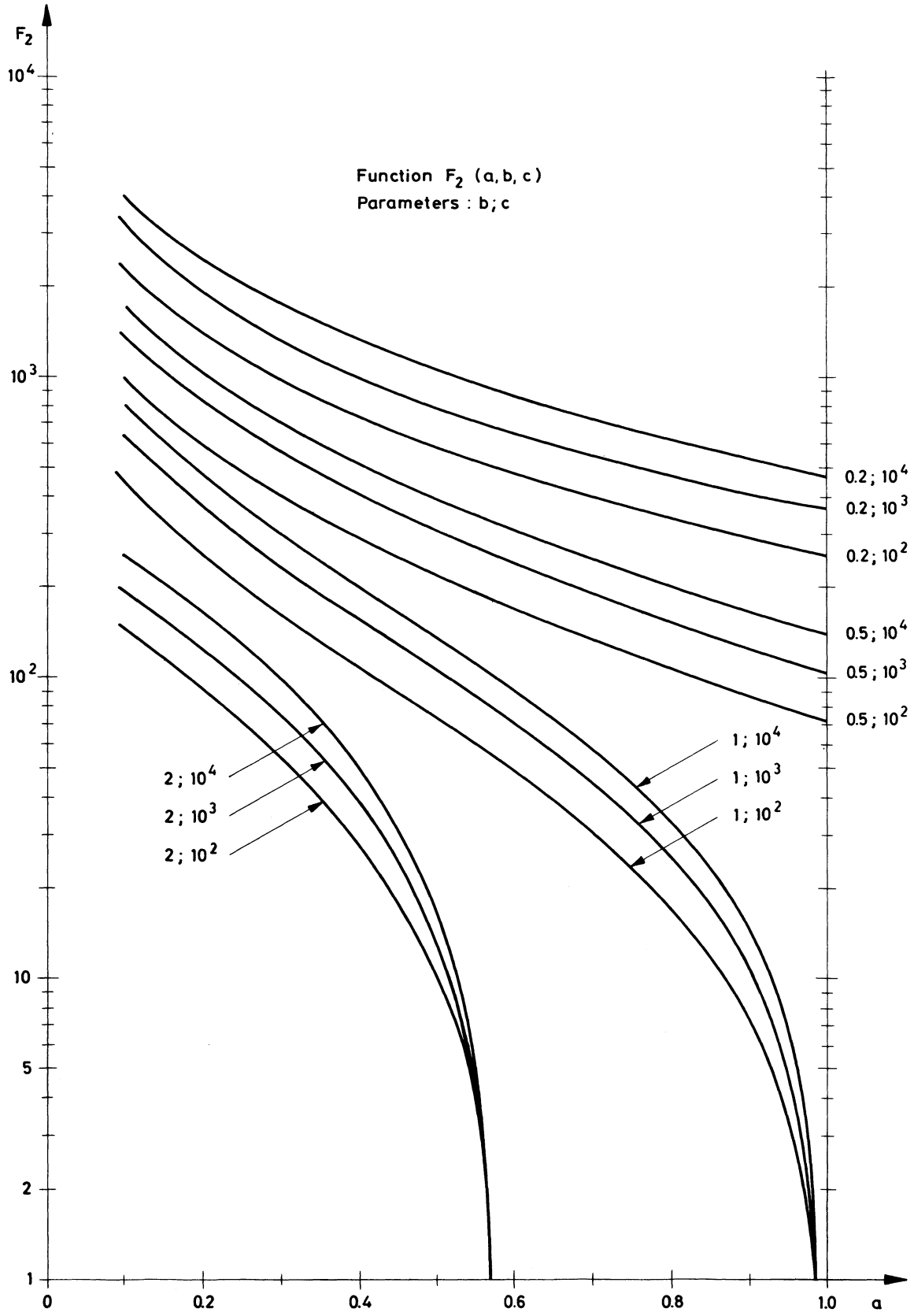

Fig. 6 Function F_2 for estimating the intra-beam scattering effect (Formula in Section 7.3)

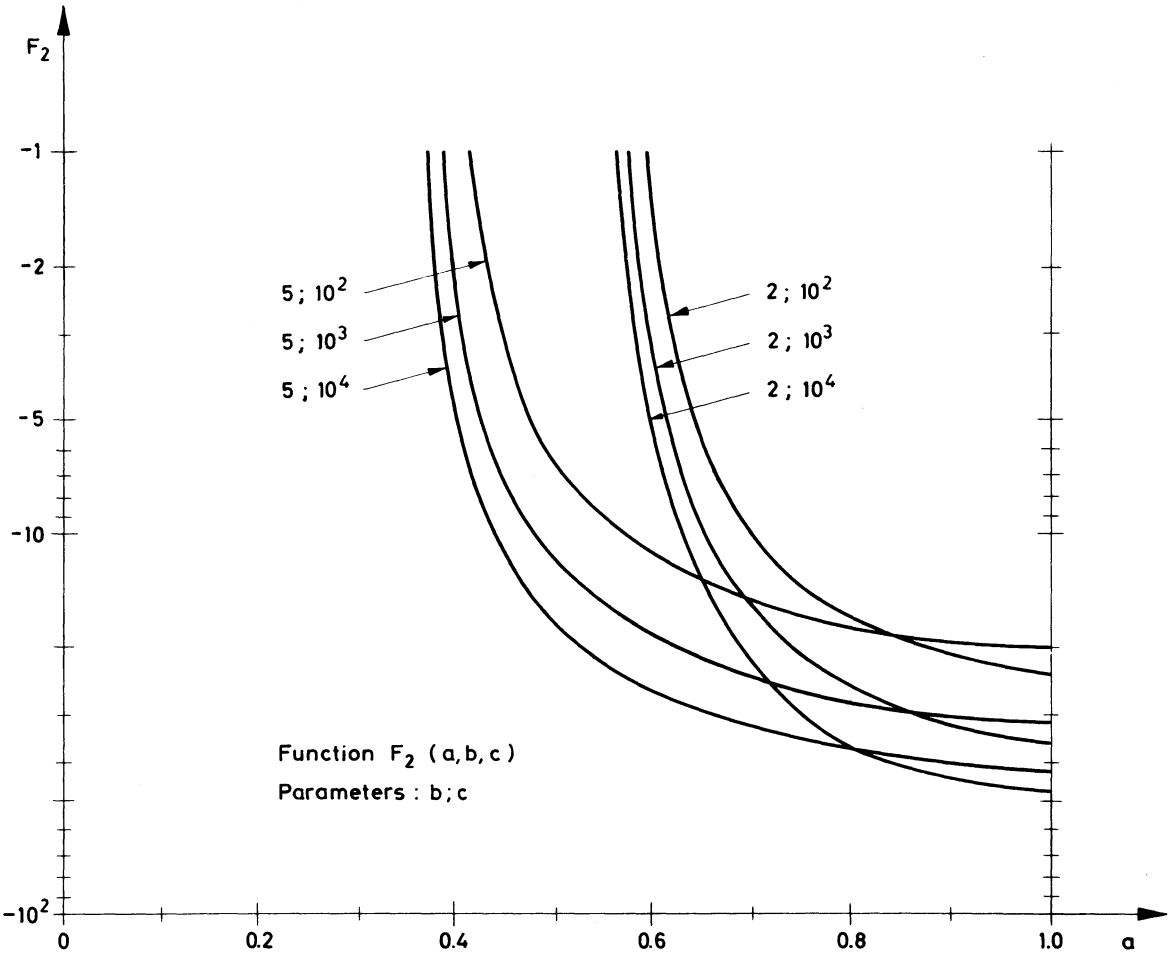

Fig. 7 Continuation of Fig. 6

7.4 Rate of stochastic cooling of momentum spread

A horizontal pick-up system is used to detect the radial position error of the centre of gravity of a short sample of particles with respect to a nominal radial position. This error is interpreted as an error in momentum with respect to the nominal momentum. A feedback system corrects a fraction g of this error further downstream as the sample passes a wide-band cavity, which accelerates or decelerates it accordingly.

The cooling rate for momentum spread is[21] $[s^{-1}]$

$$\frac{1}{\tau_p} = \frac{2W_f}{N}\left[g - \frac{g^2}{2}\left(1 + \frac{\beta_x E_x}{4\alpha_{p,x}^2 \frac{\langle\langle\Delta p^2\rangle\rangle}{p^2}} + \frac{\nu^2}{\langle\langle\Delta p^2\rangle\rangle}\right)\right]$$

where:

β_x and $\alpha_{p,x}$ are taken at the pick-up position,
W_f is the frequency bandwidth of the feedback system $[s^{-1}]$,
N is the number of particles in the ring,
g is the fraction of observed momentum error corrected per passage through the system,

Δp is the momentum deviation from the nominal value of the single particle [GeV/c],

$<\Delta p>$ is the average momentum deviation in a sample,

$<<\Delta p^2>>$ is the mean square momentum deviation over particles in many samples, i.e. over all particles in the machine,

ν is the r.m.s. electronic noise of the amplifier system, expressed at the pick-up level as a fictitious momentum error of the sample,

p is the nominal momentum [GeV/c] .

Some other interesting parameters can be defined:

i) Equivalent length of a sample [m]

$$\ell_s = \frac{c}{2}\frac{1}{W_f} \quad .$$

ii) Number of particles in a sample

$$N_s = \frac{1}{2e}\frac{I}{\beta W_f} \quad .$$

iii) Optimum gain g_o which permits the fastest cooling

$$g_o = \frac{1}{1 + \frac{\beta_x E_x}{4\alpha^2_{p,x}} \frac{<<\Delta p^2>>}{p^2} + \frac{\nu^2}{<<\Delta p^2>>}} \quad .$$

and, when the ratio of the noise power to the signal power is large

$$g_o \cong \frac{<<\Delta p^2>>}{\nu^2} \quad .$$

7.5 Fraction of error corrected in a momentum cooling system

The momentum cooling fraction g (Section 7.4) associated with an available power P [W] in the wide-band cavity is

$$g = g_o \sqrt{\frac{P}{P_{tot}}} \quad ,$$

g_o is the optimum gain (Section 7.4),

P_{tot} is the total power required for the optimum gain g_o [W]. For a large ratio of the noise power to the signal power, P_{tot} is given by

$$P_{tot} = \frac{g_o + g_o^2}{12\, N_s\, R_c} \left(\frac{c\Delta p^{tot}}{e}\right)^2 \quad ,$$

where:

N_s is the number of particles in a sample (Section 7.4),

R_c is the impedance of the wide-band cavity [Ω]

Δp^{tot} is the total momentum width of the beam for a rectangular distribution [eV/c] .

7.6 Noise to signal ratio in a momentum cooling system

The ratio of the noise power to the signal power (Section 7.4) is given by the difference signal current from the horizontal pick-up and by the electronic noise of the amplifier system

$$\frac{\nu^2}{\langle\langle \Delta p^2 \rangle\rangle} = 3 \frac{I_\nu^2}{I_{sc}^2} ,$$

I_ν is the noise current of the amplifier system [A],
I_{sc} is the signal current due to the longitudinal Schottky noise [A].

These currents are given by

$$I_{sc} = \sqrt{2e\ I\ W_f}$$

$$I_\nu = \frac{1}{R_p} \sqrt{10^{n/10}\ e\ k_B\ T\ W_f} ,$$

W_f is the frequency bandwidth of the feedback system [s^{-1}],
R_p is the impedance of the pick-up [Ω],
k_B is the constant of Boltzmann [eV K^{-1}] (Table 1),
T is the absolute temperature [K],
n is the noise figure [dB].

7.7 Horizontal betatron oscillation damping in a momentum cooling system

The momentum cooling system described in Section 7.4 can also damp the horizontal betatron oscillations. The resulting cooling rate for the radial amplitude x is[21]

$$\frac{1}{\tau_x} = \frac{W_f}{N} \left[- g_x \cos(\Delta\mu_x) - \frac{g_x^2}{2} \left(1 + \kappa_x + \frac{4\alpha_{p,x}^2(\text{P.U.}) \frac{\langle\langle \Delta p^2 \rangle\rangle}{p^2}}{\beta_x(\text{P.U.})\ E_x} \right) \right],$$

where:

$$g_x = g \frac{\alpha_{p,x}(\text{gap})}{\alpha_{p,x}(\text{P.U.})} \sqrt{\frac{\beta_x(\text{P.U.})}{\beta_x(\text{gap})}} ,$$

g, N and W_f are defined in Section 7.4, as well as $\langle\langle \Delta p^2 \rangle\rangle / p^2$,
$\Delta\mu_x$ is the horizontal phase shift from the pick-up to the cavity gap,
κ_x is the ratio of the noise power to the signal power, in which the signal current is the pick-up current due to horizontal betatron oscillations,
P.U. and gap mentioned in brackets indicate that the functions have to be taken at the pick-up and cavity positions, respectively.

The horizontal stochastic cooling is maximum if $\Delta\mu_x$ is equal to an odd number of half betatron wavelength, but appears as soon as $\cos(\Delta\mu_x) < 0$ and $g_x\ |\cos(\Delta\mu_x)|$ is larger than the second order term.

7.8 Rate of stochastic cooling of vertical betatron oscillations

A wide-band vertical difference pick-up is used to observe vertical errors of the centre of gravity of a short longitudinal sample of particles. A feedback system corrects a fraction g_z of this error further downstream as the sample passes a fast vertical kicker.

Assuming that the vertical statistical error <z> of the sample at any passage through the system is insignificantly reduced by the correction done during previous passages, the cooling rate for vertical betatron oscillations is[21] $[s^{-1}]$

$$\frac{1}{\tau_z} = \frac{W_f}{N}\left[g_z - \frac{g_z^2}{2}(1 + \kappa_z)\right] ,$$

N and W_f are defined in Section 7.4,

κ_z is the ratio of the white noise power to the signal power, in which the signal current is the pick-up current due to vertical betatron oscillations,

g_z is the fraction of observed vertical error corrected per passage through the system.

The parameters ℓ_s and N_s can be defined as in Section 7.4, but the optimum gain permitting the fastest cooling is now given by

$$g_{z,o} = \frac{1}{1 + \kappa_z} ,$$

and, when the ratio of the noise power to the signal power is large

$$g_{z,o} \cong \frac{1}{\kappa_z} .$$

7.9 Necessary power for optimum vertical cooling

It was shown in Section 7.8 that an optimum gain $g_{z,o}$ exists giving the highest cooling rate. The total power $P_{z,tot}$ [W] on the two pick-up plates required for obtaining $g_{z,o}$ is given for a large ratio of the noise power to the signal power by

$$P_{z,tot} = \frac{g_{z,o}}{8R_p N_s}\left(\frac{\sigma_z(\text{P.U.})\ \beta d\ pc}{\sqrt{\beta_z(K)\beta_z(\text{P.U.})}\ \ell e}\right)^2 ,$$

$g_{z,o}$ is given in Section 7.8,

N_s is defined in Section 7.4,

R_p is the line impedance for the plates [Ω] ,

σ_z(P.U.) is the r.m.s. value of the beam height (Section 1.6) at the pick-up [m] ,

β_z(P.U.) and β_z(K) are the vertical betatron amplitude functions at the pick-up and at the kicker, respectively [m] ,

d is the vertical spacing of the electrodes [m] ,

p is the nominal beam momentum [eV/c] ,

ℓ is the length of the vertical kicker [m] .

7.10 Noise to signal ratio in a vertical cooling system

This ratio is given by the electronic noise of the amplifier system to the difference signal current from the vertical pick-up

$$\kappa_z = 8\pi \frac{I_\nu^2}{I_{sc}^2} .$$

The currents I_ν and I_{sc} are defined in Section 7.6.

8. FORMULAE IN CONNECTION WITH TUNE SHIFTS[23,24,25,26,27,28]

Symbols frequently used in this chapter

E_o	rest energy of proton [GeV]
a	half-width of a small beam or single pulse [m]
b	half-height of a small beam or single pulse [m]
$w_{1/2}$	half-width of a large stacked beam [m]
g	half-height of a ferromagnetic gap or radius of a circular yoke [m]
h	half-height of the gap between conducting plates or of a pipe [m]
v	half-width of a conducting pipe [m]
y_1	general transverse coordinate of the centre-of-mass of the whole beam [m]
E_y	transverse component of the electrostatic field [V m^{-1}]
ε_o	permittivity of free space [As V^{-1} m^{-1}]
λ_c	line density of electrical charges [As m^{-1}]
B_f	bunching factor (Section 3.12)
η_e	neutralization factor (Section 4.8)
x	horizontal position of a particle which undergoes a given tune shift w.r.t. the centre of the perturbing beam [m]

8.1 Incoherent tune shift due to direct space charge effects

The tune shift considered here is that due to direct space charge fields of a single beam and experienced by a particle sitting in the beam itself

$$\Delta Q_y^{dir} = - k \frac{R\, I\, \bar{\beta}_y}{\beta^3\, \gamma\, B_f} \left(\frac{1}{\gamma^2} - \eta_e \right) \frac{\varepsilon_{o,y}}{b^2} ,$$

where:

$$k = \frac{2r_p}{ec} = 6.39062\ 10^{-8}\ [A^{-1}] .$$

In the case of a bunched beam, this expression gives the maximum incoherent tune shift due to direct space charge effects, experienced by the particles set at the bunch centre.

The geometric coefficient $\varepsilon_{o,y}$ associated with direct space charge fields is defined by

$$\varepsilon_{o,y} = \frac{\pi \varepsilon_o b^2}{2\lambda_c} \frac{\partial E_y}{\partial y} ,$$

E_y is the electrostatic field component due to the beam itself [V m^{-1}],
λ_c is the line density of charges [As m^{-1}] related to the averaged current I in a pulse via (Section 3.11)

$$\lambda_c = \frac{I}{\beta c} .$$

For the ISR: this formula applies either to a single pulse for which B_f is of the order of 0.1 or to a stacked beam where $B_f = 1$. If the neutralization is negligible (bunched beam), the change of the betatron frequency due to direct space charge effects is rather small, since it is proportional to $1/\gamma^3$. For large neutralization, the direct space charge effect can become of the same order of magnitude as the indirect effect (Section 8.2).

8.2 Tune shifts due to indirect space charge effects

The tune shifts considered here are those due to the presence of material boundaries around the beam excluding the direct space charge fields. It has become customary to separate the expressions for the tune shift associated with the oscillation of one single particle sitting in the perturbing beam and for the tune shifts associated with the oscillation of the whole beam. The first one is the so-called incoherent tune shift and the second one the coherent tune shift.

The incoherent tune shift (affecting, for instance, the oscillation frequency of a particle inside a stack) is

$$\Delta Q_y^{inc} = -k \frac{RI}{\beta\gamma} \left[\sum_i \bar{\beta}_y^{(i)} C_1^{(i)} \frac{\varepsilon_{1,y}^{(i)}}{h^2} \left(1 + \frac{1}{B_f \beta^2 \gamma^2} \right) (1 - \eta_e) + \sum_i \bar{\beta}_y^{(i)} C_2^{(i)} \frac{\varepsilon_{2,y}^{(i)}}{g^2} \right] .$$

The coherent tune shift valid for penetrating alternating magnetic fields at low frequency (affecting, for instance, the closed orbits) is

$$\Delta Q_y^{coh} = -k \frac{RI}{\beta\gamma} \left[\sum_i \bar{\beta}_y^{(i)} C_1^{(i)} \frac{\xi_{1,y}^{(i)}}{h^2} \left(1 + \frac{1}{B_f \beta^2 \gamma^2} \right) (1 - \eta_e) + \sum_i \bar{\beta}_y^{(i)} C_2^{(i)} \frac{\xi_{2,y}^{(i)}}{g^2} \right] .$$

The coherent tune shift valid for non-penetrating alternating magnetic fields at high frequency (affecting, for instance, the oscillation frequency of a kicked stack) is

$$\Delta Q_y^{coh} = -k \frac{RI}{\beta\gamma} \left\{ \sum_i \bar{\beta}_y^{(i)} \frac{C_1^{(i)}}{h^2} \left[\varepsilon_{1,y}^{(i)} + \xi_{1,y}^{(i)} \frac{1}{B_f \beta^2 \gamma^2} \right] (1 - \eta_e) + \sum_i \bar{\beta}_y^{(i)} C_2^{(i)} \frac{\varepsilon_{2,y}^{(i)}}{g^2} \right\} .$$

where k is defined in Section 8.1.

In the case of a bunched beam, these expressions give the maximum tune shifts due to indirect space charge effects, experienced by the particles set at the bunch centre.

The summations apply to the different possible geometries in the material boundaries, which may appear on the circumference of the machine. In each of these three expressions, the first summation concerns the electrostatic image effects (bottom index for C, ε and ξ equal to 1) and the second summation concerns the electromagnetic image effects (bottom index for C, ε and ξ equal to 2). The interdependence between the possible geometries considered in the literature, the material and the coefficients introduced here is summarized in the table below.

Index i	Geometry	Material	Coefficients
1	parallel plates	electrostatic	$C_1^{(1)}$; $\varepsilon_{1,y}^{(1)}$; $\xi_{1,y}^{(1)}$
		ferromagnetic	$C_2^{(1)}$; $\varepsilon_{2,y}^{(1)}$; $\xi_{2,y}^{(1)}$
2	circular	electrostatic (vacuum pipe)	$C_1^{(2)}$; $\varepsilon_{1,y}^{(2)}$; $\xi_{1,y}^{(2)}$
		ferromagnetic (magnet yoke)	$C_2^{(2)}$; $\varepsilon_{2,y}^{(2)}$; $\xi_{2,y}^{(2)}$
3	elliptical	electrostatic	$C_1^{(3)}$; $\varepsilon_{1,y}^{(3)}$; $\xi_{1,y}^{(3)}$

$C_1^{(i)}$ and $C_2^{(i)}$ are the fractions of the circumference occupied by an electrostatic and a ferromagnetic material in the i^{th} geometry, respectively (see table above),

$\overline{\beta}_y^{(i)}$ is the average value of the betatron amplitude function in the fraction of the circumference defined by $C^{(i)}$ [m] .

The general definitions of the geometric coefficients $\varepsilon_{1,y}$ and $\varepsilon_{2,y}$, $\xi_{1,y}$ and $\xi_{2,y}$ associated with indirect space charge fields are

$$\varepsilon_{1,y} = \frac{\pi \varepsilon_o h^2}{\lambda_c} \left.\frac{\partial E_y}{\partial y}\right|_{y_1 = 0}$$

$$\varepsilon_{2,y} = \frac{\pi \varepsilon_o g^2 c}{\lambda_c \beta} \left.\frac{\partial B_z}{\partial y}\right|_{y_1 = 0}$$

$$\xi_{1,y} = \frac{\pi \varepsilon_o h^2}{\lambda_c} \left[\frac{\partial E_y}{\partial y} + \frac{\partial E_y}{\partial y_1}\right]_{y = y_1}$$

$$\xi_{2,y} \quad \frac{\pi \varepsilon_o g^2 c}{\lambda_c \beta} \left[\frac{\partial B_z}{\partial y} + \frac{\partial B_z}{\partial y_1}\right]_{y = y_1}$$

E_y and B_z are the electromagnetic components due to the material surrounding the beam [V m^{-1}] and [T] ,

λ_c is the line density of charges given in Section 8.1 [As m^{-1}] .

For the ISR: the incoherent tune shift is the most important one and has to be compensated in order to avoid the disturbing resonances (Chapter 10). The direct space charge contribution can be neglected, since it appears that $1/\gamma^2 = \eta_e$ in the ISR at 26 GeV/c. The incoherent horizontal tune shifts are given in Fig. 8 for off-centred beams and the image space terms have been calculated with the following values:

a	$= 0.0025$ m	$C_2^{(1)} = C_1^{(3)}$	$= 0.62$	h^{ell}	$= 0.026$ m
$\bar{\beta}_x$	$= 16.854$ m	$C_1^{(2)}$	$= 0.38$	v	$= 0.08$ m
I	$= 1$ A	B_f	$= 1$	h^{circ}	$= 0.08$ m
γ	$= 20$	g	$= 0.05$ m		

For obtaining the horizontal tune shift for other values of the parameters γ, $\bar{\beta}_x$ and I, it is sufficient to scale the curves of Fig. 8 in agreement with the formula. The ratio of the horizontal to the vertical tune shift is approximately given by

$$\frac{\Delta Q_x^{inc}}{\Delta Q_z^{inc}} = - \frac{\bar{\beta}_x}{\bar{\beta}_z} \quad .$$

For a quick estimation of the incoherent tune shifts it is also possible to use the simple empirical formulae deduced from measurements performed at the ISR:

$$\Delta Q_x^{inc} = \frac{0.04}{\gamma} I \left[1 - \frac{0.2}{w_{1/2}^2} (x - x_1)^2 \right]$$

$$\Delta Q_z^{inc} = - 1.25 \, \Delta Q_x^{inc} \quad .$$

8.3 Geometric coefficients for the tune shifts due to direct fields

This concerns the coefficient $\varepsilon_{o,y}$ introduced in Section 8.1, and two cases can be considered:

a) Line charge or single pulse of elliptic cross-section and Gaussian distribution in both dimensions:

$$\varepsilon_{o,x} = \frac{b^2}{\varepsilon^2} \left\{ \frac{b}{a} \exp\left(- \frac{2x^2}{a^2} \right) - 1 + \sqrt{2\pi} \, \frac{x}{\varepsilon} \left[\operatorname{erf}\left(\sqrt{2} \, \frac{bx}{a\varepsilon} \right) - \operatorname{erf}\left(\sqrt{2} \, \frac{x}{\varepsilon} \right) \right] \exp\left(\frac{2x^2}{\varepsilon^2} \right) \right\}$$

$$\varepsilon_{o,z} = - \varepsilon_{o,x} + \frac{b}{a} \exp\left(- \frac{2x^2}{a^2} \right),$$

where:

$\varepsilon^2 = b^2 - a^2 > 0$, a and b being 2 times the r.m.s. beam dimensions.

At the pulse centre ($x = 0$), this expression simply becomes

$$\varepsilon_{o,x} = \frac{b^2}{a(a + b)} \quad ,$$

$$\varepsilon_{o,z} = \frac{b}{a + b} \quad .$$

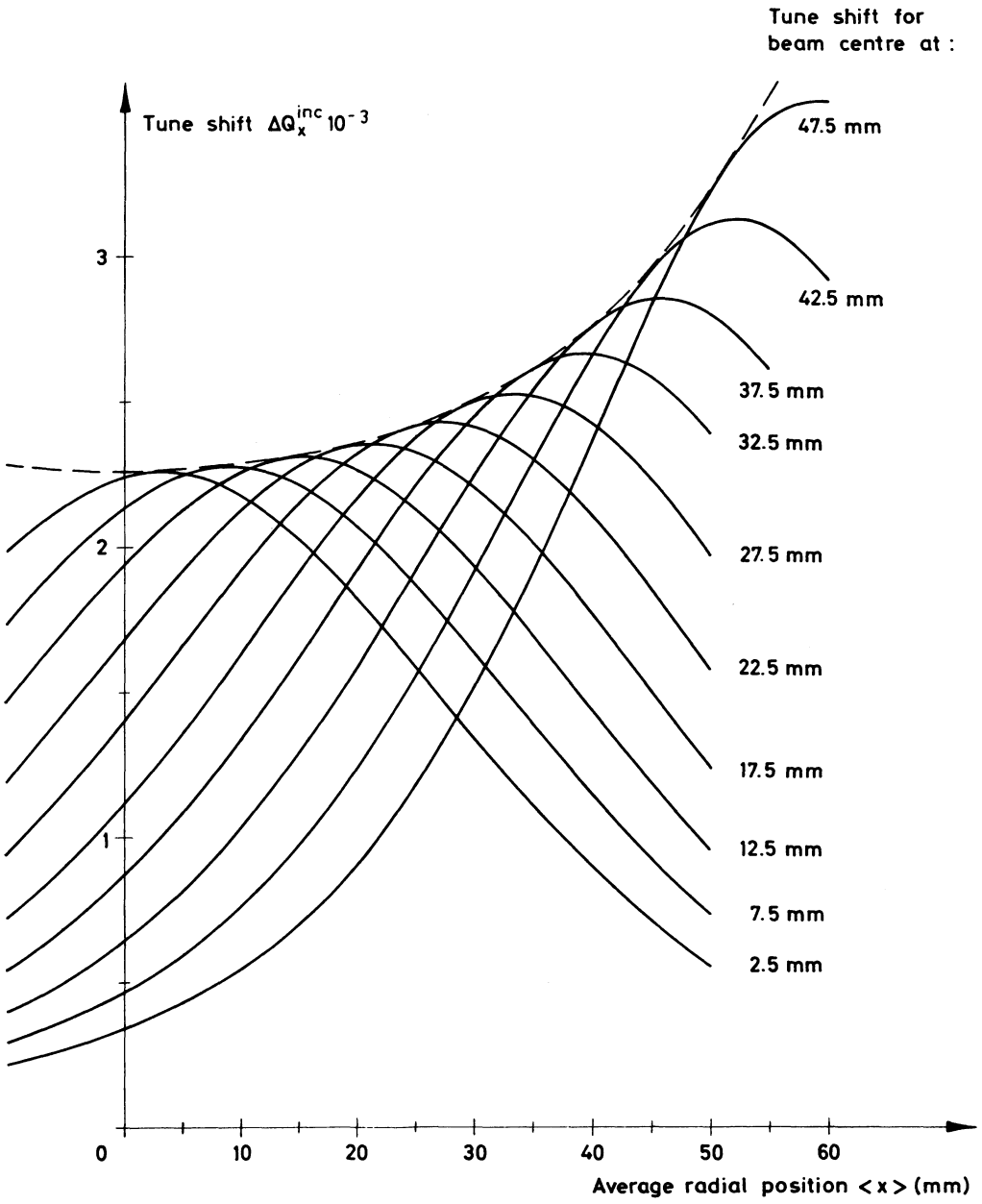

Fig. 8 Incoherent tune shifts excited by image forces in the ISR.

(Calculated for γ = 20, I = 1 A, stack width 5 mm, elliptic chamber over 62 % of ring with half-height 26 mm and half-width 80 mm, circular chamber over 38 % of ring with radius 80 mm, parallel pole pieces over 62 % of ring with half-separation 50 mm.)

b) Stacked beam with a uniform distribution and Gaussian tails in the horizontal direction and with a Gaussian profile in the vertical direction:

$$\varepsilon_{o,x} = \frac{\sqrt{\pi}}{4\sqrt{2}} \frac{b^2}{w_{1/2}\varepsilon} \left\{ \exp\left(\sqrt{2}\,\frac{x + w_{1/2}}{\varepsilon}\right)^2 \left[\operatorname{erf}\left(\sqrt{2}\,\frac{b}{\delta}\,\frac{x + w_{1/2}}{\varepsilon}\right) - \operatorname{erf}\left(\sqrt{2}\,\frac{x + w_{1/2}}{\varepsilon}\right)\right] \right.$$
$$\left. - \exp\left(\sqrt{2}\,\frac{x - w_{1/2}}{\varepsilon}\right)^2 \left[\operatorname{erf}\left(\sqrt{2}\,\frac{b}{\delta}\,\frac{x - w_{1/2}}{\varepsilon}\right) - \operatorname{erf}\left(\sqrt{2}\,\frac{x - w_{1/2}}{\varepsilon}\right)\right] \right\}$$

$$\varepsilon_{o,z} = -\varepsilon_{o,x} + \frac{\sqrt{\pi}}{4\sqrt{2}} \frac{b}{w_{1/2}} \left[\operatorname{erf}\left(\sqrt{2}\,\frac{x + w_{1/2}}{\delta}\right) - \operatorname{erf}\left(\sqrt{2}\,\frac{x - w_{1/2}}{\delta}\right)\right] ,$$

where:

$$\varepsilon^2 = b^2 - \delta^2 ,$$

δ is the width of the horizontal tails [m], i.e. twice the standard deviation of the tails, and b is twice the r.m.s. vertical beam dimension.

At the beam centre, this expression becomes

$$\varepsilon_{o,x} = \frac{\sqrt{\pi}}{2\sqrt{2}} \frac{b^2}{w_{1/2}\varepsilon} \exp\left(\sqrt{2}\,\frac{w_{1/2}}{\varepsilon}\right)^2 \left[\operatorname{erf}\left(\sqrt{2}\,\frac{b}{\delta}\,\frac{w_{1/2}}{\varepsilon}\right) - \operatorname{erf}\left(\sqrt{2}\,\frac{w_{1/2}}{\varepsilon}\right)\right]$$

$$\varepsilon_{o,z} = -\varepsilon_{o,x} + \frac{\sqrt{\pi}}{2} \operatorname{erf}\left(\sqrt{2}\,\frac{w_{1/2}}{\delta}\right) ,$$

and at the beam edge ($x = w_{1/2}$)

$$\varepsilon_{o,x} = \frac{\sqrt{\pi}}{4\sqrt{2}} \frac{b^2}{w_{1/2}\varepsilon} \exp\left(\frac{2\sqrt{2}\, w_{1/2}}{\varepsilon}\right)^2 \left[\operatorname{erf}\left(\frac{2b}{\varepsilon}\right) - \operatorname{erf}\left(\frac{2\sqrt{2}\, w_{1/2}}{\varepsilon}\right)\right]$$

$$\varepsilon_{o,z} = -\varepsilon_{o,x} + \frac{\sqrt{\pi}}{4\sqrt{2}} \frac{b}{w_{1/2}} \operatorname{erf}(2) .$$

Typical curves for $\varepsilon_{o,x}$ and $\varepsilon_{o,z}$ corresponding to stacks with $b/w_{1/2} = 7/12$ are given in Fig. 9.

8.4 Geometric coefficients for the tune shifts due to indirect fields in a geometry with horizontal parallel plates

This concerns the coefficients $\varepsilon^{(1)}_{1,y}$, $\varepsilon^{(1)}_{2,y}$, $\xi^{(1)}_{1,y}$ and $\xi^{(1)}_{2,y}$ introduced in the table of Section 8.2.

For horizontal parallel plates, two coefficients vanish and some relations between the coefficients exist

$$\xi^{(1)}_{1,x} = \xi^{(1)}_{2,x} = 0$$
$$\xi^{(1)}_{1,z} = \xi^{(1)}_{2,z}$$
$$\varepsilon^{(1)}_{1,z} = -\varepsilon^{(1)}_{1,x}$$
$$\varepsilon^{(1)}_{2,z} = -\varepsilon^{(1)}_{2,x}$$

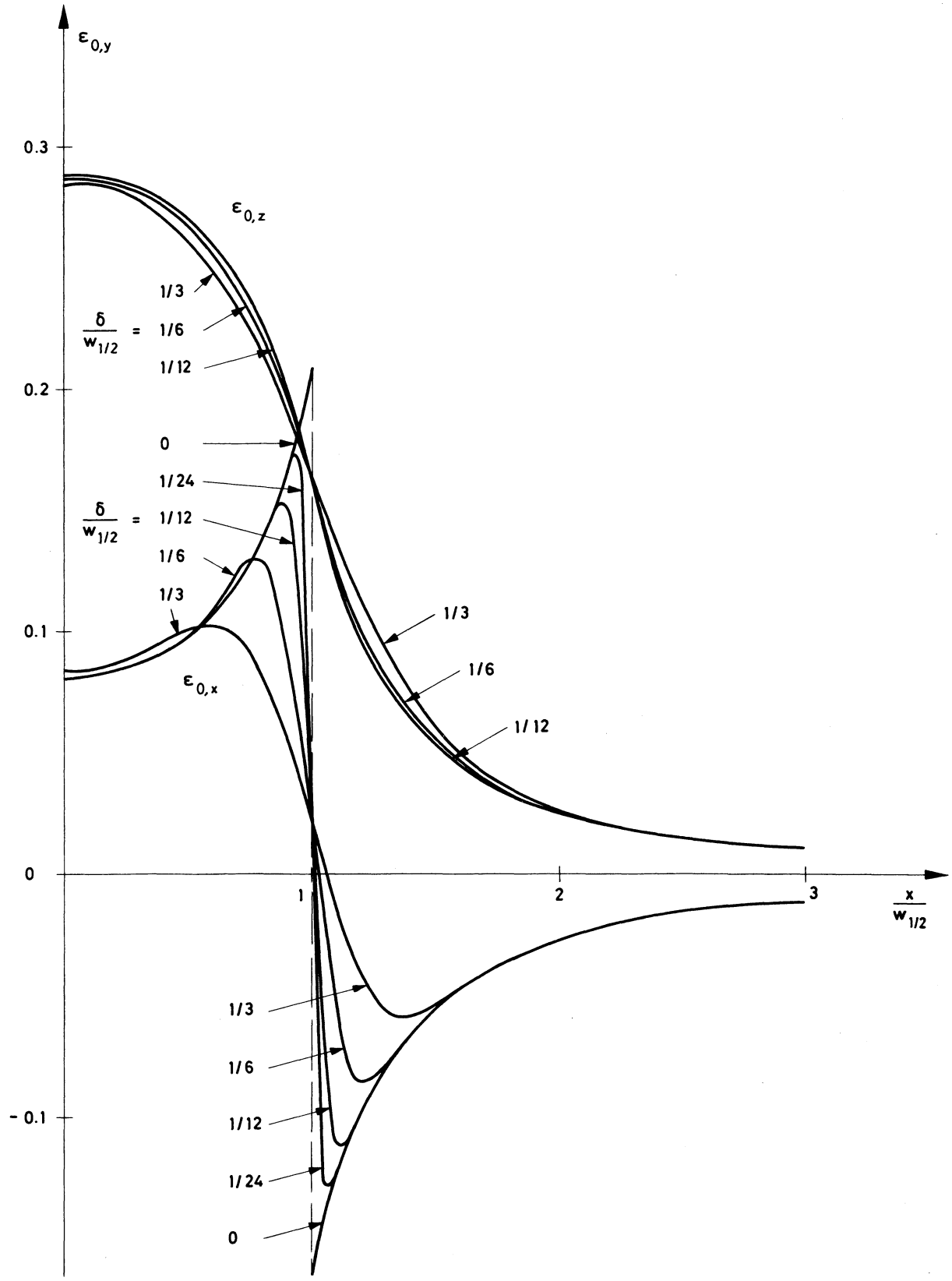

Fig. 9 Geometric coefficients for the tune shifts due to direct fields (Calculated for stacks having the following distributions: horizontal uniform ($w_{1/2}$) with tails (δ), vertical Gaussian (b), $b/w_{1/2}$ = 7/12.)

Using the parameters

$$\alpha_1 \equiv \frac{\pi}{2h} \qquad \text{and} \qquad \alpha_2 \equiv \frac{\pi}{2g} ,$$

the expressions for the three coefficients, which are independent, are given below for two different cases with the beam vertically centred ($z_1 = 0$):

a) Line-charge or single pulse at x_1:

$$\varepsilon^{(1)}_{1,z} = \frac{\pi^2}{8} \frac{\mathrm{ch}\left[\alpha_1 (x-x_1)\right]}{\mathrm{sh}^2\left[\alpha_1 (x-x_1)\right]} - \frac{h^2}{2(x-x_1)^2} ,$$

$$\varepsilon^{(1)}_{2,z} = \frac{g^2}{2(x-x_1)^2} - \frac{\pi^2}{8\ \mathrm{sh}^2\left[\alpha_2 (x-x_1)\right]} ,$$

$$\xi^{(1)}_{1,z} = \frac{\pi^2}{16\ \mathrm{ch}^2\left[\frac{1}{2}\alpha_1 (x-x_1)\right]} .$$

At the pulse location ($x = x_1$), these expressions simply become

$$\varepsilon^{(1)}_{1,z} = \frac{\pi^2}{48} ; \qquad \varepsilon^{(1)}_{2,z} = \frac{\pi^2}{24} ; \qquad \xi^{(1)}_{1,z} = \frac{\pi^2}{16} .$$

b) Flat stacked beam centred on x_1:

$$\varepsilon^{(1)}_{1,z} = \frac{\pi h}{4w_{1/2}} \frac{\mathrm{ch}\left[\alpha_1 (x-x_1)\right] \mathrm{sh}(\alpha_1 w_{1/2})}{\mathrm{sh}^2\left[\alpha_1 (x-x_1)\right] - \mathrm{sh}^2(\alpha_1 w_{1/2})} - \frac{1}{2} \frac{h^2}{(x-x_1)^2 - w^2_{1/2}} ,$$

$$\varepsilon^{(1)}_{2,z} = \frac{1}{2} \frac{g^2}{(x-x_1)^2 - w^2_{1/2}} - \frac{\pi g}{8w_{1/2}} \frac{\mathrm{sh}(2\alpha_2 w_{1/2})}{\mathrm{sh}^2\left[\alpha_2 (x-x_1)\right] - \mathrm{sh}^2(\alpha_2 w_{1/2})} ,$$

$$\xi^{(1)}_{1,z} = \frac{\pi h}{4w_{1/2}} \frac{\mathrm{sh}(\alpha_1 w_{1/2})}{\mathrm{ch}\left[\alpha_1 (x-x_1)\right] + \mathrm{ch}(\alpha_1 w_{1/2})} .$$

At the beam centre ($x = x_1$), these expressions become

$$\varepsilon^{(1)}_{1,z} = \frac{h^2}{2w^2_{1/2}} \left[1 - \frac{\alpha_1 w_{1/2}}{\mathrm{sh}(\alpha_1 w_{1/2})}\right] ,$$

$$\varepsilon^{(1)}_{2,z} = \frac{g^2}{2w^2_{1/2}} \left[\alpha_2 w_{1/2} \coth(\alpha_2 w_{1/2}) - 1\right] ,$$

$$\xi^{(1)}_{1,z} = \frac{\pi^2}{8\alpha_1 w_{1/2}} \mathrm{th}\left(\frac{\alpha_1 w_{1/2}}{2}\right) ,$$

and at the beam edges ($x = x_1 \pm w_{1/2}$)

$$\varepsilon^{(1)}_{1,z} = \frac{h^2}{8w^2_{1/2}} \left[1 - \frac{2\alpha_1 w_{1/2}}{\mathrm{sh}(2\alpha_1 w_{1/2})}\right] ,$$

$$\varepsilon^{(1)}_{2,z} = \frac{g^2}{8w^2_{1/2}} \left[2\alpha_2 w_{1/2} \coth(2\alpha_2 w_{1/2}) - 1\right] ,$$

$$\xi^{(1)}_{1,z} = \frac{\pi^2}{16\alpha_1 w_{1/2}} \mathrm{th}\ (\alpha_1 w_{1/2}) .$$

In all these expressions, h and g are the half-distances between the two conducting and ferromagnetic plates, respectively [m] .

Typical curves for $\varepsilon^{(1)}_{1,z}$ and $\varepsilon^{(1)}_{2,z}$ with different ratios $w_{1/2}/h$ and $w_{1/2}/g$ are given in Fig. 10.

For the ISR: since the main magnets are not pure dipoles but are gradient magnets, the above formulae for $\varepsilon^{(1)}_{2,z}$ do not apply exactly. However, a correction factor has been estimated[23] for a wedge-shaped gap and a single pulse:

$$\varepsilon^{(1)}_{2,z}\ (\text{wedge gap}) \;=\; \varepsilon^{(1)}_{2,z}\left[1 \pm \frac{6}{\pi}\left|\frac{gB}{G}\right| + \left(\frac{2}{3} + \frac{5}{\pi^2}\right)\left(\frac{gB}{G}\right)^2\right] \quad .$$

The negative sign applies to magnets which have a gap open towards the outside of the machine and a return yoke on the inside (so-called D-units). The positive sign applies to magnets which have a gap open towards the inside of the machine and a return yoke on the outside (so-called F-units). Since in the ISR there are en equal number of both types of magnets, the linear correction term cancels and only the quadratic correction term, which is much smaller, has to be considered.

g is the half gap [m] at the pulse position and G is the magnet gradient [Tm^{-1}]. The values of G/B = - n/ρ for the ISR are given in Table 2.

8.5 Geometric coefficients for the tune shifts due to indirect fields in a circular geometry

This concerns the coefficients $\varepsilon^{(2)}_{1,y}$, $\varepsilon^{(2)}_{2,y}$ and $\xi^{(2)}_{1,y}$ introduced in the table of Section 8.2 ($\xi^{(2)}_{2,y}$ is not given in the literature).

In this geometry, there are two relations between the coefficients:

$$\varepsilon^{(2)}_{1,z} \;=\; -\,\varepsilon^{(2)}_{1,x}$$

$$\varepsilon^{(2)}_{2,z} \;=\; \frac{\mu-1}{\mu+1}\,\varepsilon^{(2)}_{1,z}(g) \quad ,$$

μ is the constant relative permeability of a circular magnetic yoke,
$\varepsilon^{(2)}_{1,z}(g)$ means that g must replace h in the expression of $\varepsilon^{(2)}_{1,z}$.

The expressions of the three independent coefficients are given below for two different cases, the beam being vertically centred ($z_1 = 0$):

a) Line-charge or single pulse at x_1:

$$\varepsilon^{(2)}_{1,z} \;=\; -\,\frac{h^2}{2}\,\frac{x_1^2}{(h^2 - xx_1)^2} \quad ,$$

$$\xi^{(2)}_{1,z} \;=\; \frac{h^2}{2}\,\frac{h^2 - x_1^2}{(h^2 - xx_1)^2} \quad ,$$

$$\xi^{(2)}_{1,x} \;=\; \frac{h^2}{2}\,\frac{h^2 + x_1^2}{(h^2 - xx_1)^2} \quad .$$

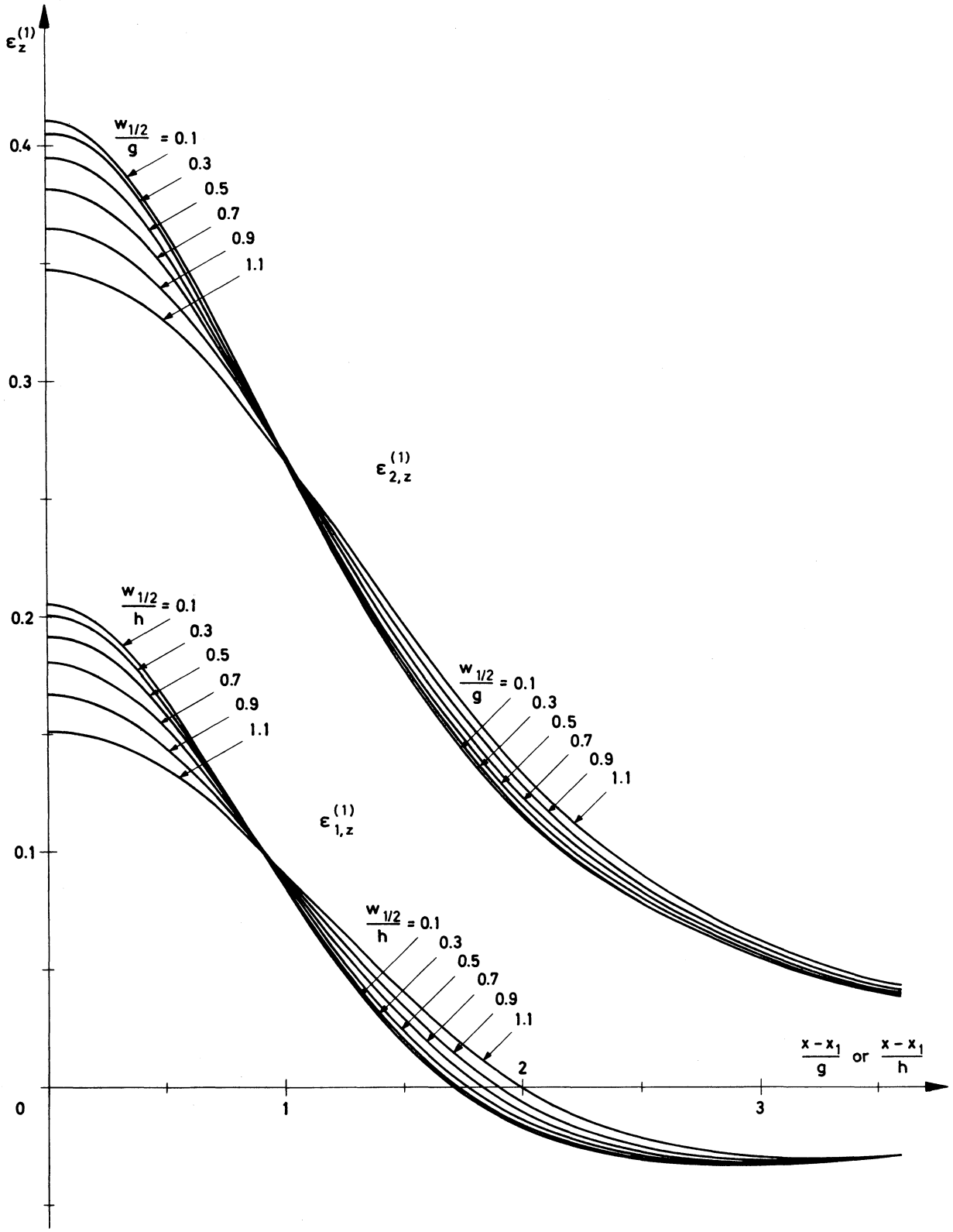

Fig. 10 Geometric coefficients $\varepsilon_{1,z}^{(1)}$ and $\varepsilon_{2,z}^{(1)}$ in a geometry with horizontal parallel plates

At the pulse location ($x = x_1$), these expressions become

$$\varepsilon^{(2)}_{1,z} = -\frac{h^2}{2}\frac{x_1^2}{(h^2 - x_1^2)^2} ,$$

$$\xi^{(2)}_{1,z} = \frac{h^2}{2}\frac{1}{h^2 - x_1^2} ,$$

$$\xi^{(2)}_{1,x} = \frac{h^2}{2}\frac{h^2 + x_1^2}{(h^2 - x_1^2)^2} ,$$

and for the pulse at the chamber centre ($x = x_1 = 0$)

$$\varepsilon^{(2)}_{1,z} = \varepsilon^{(2)}_{1,x} = 0 \; ; \quad \xi^{(2)}_{1,z} = \xi^{(2)}_{1,x} = \frac{1}{2} .$$

b) Flat stacked beam centred on x_1:

$$\varepsilon^{(2)}_{1,z} = -\frac{h^2}{2x^2}\left(1 + \frac{h^2}{C} + \frac{h^2}{w_{1/2}x}\,\ell n\, D\right) ,$$

$$\xi^{(2)}_{1,z} = -\frac{h^2}{2x^2}\left(1 + \frac{h^2 - x^2}{C} + \frac{h^2}{w_{1/2}x}\,\ell n\, D\right) ,$$

$$\xi^{(2)}_{1,x} = -\frac{h^2}{2x^2}\left(1 + \frac{h^2 + x^2}{C} + \frac{h^2}{w_{1/2}x}\,\ell n\, D\right) ,$$

where:

$$C = \frac{1}{h^2}\left[(h^2 - xx_1)^2 - w^2_{1/2}\,x^2\right] ,$$

$$D = \frac{h^2 - xx_1 - w_{1/2}\,x}{h^2 - xx_1 + w_{1/2}\,x} .$$

At the chamber centre ($x = 0$), these expressions become

$$\varepsilon^{(2)}_{1,z} = -\frac{3x_1^2 + w^2_{1/2}}{6\,h^2} ,$$

$$\xi^{(2)}_{1,z} = \frac{1}{2}\left(1 - \frac{3x_1^2 + w^2_{1/2}}{3\,h^2}\right) ,$$

$$\xi^{(2)}_{1,x} = \frac{1}{2}\left(1 + \frac{3x_1^2 + w^2_{1/2}}{3\,h^2}\right) .$$

In all these expressions, h and g are the radii of the electrostatic and ferromagnetic boundaries, respectively [m] .

The parameter $\varepsilon^{(2)}_{1,z}$ gives all the other parameters ε by virtue of the above relations. For stacks in a circular pipe, typical curves for $\varepsilon^{(2)}_{1,z}$ with different ratios $w_{1/2}/h$ and two positions of the stack ($x_1 = 0$ and $x_1 = 0.2\ h$) are given in Figs. 11 and 12.

For the ISR: the curves of Figs. 11 and 12 can directly be used when the stacked beam is either centred by decreasing the magnetic field or left at the position obtained after stacking, i.e. $x_1/h \cong 0.2$.

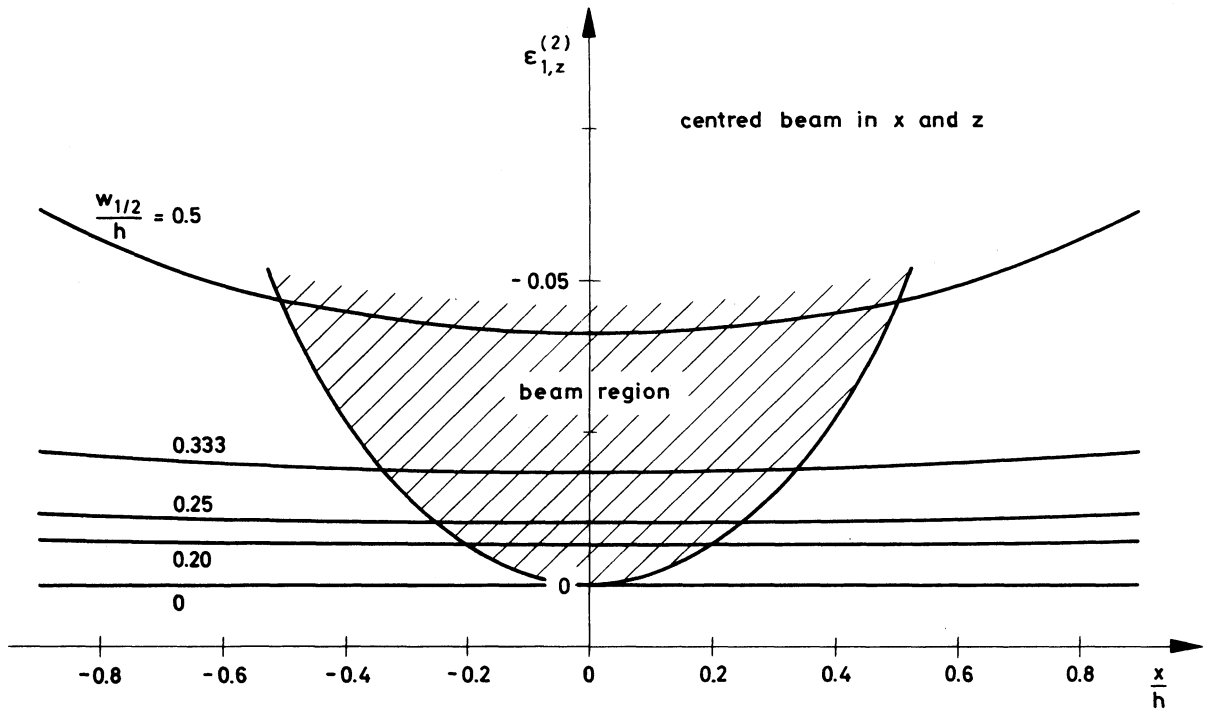

Fig. 11 Geometric coefficient $\varepsilon^{(2)}_{1,z}$ in a circular geometry for centred beams

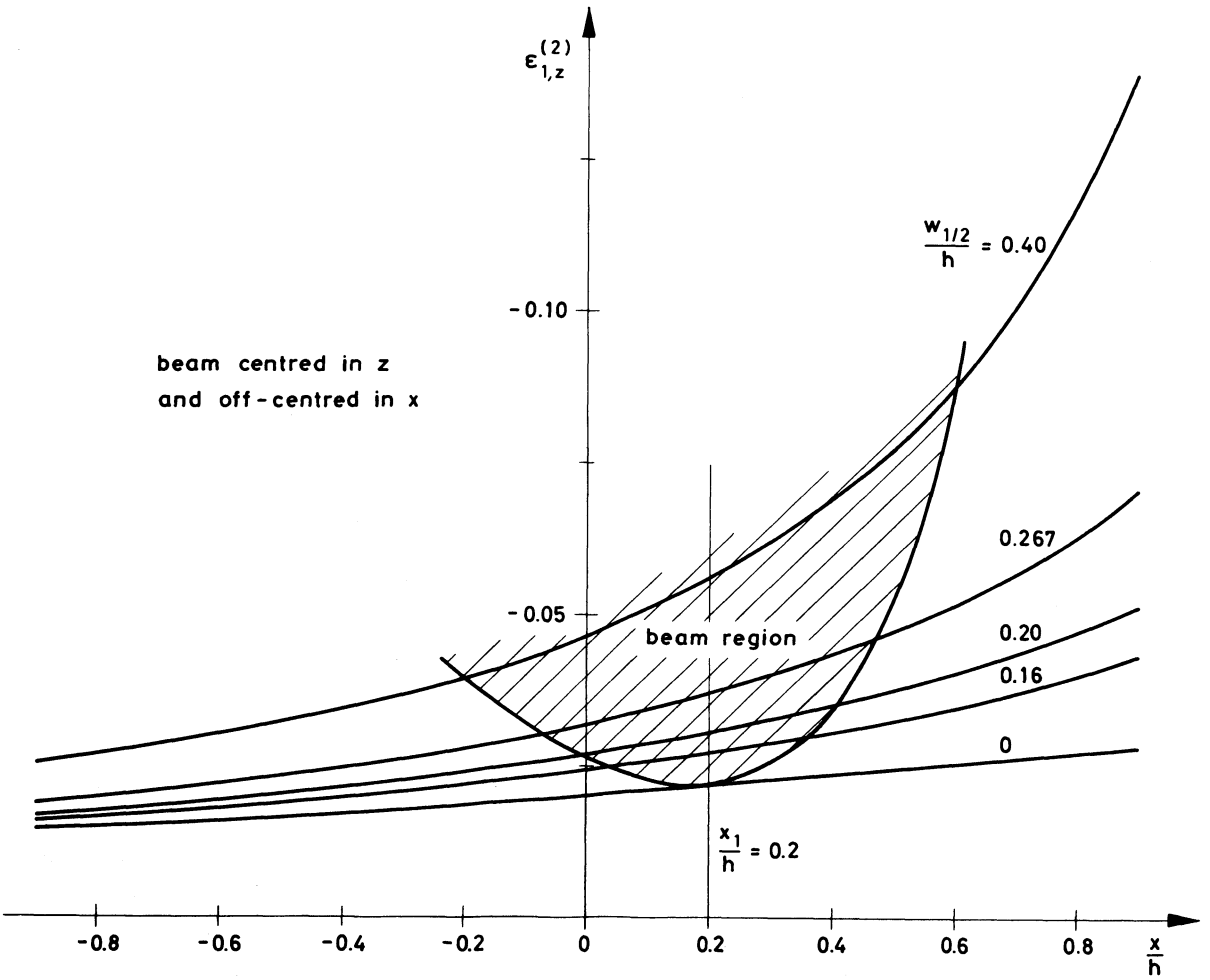

Fig. 12 Geometric coefficient $\varepsilon^{(2)}_{1,z}$ in a circular geometry for off-centred beams

8.6 Geometric coefficients for the tune shifts due to indirect fields in an elliptical geometry

This concerns the coefficients $\varepsilon^{(3)}_{1,y}$ and $\xi^{(3)}_{1,y}$ introduced in the table of Section 8.2 (a magnetic yoke of elliptical section having never been considered in the literature).

In this geometry, the following relation between the coefficients exists:

$$\varepsilon^{(3)}_{1,z} = - \varepsilon^{(3)}_{1,x} .$$

The expressions of the three remaining coefficients are very complex and are given here only for a line-charge or single pulse, at x_1 on the major axis inside focal points ($|x_1| < d$, $z_1 = 0$):

$$\varepsilon^{(3)}_{1,z} = \frac{h^2}{2}\left[\left(\frac{2K}{\pi}\right)^2 \frac{DD_1}{F^2}\,\frac{1-SS_1}{(S-S_1)^2} - \frac{2xK}{\pi F^3}\,\frac{CD_1}{S-S_1} - \frac{1}{(x-x_1)^2}\right] ,$$

$$\xi^{(3)}_{1,z} = \frac{h^2}{2}\left[\left(\frac{2K}{\pi}\right)^2 \frac{DD_1}{(S-S_1)^2}\left(\frac{1-SS_1}{F^2} - \frac{CC_1}{FF_1}\right) - \frac{2xK}{\pi F^3}\,\frac{CD_1}{S-S_1}\right] ,$$

$$\xi^{(3)}_{1,x} = \frac{h^2}{2}\left[\left(\frac{2K}{\pi}\right)^2 \frac{1}{(S-S_1)^2}\left(CC_1\,\frac{1-k^2SS_1}{FF_1} - DD_1\,\frac{1-SS_1}{F^2}\right) + \frac{2xK}{\pi F^3}\,\frac{CD_1}{S-S_1}\right] ,$$

where:

S, C and D are the Jacobian elliptic functions[7,16] sn, cn and dn of argument u (respectively u_1 for subscript 1) with

$$u_{(1)} = \frac{2K}{\pi}\,\arcsin\frac{x_{(1)}}{d} ,$$

and $d = \sqrt{v^2 - h^2}$,

K(k) is the complete elliptic integral of the first kind[7,16] and the modulus k is determined by the algebraic equation

$$q = \frac{v-h}{v+h} ,$$

where the "nome" q is defined by

$$q = \exp\,(-\pi K'/K) ,$$

K' = K(k') is the complete elliptic integral of the complementary modulus $k' = \sqrt{1-k^2}$,

F and F_1 are defined according to

$$F_{(1)} = \sqrt{d^2 - x^2_{(1)}} .$$

At the pulse location coinciding with the chamber centre ($x = x_1 = 0$), these expressions become

$$\varepsilon^{(3)}_{1,z} = \frac{h^2}{12d^2}\left[(1 + k'^2)\left(\frac{2K}{\pi}\right)^2 - 2\right] ,$$

$$\xi^{(3)}_{1,z} = \frac{h^2}{4d^2}\left[\left(\frac{2K}{\pi}\right)^2 - 1\right] ,$$

$$\xi^{(3)}_{1,x} = \frac{h^2}{4d^2}\left[1 - \left(\frac{2Kk'}{\pi}\right)^2\right] .$$

with the same definitions as above.

For stacked beams of finite width, it is not possible to integrate analytically the expressions valid for a line-charge. However, the integrals have been evaluated numerically by computer[26] for the parameter $\varepsilon^{(3)}_{1,z}$. For stacks in an elliptical pipe (v/h = 3), typical curves for $\varepsilon^{(3)}_{1,z}$ with different ratios $w_{1/2}/v$ and two positions of the stack ($x_1 = 0$ and $x_1 = 0.2\ v$) are given in Figs. 13 and 14.

For the ISR: the curves of Figs. 13 and 14 can be used directly, since the aspect ratio v/h of the elliptical chamber is very close to 3 and since the stacked beam is either centred by decreasing the magnetic field or left at the position obtained after stacking, i.e. $x_1/v \cong 0.2$.

8.7 Tune shift of a particle crossing a cylindrical coasting beam

A particle crossing with a horizontal angle ψ, an azimuthally uniform, Gaussian beam of circular cross-section undergoes a linear tune shift per intersection in the plane (y,s) of[28]

$$\Delta Q^{bb}_{y_1} = k^{bb}\,\frac{1 + \beta_1\beta_2}{\beta_1\beta_2 p_1}\,\frac{I_2\,\beta_{y,I}\,d}{\sigma^2_{y_2,I}}\,J_y\left(\zeta = \frac{d}{2\beta_{y,I}}\ ;\ \omega = \frac{\beta_{y,I}\sin\psi}{\sigma_{y_2,I}}\right) ,$$

where:

$$k^{bb} = \frac{r_p E_o}{4\pi\, e\, c^2} = 2.385611\ 10^{-9}[A^{-1}\ GeV/c] ,$$

$$J_x(\zeta,\omega) = \frac{\cos^2\psi}{\zeta\omega^2}\int_{-\zeta}^{\zeta}\frac{t^2+1}{t^2}\left\{\left(1 + \frac{\omega^2 t^2}{1 + t^2\cos^2\psi}\right)\exp\left[-\frac{1}{2}\,\frac{\omega^2 t^2}{(1 + t^2\cos^2\psi)}\right] - 1\right\} dt ,$$

$$J_z(\zeta,\omega) = \frac{1}{\zeta\omega^2}\int_{-\zeta}^{\zeta}\frac{t^2+1}{t^2}\left\{1 - \exp\left[-\frac{1}{2}\,\frac{\omega^2 t^2}{(1 + t^2\cos^2\psi)}\right]\right\} dt ,$$

Index 1 refers to the perturbed particle,

Index 2 refers to the perturbing beam,

$\beta_{y,I}$ is the minimum of the betatron amplitude function which is assumed to be at the point where the particle crosses the beam centre [m]. The variation of β_x is quadratic with the longitudinal coordinate and $\beta_x = \beta_z$ since the beam is circular. Furthermore, the functions β_y associated with the particle and with the beam are assumed to be equal,

$\sigma_{y_2,I}$ is the r.m.s. value of the beam 2 radius, taken at the point where β_y is minimum [m],

d is the interaction length [m] ,

ψ is the horizontal colliding angle [rad] ,

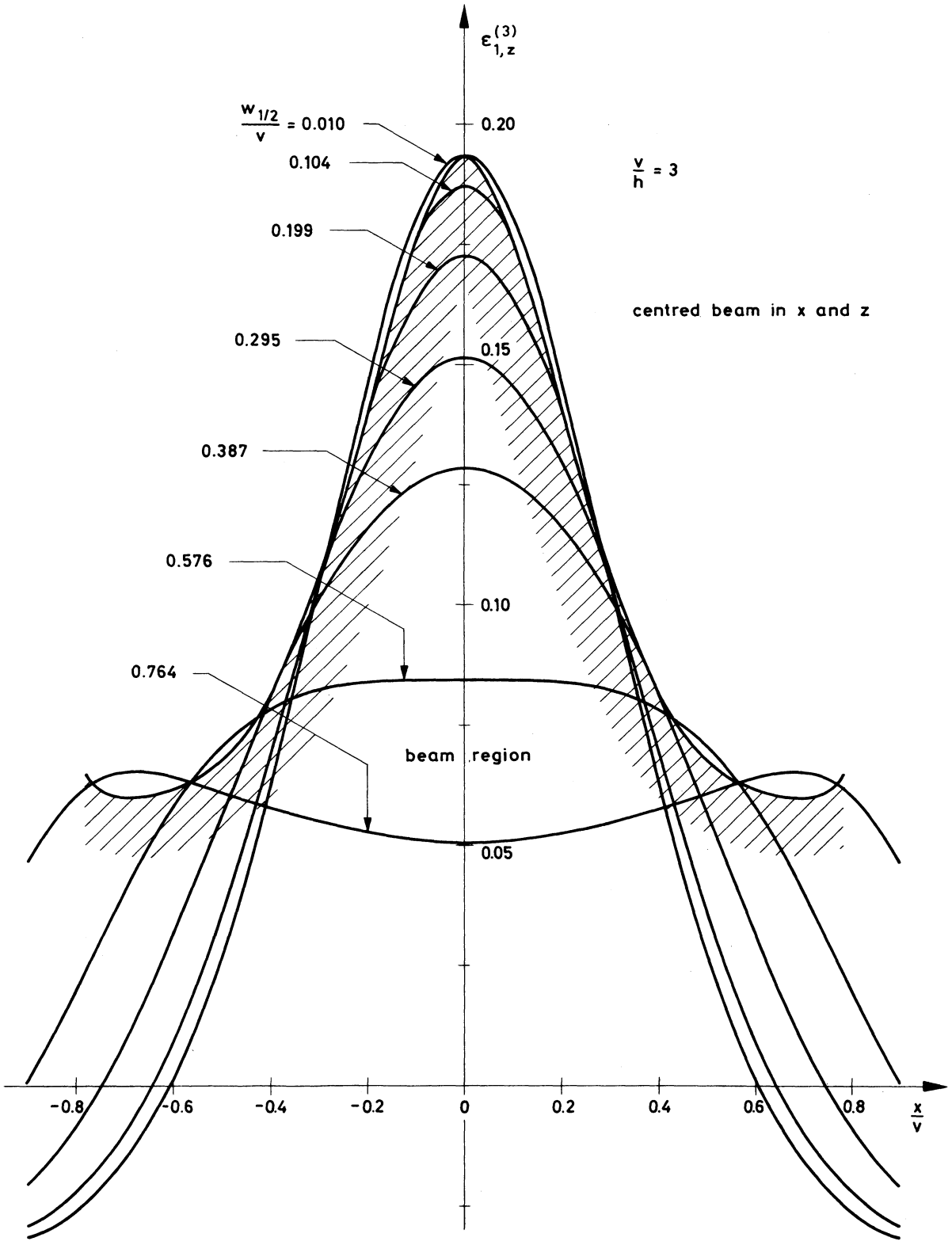

Fig. 13 Geometric coefficient $\varepsilon^{(3)}_{1,z}$ in an elliptical geometry for centred beams

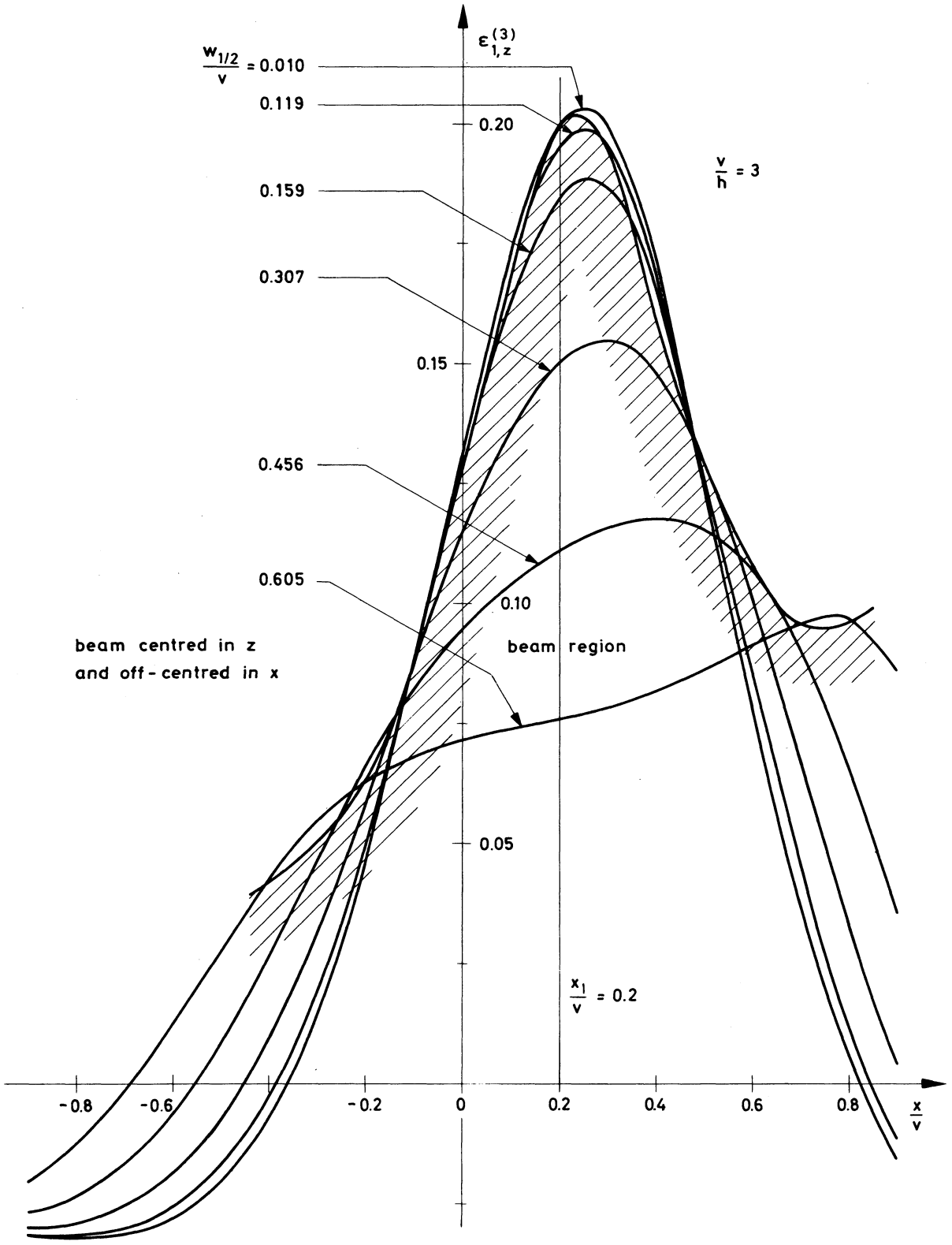

Fig. 14 Geometric coefficient $\varepsilon^{(3)}_{1,z}$ in an elliptical geometry for off-centred beams

J_x and J_z are integrals, which are given in Figs. 15 and 16 for different values of the parameters ζ and ω, and for $\cos \psi \cong 1$.

If the crossing angle is vertical, the expression for $\Delta Q_{y_1}^{bb}$ remains valid, provided that the definitions of J_x and J_z are exchanged.

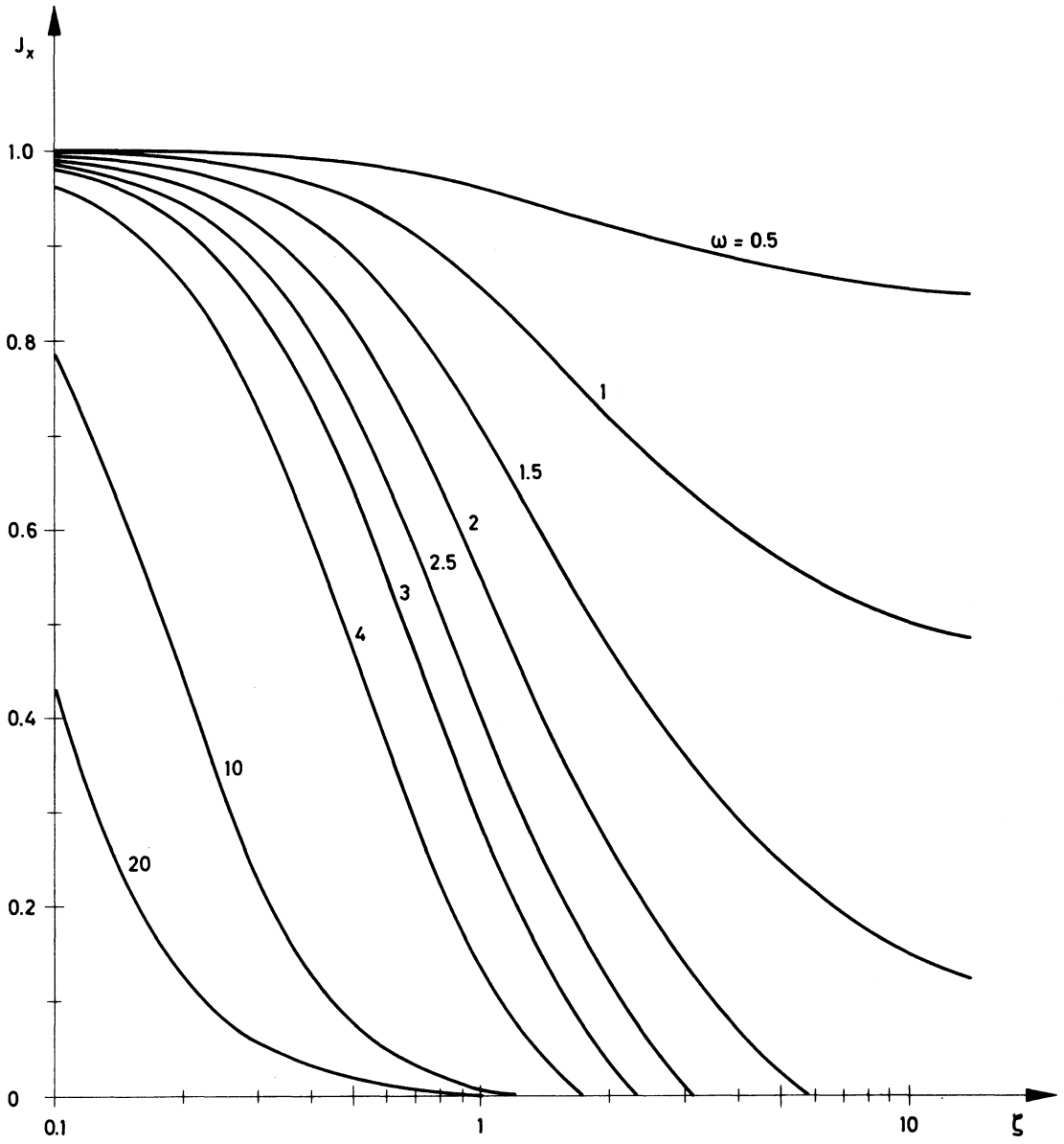

Fig. 15 Integral J_x (ζ,ω) for estimation of particle-beam tune shifts (formula in Section 8.7)

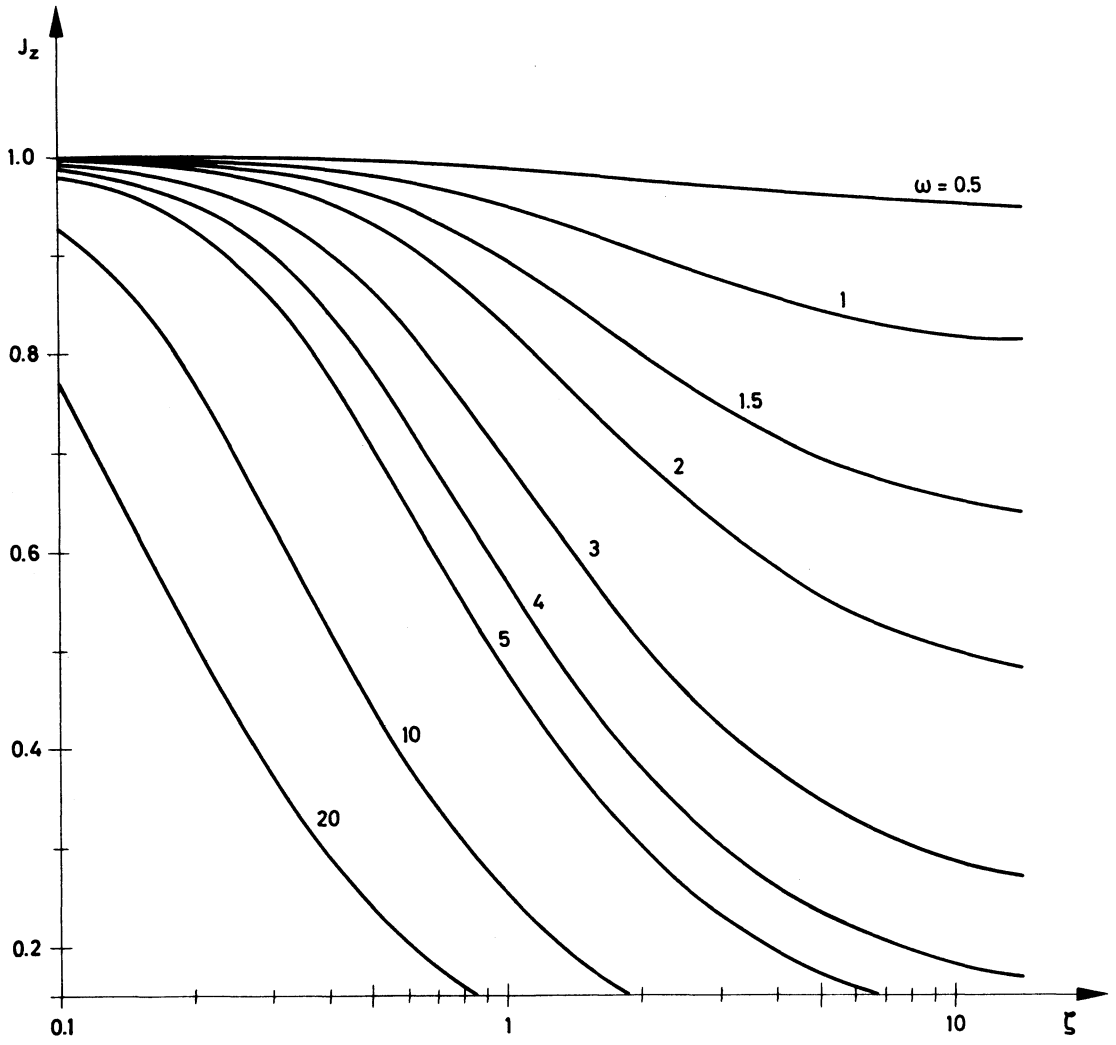

Fig. 16 Integral J_z (ζ,ω) for estimation of particle-beam tune shifts (formula in Section 8.7)

8.8 Tune shift of a particle crossing a coasting or bunched beam at zero angle

A particle crossing with zero angle a strong beam of any cross-section undergoes a linear tune shift per intersection in the plane (y,s) of

$$\Delta Q_{y_1}^{bb} = 2k^{bb} \frac{1 + \beta_1\beta_2}{\beta_1\beta_2 p_1} \int_0^d \beta_{y_1} I_2 \frac{\varepsilon_{o,y}}{\sigma_{z_2}^2} \, ds \quad ,$$

k^{bb} is given in Section 8.7, as well as the meaning of the indices 1 and 2,

d is the interaction length [m] ,

β_{y_1} is the betatron amplitude function associated with the particle inside the interaction region [m] ,

σ_{z_2} is the r.m.s. value of the beam 2 height [m] ,

$\varepsilon_{o,y}$ is the geometric coefficient for direct fields. It is explicitly given in Section 8.3 for a Gaussian pulse of elliptic cross-section and for a stacked beam of uniform distribution with tails in the horizontal direction and of Gaussian profile in the vertical direction. The variable x used in Section 8.3 represents in this case the radial distance of the particle from the strong beam centre. All the parameters a, b, x, $w_{1/2}$ and δ appearing in Section 8.3 can be functions of the coordinate s.

In the special case where the functions β_{y_1}, β_{y_2} and the radial position x of the particle are constant through the interaction region, the linear tune shift per intersection for an either coasting or bunched beam becomes

$$\Delta Q_{y_1}^{bb} = 2k^{bb} \frac{1 + \beta_1\beta_2}{\beta_1\beta_2 p_1} \frac{\beta_{y_1,I}\, I_2\, \varepsilon_{o,y}}{\sigma_{z_2,I}^2} \begin{cases} d & \text{coasting beam} \\ \dfrac{2\beta_1}{\beta_1 + \beta_2} \dfrac{\pi R}{M} & \text{bunched beam} \end{cases}$$

$\beta_{y_1,I}$ is the betatron amplitude function associated with the particle in the crossing region [m] ,

$\sigma_{z_2,I}$ is the r.m.s. value of the strong beam height in the crossing region [m] ,

M is the number of bunches in the strong beam.

For a strong bunched beam, it has been assumed that the perturbed particle was synchronous with the bunches.

If the strong beam has an elliptic cross-section and the particle remains radially centred w.r.t. the perturbing beam, the expressions given in Section 8.3.a) for x = 0 apply (with the convention a = $2\sigma_{x,I}$ and b = $2\sigma_{z,I}$) and the relation for $\Delta Q_{y_1}^{bb}$ takes the more usual form

$$\Delta Q_{y_1}^{bb} = 2k^{bb} \frac{1 + \beta_1\beta_2}{\beta_1\beta_2 p_1} \frac{\beta_{y_1,I}\, I_2}{\sigma_{y_2,I}(\sigma_{x_2,I} + \sigma_{z_2,I})} \begin{cases} d & \text{coasting beam} \\ \dfrac{2\beta_1}{\beta_1 + \beta_2} \dfrac{\pi R}{M} & \text{bunched beam} \end{cases}$$

$\sigma_{x_2,I}$ is the r.m.s. value of the strong beam width in the crossing region [m] .

8.9 Tune shift of a particle crossing a coasting beam at a large angle

For a particle crossing with a relatively large horizontal angle ψ a circular pulse of Gaussian transverse distribution, the following condition and approximation apply to the relations given in Section 8.7:

$$\omega(z) >> 1 \; ; \quad \cos\psi \approx 1 \; ,$$

$$J_z(\zeta,\omega >> 1) \cong \frac{2}{\omega^2} - \frac{2}{\zeta^2\omega^2}\left[1 - \exp\left(-\frac{1}{2}\zeta^2\omega^2\right)\right] + \frac{\sqrt{2\pi}}{\zeta\omega}\,\mathrm{erf}\left(\frac{1}{\sqrt{2}}\zeta\omega\right) ,$$

$\omega(z)$ means that ω, defined in Section 8.7, has to be taken for $y \equiv z$.

If, furthermore, the conditions $\omega(z)\,\zeta(z) >> 1$ and $\omega(z) >> \zeta(z)$ are verified, J_z tends towards

$$J_z \cong \frac{\sqrt{2\pi}}{\zeta\omega} \; ,$$

$\zeta(z)$ means that ζ, defined in Section 8.7, has to be taken for $y \equiv z$.

Using the last approximation for J_z, the linear tune shift per intersection of a particle crossing a coasting beam at a large horizontal angle is

$$\Delta Q_{x_1}^{bb} = 0 \ ,$$

$$\Delta Q_{z_1}^{bb} = 2\sqrt{2\pi}\, k^{bb} \frac{1 + \beta_1\beta_2}{\beta_1\beta_2 p_1} \frac{I_2\ \beta_{z_1,I}}{\sigma_{z_2,I}\ \sin\psi} \ ,$$

k^{bb} is given in Section 8.7 as well as the meaning of the indices 1 and 2, $\beta_{z_1,I}$ and $\sigma_{z_2,I}$ are defined in Section 8.8 and the angle ψ in Section 8.7.

For a stacked beam consisting of a radial succession of circular pulses with Gaussian transverse distribution, I_2 represents the total current and $\sigma_{z_2,I}$ is the r.m.s. value of the thin dimension of the beam.

It is interesting to note that the octupole terms in the tune shift, seen by an off-centred particle, are opposed to the linear one given above, so that the total tune shift seen by the particles of a wide beam is distributed between 0 and $\Delta Q_{z_1}^{bb}$ around an average value which is[29)]

$$\overline{\Delta Q}_{z_1,tot}^{bb} \cong 0.7\ \Delta Q_{z_1}^{bb} \ .$$

If the crossing angle ψ is vertical, the above expression of $\Delta Q_{z_1}^{bb}$ applies to $\Delta Q_{x_1}^{bb}$, provided that the parameters $\beta_{x,I}$ and $\sigma_{x,I}$ are used instead of $\beta_{z,I}$ and $\sigma_{z,I}$. $\Delta Q_{z_1}^{bb}$ becomes equal to zero.

For the ISR: the crossing plane is horizontal and the nominal angle ψ is equal to 0.2578 rad. In agreement with the above formulae, the total vertical averaged tune shift of a wide beam can be estimated from

$$\overline{\Delta Q}_{z_1,tot}^{bb} = 6.567\ 10^{-8} \frac{I_2\ \beta_{z_1,I}}{p_1\ \sigma_{z_2,I}} \ ,$$

while the horizontal tune shift is zero. The measurements made in the ISR with pulses give values of $\overline{\Delta Q}_{z_1,tot}^{bb}$ which are close to this theoretical value (remembering that the linear tune shift $\Delta Q_{z_1}^{bb}$ is $\sim$1.43 larger).

When the Split Field Magnet is set, the crossing angle ψ changes in intersection 4. The values of ψ and the orbit characteristics in intersection 4 are given in Table 10 for different field levels.

The values of $\beta_{z,I}$ are given in Table 3 and the relativistic parameters in Table 5.

8.10 Tune shift of a particle crossing a bunched beam at a large angle

The conditions and approximations given in Section 8.9 remain valid for a bunched beam, the sole difference coming from the non-uniform azimuthal distribution of the current I_2. If the perturbed particle is synchronous with the bunches of the strong beam, the expressions for the linear tune shifts per intersection can be written as follows:

$$\Delta Q_{x_1}^{bb} = 0 \quad ,$$

$$\Delta Q_{z_1}^{bb} = 2\sqrt{2\pi}\, k^{bb} \frac{1 + \beta_1\beta_2}{\beta_1\beta_2 p_1} \frac{\beta_{z_1,I}}{\sigma_{z_2,I} \sin\psi} \int_{\theta}^{\theta+(1+\frac{\beta_2}{\beta_1})\frac{w_2}{R \sin\psi}} I_{\theta,2}\, d\theta \quad ,$$

k^{bb} is given in Section 8.7 as well as the meaning of the indices 1 and 2,
$\beta_{z_1,I}$ and $\sigma_{z_1,I}$ are defined in Section 8.8 and the angle ψ in Section 8.7,
θ is the angular shift of the perturbed particle w.r.t. the bunch centre [rad],
w_2 is the total width of the strong beam [m],
$I_{\theta,2}$ is the azimuthal current distribution inside a bunch of the perturbing beam [A] (Section 3.10).

If the interaction length is small compared with the bunch length, $I_{\theta,2}$ can be taken as constant in the integration interval $\Delta\theta$, so that the integral can be replaced by $I_{\theta,2}\, \Delta\theta$, where

$$\Delta\theta = \left(1 + \frac{\beta_2}{\beta_1}\right) \frac{w_2}{R \sin\psi} \quad .$$

9. FORMULAE IN CONNECTION WITH LINEAR COUPLING[30,31,32]

Symbols frequently used in this chapter

C complex coefficient of linear coupling

Δ distance from a linear coupling resonance
($= Q_x + nQ_z - p$, n and p being integers, $n = \pm 1$)

9.1 Complex coefficients of linear coupling

For both sum and difference resonances $Q_x + nQ_z = p$, $(n = \pm 1)$, which are associated with a linear coupling of transverse betatron oscillations, a general complex coefficient can be defined:

$$C = \frac{1}{4\pi R} \int_0^{2\pi} \sqrt{\beta_x\beta_z} \left[K + \frac{1}{2} MR\left(\frac{\alpha_x}{\beta_x} - \frac{\alpha_z}{\beta_z}\right) - \frac{i}{2} MR\left(\frac{1}{\beta_x} - \frac{n}{\beta_z}\right)\right]$$
$$\exp\left\{i\left[(\mu_x - Q_x\theta) + n(\mu_z - Q_z\theta) + p\theta\right]\right\} d\theta \quad ,$$

with the following definitions:

$$K(\theta) = \frac{1}{2} \frac{R^2}{B\rho} \left(\frac{\partial B_x}{\partial x} - \frac{\partial B_z}{\partial z}\right) \quad ,$$

$$M(\theta) = \frac{R}{B\rho} B_\theta \quad ,$$

$$n = \pm 1 \text{ (depending on the resonance)},$$

α_y is the Twiss parameter (Section 1.1),

μ_y is the phase of the betatron oscillation (Section 1.1),

$\theta = s/R$ is the azimuthal angle (Fig. 1),

$\partial B_y/\partial y$ is the skew gradient in the horizontal or vertical direction $[Tm^{-1}]$.

For the ISR: using the above formula and taking, for example, the value of α_y, β_y, μ_y and Q_y for the 8C working line, it is possible to estimate the effect on the coupling due to random main magnet tilts

$$|C| = 10\ \phi_{r.m.s.} ,$$

$\phi_{r.m.s.}$ is the root mean square value of the distributed tilts [rad] .

9.2 Fraction of energy interchanged in a kicked beam

The energy associated with betatron oscillations in a transverse plane is defined here as a square of the amplitude of the oscillation envelope. For the difference resonance $Q_x - Q_z = p$, there is an interchange of energy between horizontal and vertical oscillations following a kick in a transverse plane and the fraction of interchanged energy is

$$F = \frac{|C|^2}{\Delta^2 + |C|^2} ,$$

where $|C|$ indicates the modulus of C.

9.3 Parameters of the coherent oscillations of a kicked beam

When close to the difference resonance $Q_x - Q_z = p$, the coupling provokes a modulation of the amplitude of the oscillations in the same plane as an angular kick is given.

$$S = \frac{|\Delta|}{\sqrt{\Delta^2 + |C|^2}} ,$$

$$T = \frac{1}{f_{rev}\sqrt{\Delta^2 + |C|^2}} ,$$

S is the ratio of the minimum to the maximum of the amplitude modulation,

T is the period of the modulation [s] ,

f_{rev} is the revolution frequency $[s^{-1}]$ (Section 3.3).

The above formulae provide a simple method for measuring $|C|$ and $|\Delta|$ (see also Section 9.5).

For the ISR: f_{rev} is given in Table 2.

9.4 Time shift of the coherent oscillations of a kicked beam

When kicking a pulse at an angle $dz/dx = \sqrt{\beta_x/\beta_z}$ while being close to the resonance $Q_x - Q_z = p$, the amplitude modulation observed in the horizontal or vertical direction is shifted, compared with the modulation following a simple horizontal or vertical kick.

$$\delta_t = \frac{T}{2\pi}\ \mathrm{arctg}\ \frac{\sqrt{\Delta^2 + |C|^2}\ (\mathrm{Im}.C)}{\Delta\ (\mathrm{Re}.C)} ,$$

(Im.C) and (Re.C) are the imaginary and real parts of C (Section 9.1),

T is given in Section 9.3,

δ_t is the time shift of the amplitude modulation [s] .

9.5 Measurement of the coupling coefficient

By combining the formulae of Sections 9.3 and 9.4, $|\Delta|$, Re.C, Im.C and $|C|$ can be expressed in terms of measurable quantities

$$\left.\begin{aligned} |\Delta| &= \frac{S}{T\, f_{rev}} \\ |C| &= \frac{1}{T\, f_{rev}} \sqrt{1 - S^2} \end{aligned}\right\} \text{ kicking in a transverse plane,}$$

$$\frac{\text{Im.C}}{\text{Re.C}} = \frac{S\Delta}{|\Delta|} \operatorname{tg}\left(2\pi \frac{\delta_t}{T}\right) \quad \text{kicking at an angle } dz/dx = \sqrt{\beta_x/\beta_z}.$$

S, T and f_{rev} are defined in Section 9.3 and δ_t is defined in Section 9.4

9.6 Changes in beam dimensions due to linear coupling

Averaging on time the modulation of the amplitude of the betatron oscillations due to linear coupling with n = -1 (Section 9.1) gives the apparent beam sizes. Without shaving, the sizes are[32)]

$$\frac{\sigma_x}{\sigma_{x,o}} = \sqrt{\frac{\beta_x}{\beta_{x,o}}} \sqrt{1 + \frac{1}{2}\left[\left(\frac{\sigma_{z,o}}{\sigma_{x,o}}\right)^2 - 1\right] \frac{|C|^2}{\Delta^2 + |C|^2}} \ ,$$

$$\frac{\sigma_z}{\sigma_{z,o}} = \sqrt{\frac{\beta_z}{\beta_{z,o}}} \sqrt{1 + \frac{1}{2}\left[\left(\frac{\sigma_{x,o}}{\sigma_{z,o}}\right)^2 - 1\right] \frac{|C|^2}{\Delta^2 + |C|^2}} \ ,$$

σ_x and σ_z are the r.m.s. values of the horizontal and vertical distributions of the amplitudes, respectively, at the azimuthal position θ [m] ,

β_x and β_z are the betatron amplitude functions at θ [m] ,

$\sigma_{x,o}$ and $\sigma_{z,o}$ are the initial values of σ_x and σ_z at the position θ_o [m] ,

$\beta_{x,o}$ and $\beta_{z,o}$ are the initial values of β_x and β_z at θ_o [m] ,

C is explicitly given in Section 9.1.

Considering a vertical shaving of the beam, the remaining particles are initially in a 4-dimensional phase space volume, which is given by

$$v_o^2 + v_o^{*2} + (A + \sqrt{A^2 + B^2}) \leq \frac{z_s^2}{\beta_{z,s}} \ ,$$

where:

$$A = \frac{|C|^2}{2\eta_c^2}(u_o^2 + u_o^{*2} - v_o^2 - v_o^{*2}) - \frac{(\text{Re.C})\Delta}{\eta_c^2}(u_o v_o + u_o^* v_o^*) + \frac{(\text{Im.C})\Delta}{\eta_c^2}(u_o v_o^* - u_o^* v_o),$$

$$B = -\frac{(\text{Im.C})}{\eta_c}(u_o v_o + u_o^* v_o^*) - \frac{(\text{Re.C})}{\eta_c}(u_o v_o^* - u_o^* v_o) \ ,$$

with

$$u_o = \frac{x_o}{\sqrt{\beta_{x,o}}} ,$$

$$v_o = \frac{z_o}{\sqrt{\beta_{z,o}}} ,$$

$$u_o^* = \frac{\beta_{x,o}\, x_o' + \alpha_{x,o}\, x_o}{\sqrt{\beta_{x,o}}} ,$$

$$v_o^* = \frac{\beta_{z,o}\, z_o' + \alpha_{z,o}\, z_o}{\sqrt{\beta_{z,o}}} ,$$

$$\eta_c = \sqrt{\Delta^2 + |C|^2} ,$$

(Re.C) and (Im.C) are the real and imaginary parts of C (Section 9.1),
x_o, x_o', z_o and z_o' are the initial coordinates of the particles,
z_s is the position of the scraper blade [m],
$\beta_{z,s}$ is the betatron amplitude function at the scraper [m],
$\alpha_{x,o}$ and $\alpha_{z,o}$ are the initial values of α_x and α_z at θ_o.

Averaging on time the amplitude of the oscillations inside the phase-space volume defined above gives the change of the vertical beam size as a function of the shaver position or of the fraction of particles left. Typical curves giving the remaining fraction of a shaved beam $F_{s,z}$ as a function of the ratio of the final to the initial beam height $\sigma_z/\sigma_{z,o}$ are represented in Figs. 17 and 18 for different emittance ratios and different values of F (Section 9.2). These results can be used for horizontally shaved beams, provided the corresponding variables are used.

10. FORMULAE IN CONNECTION WITH SUM AND DIFFERENCE RESONANCES[5,30,33,34,35,36]

Symbols frequently used in this chapter

α_y	Twiss parameter (Section 1.1)
μ_y	phase of betatron oscillation (Section 1.1)
E_{y_o}	initial transverse emittances associated with one particle and assumed different from zero [m rad]
n_x, n_z	integers defining the resonance of interest
N	order of the resonance: $N = \|n_x\| + \|n_z\|$
$g_y = \sqrt{E_y/E_{y_o}}$	amplitude growth in a resonance
e	distance from the resonance
$B\rho$	magnetic rigidity [Tm] (Section 2.1)

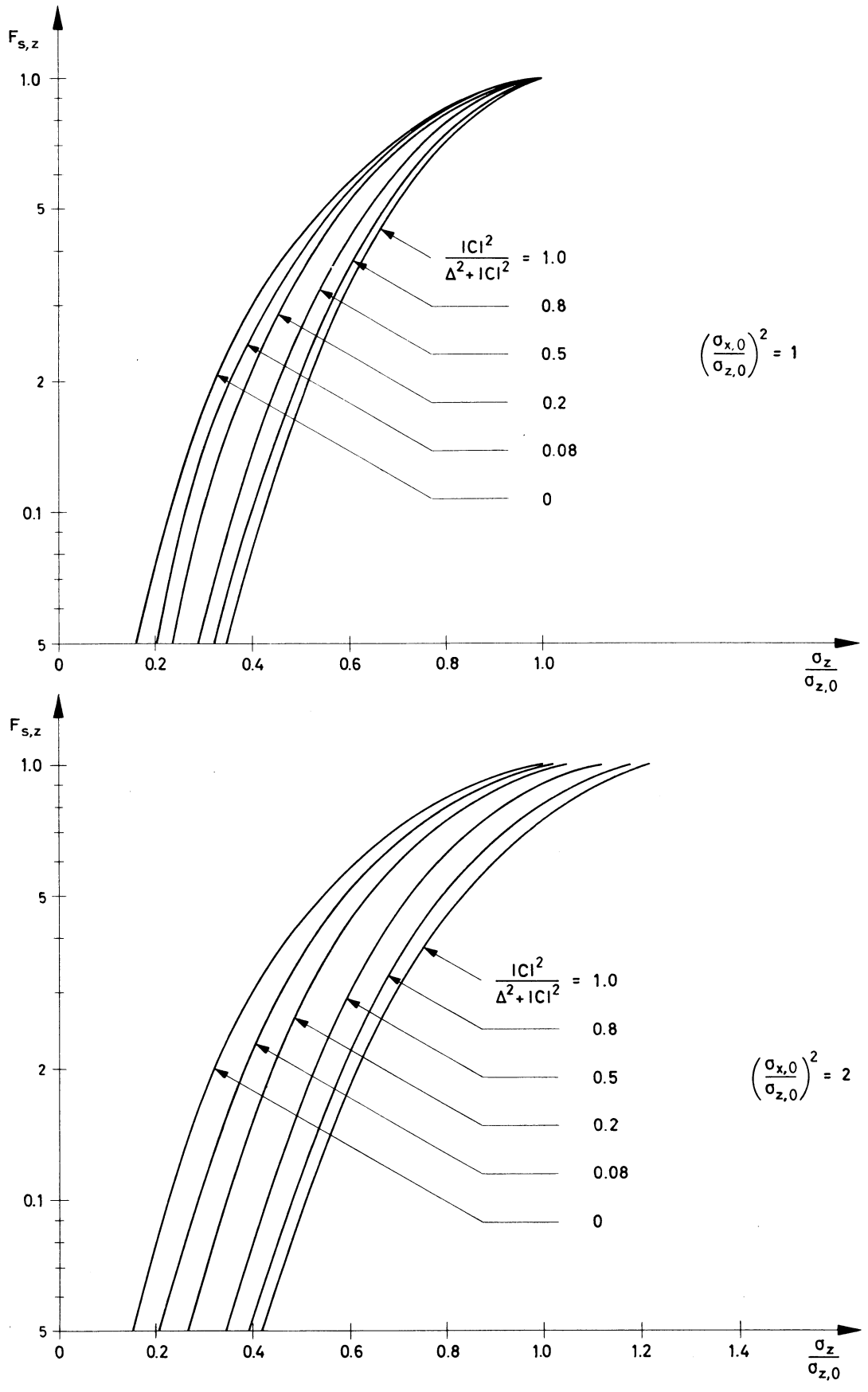

Fig. 17 Vertical blow-up due to linear coupling for different rates of vertical shaving and low emittance ratios

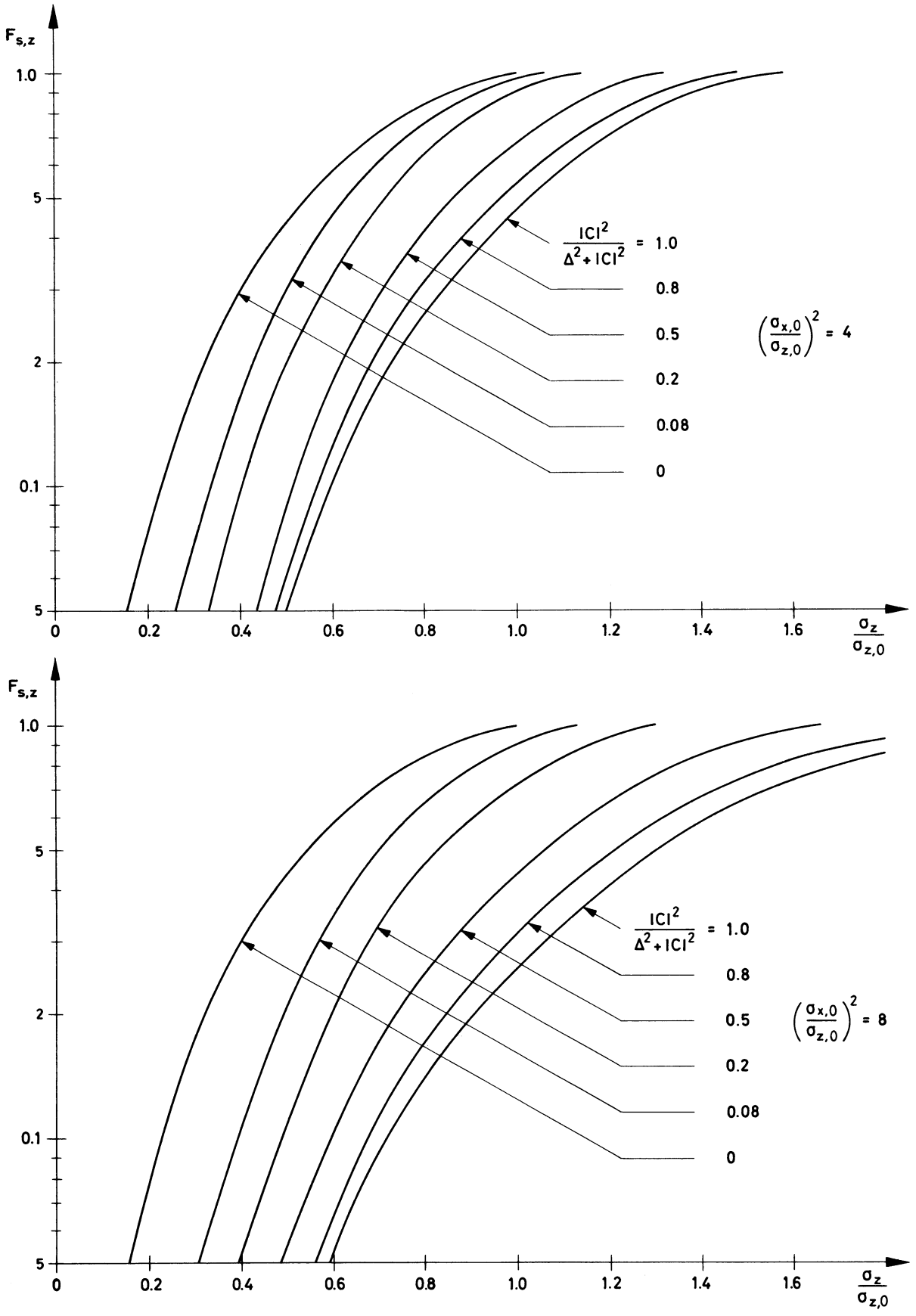

Fig. 18 Vertical blow-up due to linear coupling for different rates of vertical shaving and high emittance ratios

10.1 Resonances in a coasting beam due to the magnetic fields of the machine magnets

The presence of a three-dimensional magnetic field can provoke instabilities and resonances in the transverse motions of the particles in a circulating coasting beam. The condition that a resonance may occur in the two-dimensional oscillations of the particles is

$$e = n_x Q_x + n_z Q_z - p = 0 .$$

The excitation terms, which characterize the perturbation, have the following forms in the case of a three-dimensional magnetic field verifying $\vec{\text{rot}}\,\vec{B} = 0$:

$$\left.\begin{matrix} d_p \\ f_p \end{matrix}\right\} = \frac{1}{2\pi}\int_0^{2\pi} \beta_x^{(|n_x|/2)}\ \beta_z^{(|n_z|/2)}\ \frac{B\rho}{R^2}\left[(-1)^{(|n_z|+2)/2}\ \underset{x}{K_z^{(N-1)}} + \right.$$

$$\left. + \underset{x}{RF_z^{(N-1)}}\left(|n_x|\,\frac{\alpha_x}{\beta_x} - |n_z|\,\frac{\alpha_z}{\beta_z}\right) - i\,\underset{x}{RF_z^{(N-1)}}\left(\frac{n_x}{\beta_x} - \frac{n_z}{\beta_z}\right)\right]$$

$$\exp\left\{i\left[n_x\mu_x + n_z\mu_z - (n_xQ_x + n_zQ_z - p)\theta\right]\right\}\,d\theta \quad ,$$

the indices z and x of $K^{(N-1)}$ and $F^{(N-1)}$ being associated with d_p and f_p, respectively, with, for N = 2:

$$\left\{\begin{matrix} K_x^{(1)} = \frac{R^2}{2B\rho}\left(\frac{\partial B_x}{\partial x} - \frac{\partial B_z}{\partial z}\right)_{x=z=0} \\ F_x^{(1)} = \frac{R}{2B\rho}\,B_\theta\ (x=z=0) \end{matrix}\right. \qquad \left\{\begin{matrix} K_z^{(1)} = \frac{R^2}{B\rho}\,\frac{\partial B_x}{\partial z}\Big|_{x=z=0} \\ F_z^{(1)} = 0 \end{matrix}\right. \quad ,$$

and, for $N \geqslant 3$:

$$\left.\begin{matrix} k_2 \text{ even} \quad K_x^{(N-1)} \\ k_2 \text{ odd} \quad K_z^{(N-1)} \end{matrix}\right\} = \left\{\begin{matrix} (-1)^{(k_2+2)/2} \\ (-1)^{(k_2+1)/2} \end{matrix}\right\} \frac{R^2}{2B\rho}\,\frac{(k_2+1)!\,(N-k_2-2)!}{(N-1)!}$$

$$\left[\frac{\partial^{(N-1)}B_z}{\partial x^{(N-k_2-2)}\,\partial z^{(k_2+1)}}\Big|_{x=z=0} - \frac{N-k_2-1}{k_2+1}\,\frac{\partial^{(N-1)}B_x}{\partial x^{(N-k_2-1)}\,\partial z^{k_2}}\Big|_{x=z=0}\right]$$

$$\left.\begin{matrix} k_2 \text{ even} \quad F_x^{(N-1)} \\ k_2 \text{ odd} \quad F_z^{(n-1)} \end{matrix}\right\} = \frac{R}{2B\rho}\,\frac{k_2!\,(N-k_2-2)!}{(N-2)!}\,\frac{\partial^{(N-2)}B_\theta}{\partial x^{(N-k_2-2)}\,\partial z^{k_2}}\Big|_{x=z=0} \quad ,$$

where the integer k_2 is free within the limits given by $0 \leq k_2 \leq (N-2)$.

For a two-dimensional magnetic field, the parameters K and F simply become:

$$F_x^{(N-1)} = F_z^{(N-1)} = 0 \ ,$$

$$K_x^{(N-1)} = \frac{R^2}{B\rho} \frac{\partial^{(N-1)} B_x}{\partial x^{(N-1)}} \ ,$$

$$K_z^{(N-1)} = \frac{R^2}{B\rho} \frac{\partial^{(N-1)} B_z}{\partial x^{(N-1)}} \ .$$

The magnetic resonances can be damped by some zero harmonics of the field. These damping terms associated with the field of the machine magnets are

$$h_{qs}^{(2\nu)} = \frac{1}{2\pi (2R)^{\nu} (q!s!)^2} \int_0^{2\pi} \beta_x^q \beta_z^s \left[(-1)^{s+1} K_z^{(2\nu-1)} + F_z^{(2\nu-1)} \, 2R \left(q \frac{\alpha_x}{\beta_x} - s \frac{\alpha_z}{\beta_z} \right) \right] d\theta \ ,$$

with $\nu = q + s$; ν, q, s = integers; $\nu \leq \bar{N}/2$ ($\bar{N}/2$ is the smallest integer $\geq N/2$).

$K_z^{(2\nu-1)}$ and $F_z^{(2\nu-1)}$ are defined as above using 2ν instead of N.

10.2 Betatron-synchrotron resonances due to the magnetic fields of the machine magnets[37]

The presence of a magnetic field can provoke instabilities and resonances in the transverse motions of the particles in a bunched beam. These resonances are called betatron-synchrotron resonances, since the synchrotron oscillations of the particles inside the bunches are coupled with the betatron oscillations to induce transverse instabilities. In this mechanism, the synchrotron motion manifests itself by an oscillation of the momentum of nonsynchronous particles given in Section 3.2. Analysing this oscillation in harmonics of the revolution frequency, it is possible to write

$$\frac{\Delta p}{p} = \frac{p - p_o}{p} = \sum_{k=0}^{\infty} u_k \exp (i \, k \, Q_s \, \theta) \ ,$$

k is an integer,

p and p_o are the momentum of the nonsynchronous and synchronous particles, respectively [eV/c],

Q_s is the number of synchrotron oscillations per revolution. $Q_s = f_p / f_{rev}$, these frequencies being defined in Section 3.3.

The horizontal position x_p of an off-momentum particle is related to $\alpha_{p,x}$ (Section 1.1), but this is no longer an oscillation of period 2π in θ. Using the form of $\Delta p/p$ given above, the position x_p for a nonsynchronous particle sitting in a bunch can be written as follows:

$$x_p = \sum_{\ell} \sqrt{\frac{\beta_x R}{2}} \frac{R \, u_{k_\ell} \, c_{b_\ell}}{\rho_o \, \Delta_\ell} \exp \left[i \, (\mu_x - \Delta_\ell \, \theta) \right] \ ,$$

where:

$$c_b = \frac{1}{2\pi}\int_0^{2\pi}\sqrt{\frac{\beta_x}{2R}}\exp\left\{i\left[(Q_x - b)\theta - \mu_x\right]\right\}d\theta \ ,$$

$$u_k = \frac{Q_s}{2\pi}\int_0^{2\pi/Q_s}\frac{\Delta p}{p}\exp\left(-\,i\,k\,Q_s\,\theta\right)d\theta \ ,$$

$$\Delta = Q_x - b - k\,Q_s \ .$$

The index ℓ (integer) has been introduced for numbering the two integers k and b, in order to replace the double summation on k and b by a single summation on ℓ. With every ℓ, a pair of values (b_ℓ, k_ℓ) is associated. Δ_ℓ means that Δ is taken for this pair of values, while c_{b_ℓ} and u_{k_ℓ} mean that c_b and u_k are taken for the values b_ℓ and k_ℓ of the pair, respectively.

ρ_o is the radius of curvature of the synchronous particle [m].

This expression of x_p obviously shows the existence of dipole resonances in the absence of perturbing fields. These resonances are given by

$$\Delta = Q_x - b - k\,Q_s = 0 \ ,$$

so that x_p goes to infinity.

Considering now two-dimensional perturbing fields of the machine magnets, the condition that a resonance may occur in the transverse oscillations of the particles will be

$$e = n_x Q_x + n_z Q_z - p - m Q_s - \sum_\ell (b_\ell + k_\ell Q_s) j_\ell = 0 \ ,$$

p, m, j_ℓ being also integers and $\sum_\ell j_\ell = n - N + 1$, with $n \geq N-1$.

In this case, the excitation terms characterizing the perturbation are

$$\left.\begin{matrix} d_p \\ f_p \end{matrix}\right\} = \frac{(n-N+1)!\,(N-1)!}{n!\prod_\ell (j_\ell!)}\left(\sqrt{\frac{R}{2}}\,\frac{R}{\rho_o}\right)^{n-N+1}(-u_m)\prod_\ell\left(\frac{u_{k_\ell}\,c_{b_\ell}}{\Delta_\ell}\right)^{j_\ell}\frac{1}{2\pi}\int_0^{2\pi}d\theta\,\frac{\partial^n B_z}{\partial x^n}$$

$$\beta_x^{(|n_x|+n-N+1)/2}\,\beta_z^{|n_z|/2}\exp\left\{i\left[(n_x + n - N + 1)(\mu_x - Q_x\,\theta) + n_z(\mu_z - Q_z\,\theta) + p\theta\right]\right\} ,$$

the indices z and x of B are associated with d_p and f_p, respectively,
the symbol $\prod_\ell$ indicates a product of terms numbered by the index ℓ,
n is any integer $\geq N-1$,
j_ℓ are integers verifying $\sum_\ell j_\ell = n-N+1$,
p, m are any integers.

The coefficients Δ_ℓ, u_{k_ℓ} and c_{b_ℓ} are those appearing in the expression for x_p given above. The coefficient u_m is any harmonics amplitude of $\Delta p/p$.

The two products appearing in this expression should contain exactly the terms appearing in x_p and no others. Nevertheless, only the dominant terms corresponding to small Δ_ℓ can be considered for x_p, d_p and f_p in order to limit the number of terms in a practical case.

The resonances can be damped as mentioned in Section 10.1. The damping terms are

$$h_{qs}^{(2\nu)} = \frac{R^2}{B\rho_o (2R)^\nu (q!s!)^2 2\pi} \frac{(2\nu-1)!\ (n-2\nu+1)!}{n! \prod_\ell (j_\ell!)} \left(\sqrt{\frac{R}{2}}\,\frac{R}{\rho_o}\right)^{n-2\nu+1} (-u_m) \prod_\ell \left(\frac{u_{k_\ell}\, c_{b_\ell}}{\Delta_\ell}\right)^{j_\ell}$$

$$\int_o^{2\pi} d\theta\, \frac{\partial^n B_z}{\partial x^n}\, \beta_x^{(q-\nu+\frac{n+1}{2})}\, \beta_z^s \exp\left\{ i\left[(n-2\nu+1)(\mu_x - Q_x\,\theta) + p\theta\right]\right\} ,$$

with $\nu = q + s$; ν, q, s = integers,

n is any integer $\geq 2\nu - 1$,

j_ℓ are integers verifying $\sum_\ell j_\ell = n - 2\nu + 1$,

m, p are integers verifying

$$p + m\,Q_s = -\sum_\ell (b_\ell + k_\ell\, Q_s)\, j_\ell \ .$$

10.3 Resonances due to coasting beams crossing each other

When two coasting beams are crossing at a small angle ψ, a particle of the beam 1 sees the electric and magnetic fields of beam 2. As for the case mentioned in Section 10.1, these fields can provoke instabilities and resonances in the transverse motions of the particles of beam 1. The condition that such a resonance may occur in beam 1 is again (Section 10.1)

$$e = n_x Q_{x_1} + n_z Q_{z_1} - p = 0 \ .$$

The index 1 means that the tunes are those of beam 1 particles.

The excitation terms have the following forms using the coordinate system of Fig. 19:

$$\left.\begin{matrix} d_p \\ f_p \end{matrix}\right\} = \frac{1}{2\pi\ \beta_1\ c} \int_o^{2\pi} \beta_{x_1}^{(|n_x|/2)}\, \beta_{z_1}^{(|n_z|/2)}\, \frac{\partial^N V}{\partial x_1^{|n_x|}\, \partial z_1^{|n_z|}}$$

$$\exp\left\{ i\left[n_x \mu_{x_1} + n_z \mu_{z_1} - (n_x Q_{x_1} + n_z Q_{z_1} - p)\,\theta_1 \right]\right\} d\theta_1 \ .$$

V is a force potential which does not necessarily obey Laplace's equation [V].

The index 1 in the coordinates x, z, θ and in the parameter β means that the functions such as β_y, V, μ_y and Q_y and the longitudinal speed have to be taken in the coordinate system of the beam 1 particles (Fig. 19).

Since the fields are due to the particles of beam 2, the potential V is given by the following relations:

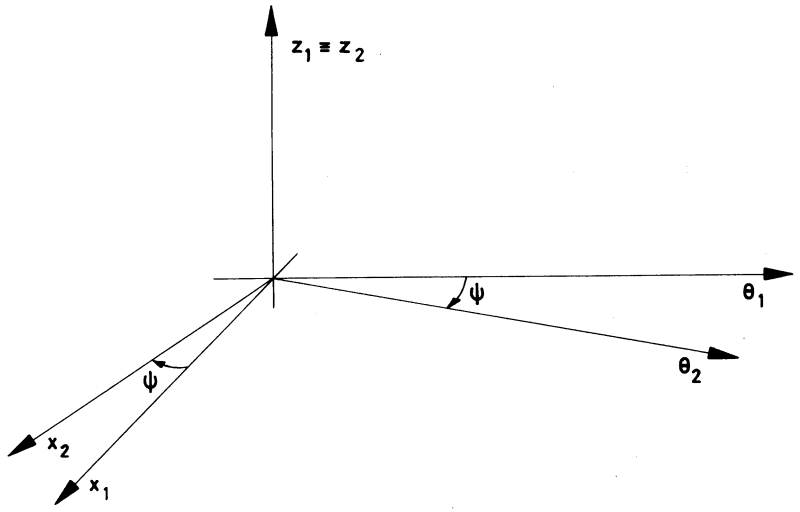

Fig. 19 Coordinate systems used at the crossing point of two beams

$$\frac{\partial^N V}{\partial x_1^{|n_x|}\,\partial z_1^{|n_z|}} = \begin{cases} (1+\beta_1\beta_2)\,\dfrac{\partial^{(N-1)} E_{x_1}}{\partial x_1^{|n_x-1|}\,\partial z_1^{|n_z|}} & |n_x| \geq 1 \\ (1+\beta_1\beta_2)\,\dfrac{\partial^{(N-1)} E_{z_1}}{\partial x_1^{|n_x|}\,\partial z_1^{|n_z-1|}} & |n_z| \geq 1 \end{cases} ,$$

β_2 is the relative longitudinal speed of beam 2.

The electric field components [V m^{-1}] in the coordinate system of beam 2 (Fig. 19) for Gaussian transverse distributions of particles are given by

$$E_{y_2} = \frac{I_2}{\pi\,\varepsilon_o\,\beta_2\,c} \int_o^\infty \frac{y_2 \exp\left[-\left(\dfrac{2x_2^2}{a_2^2+t} + \dfrac{2z_2^2}{b_2^2+t}\right)\right]}{(a_2^2+t)\sqrt{(a_2^2+t)\,(b_2^2+t)}}\,dt ,$$

where index 2 means that all the functions are taken for beam 2,

ε_o is the free-space permittivity [As V^{-1} m^{-1}] (Table 1),

a_2 is the half-beam 2 width (twice the r.m.s. of the radial dimension) [m],

b_2 is the half-beam 2 height (twice the r.m.s. of the vertical dimensions) [m].

In general, a_2 and b_2 are quadratically varying with θ_2.

The passage from the field components E_{y_2} to the components E_{y_1} depends on the colliding angle ψ, since the coordinates transformation from beam 2 to beam 1 only depends on this angle (Fig. 19).

For beam-beam resonances, the damping terms mentioned in Section 10.1 are

$$h_{qs}^{(2\nu)} = \frac{1}{2\pi\,\beta_1\,c\,(2R)^\nu (q!s!)^2} \int_o^{2\pi} \beta_{x_1}^q\,\beta_{z_1}^s\,\frac{R^2}{B\rho}\,\frac{\partial^{(2\nu)} V}{\partial x_1^{(2q)}\,\partial z_1^{(2s)}}\,d\theta_1 ,$$

ν, q, s are integers satisfying $\nu = q + s$,
V is the potential given above [V] .

In actual fact, the integrals for d_p, f_p and $h_{qs}^{(2\nu)}$ are different from zero only in the interval $(\theta_I - d/2R, \theta_I + d/2R)$, if d is the length [m] of the crossing region in which the two beams interact and θ_I is the azimuth of the considered crossing point.

10.4 Resonances due to overlap knock-out[38)]

The interaction between a coasting beam (beam 1) and a bunched beam (beam 2) can provoke instabilities and resonances in the transverse motions of the particles. The condition for a resonance to occur in the coasting beam is

$$e = n_x Q_{x_1} + n_z Q_{z_1} - p - q \frac{f_{rev_2}}{f_{rev_1}} = 0 .$$

The indices 1 and 2 refer to the coasting and bunched beams, respectively.

q is the harmonic of the bunch frequency exciting the resonance (Section 3.13),
f_{rev_2} is the revolution frequency of the bunches [s^{-1}] (Section 3.3),
f_{rev_1} is the revolution frequency of the particle at resonance [s^{-1}] (Section 3.3).

The excitation terms characterizing the perturbation have the following forms in the case of the fields induced by the bunches:

$$\left.\begin{matrix} d_p \\ f_p \end{matrix}\right\} = \frac{1}{2\pi \beta_1 c} \int_0^{2\pi} \beta_{x_1}^{(|n_x|/2)} \beta_{z_1}^{(|n_z|/2)} \frac{\partial^N V}{\partial x_1^{|n_x|} \partial z_1^{|n_z|}} d\theta_1$$

$$\exp\left\{ i\left[n_x \mu_{x_1} + n_z \mu_{z_1} - (n_x Q_{x_1} + n_z Q_{z_1} - p)\,\theta_1 + q\theta_2 \right] \right\}$$

$$\frac{1}{2\pi \hat{I}_2} \int_0^{2\pi} I_{\theta,2} \exp(i\, q\, \theta)\, d\theta$$

θ_1 is the azimuthal angle of the particle at resonance [rad] ,
θ_2 is the angular position taken in the bunch frame and corresponding to the particle position θ_1 [rad] (Fig. 20),
θ is the azimuthal variable of integration taken in the bunch frame [rad] ,
β_1 is the relativistic parameter of the coasting beam,
$I_{\theta,2}$ is the azimuthal current distribution inside one bunch of beam 2 [A] (Section 3.10),
$\hat{I}_2$ is the peak current inside a bunch of beam 2 [A] (Section 3.10).

The last integral on θ gives exactly the coefficients c_q defined in Section 3.13.

V is the potential [V] of the electromagnetic forces due to the peak current of the bunched beam and V does not obey Laplace's equation. Looking at these excitation forces, two different cases of overlap knock-out can be considered:

i) Single-beam overlap knock-out:

The bunched beam and the coasting beam are two parts of the same beam (Fig. 20). Then, the potential V comes from the electromagnetic forces of the bunched beam and also from the coupling forces induced by the bunches via the material close to the beam.

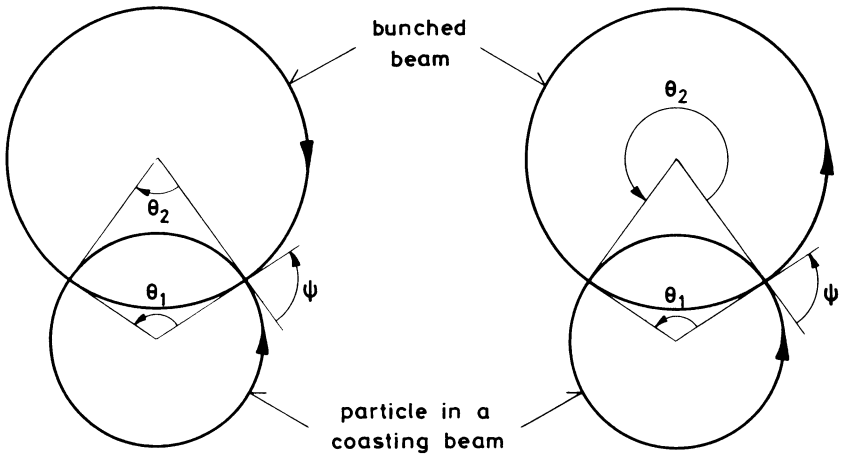

Angle definition for two-beam overlap knock-out,
depending on the directions of propagation

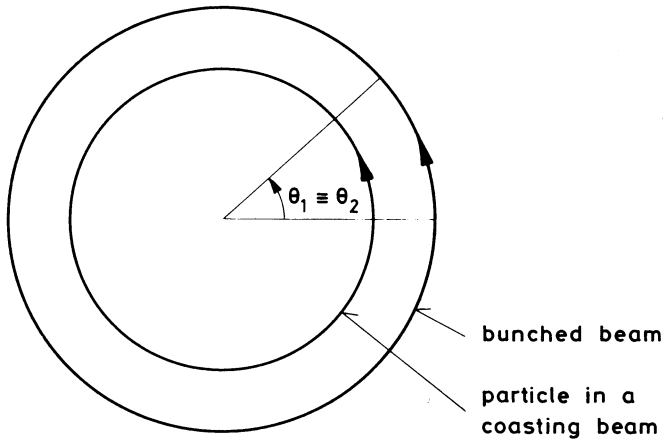

Angle definition for single beam overlap knock-out

Fig. 20 Definition of the azimuthal variables used in Section 10.4

ii) Two-beam overlap knock-out:

The bunched beam is different from the coasting beam and crosses it at a finite number of intersections (Fig. 20). In this case, the effect of the surrounding material is less important and the potential V is essentially due to the direct electromagnetic forces.

For the direct forces, the potential V is given by the following relations:

$$\frac{\partial^N V}{\partial x_1^{|n_x|}\,\partial z_1^{|n_z|}} = \begin{cases} (1 + \text{sign}\ \beta_1\beta_2)\dfrac{\partial^{(N-1)} E_{x_1}}{\partial x_1^{|n_x-1|}\,\partial z_1^{|n_z|}} & |n_x| \geq 1 \\ (1 + \text{sign}\ \beta_1\beta_2)\dfrac{\partial^{(N-1)} E_{z_1}}{\partial x_1^{|n_x|}\,\partial z_1^{|n_z-1|}} & |n_z| \geq 1 \end{cases} ,$$

where:

E_{x_1} and E_{z_1} are the electric field components in the coordinate system of beam 1. The corresponding components E_{y_2} in the coordinate system of beam 2 are given in Section 10.3 for a beam of elliptic cross-section,

β_1 is the relativistic parameter of the coasting beam,

β_2 is the relativistic parameter of the bunched beam,

sign is + 1 if the two beams go in opposed directions and is - 1 in the other case.

10.5 Bandwidth for a sum resonance

Given a single resonance e = 0 (Sections 10.1 to 10.4) and a point (Q_x, Q_z) in the tune diagram, the distance of this point from the resonance is defined as the value of e with these tunes. Knowing the limits e_1 and e_2 on each side of the resonance beyond which the motion becomes stable, the bandwidth is defined as $\Delta e = |e_1| + |e_2|$ (Fig. 21)

$$\Delta e = \frac{R}{2^{(N-2)}\, B\rho\, |n_x|!\, |n_z|!}\, E_{x_o}^{(|n_x|-2)/2}\, E_{z_o}^{(|n_z|-2)/2} \left(n_x^2 E_{z_o} + n_z^2 E_{x_o}\right) \begin{cases} |d_p| & \text{for } n_z \text{ even} \\ |f_p| & \text{for } n_z \text{ odd} \end{cases}$$

$$n_x,\ n_z \geq 0 \quad \text{or} \quad n_x,\ n_z \leq 0 \ ,$$

where the excitation terms d_p and f_p are given in Sections 10.1 to 10.4 depending on the type of instability considered.

10.6 Trapping condition for the particles crossing a sum resonance

When the tunes, the synchrotron frequency and/or the revolution frequencies are changing with the time in such a way that the particles are crossing a sum resonance, these particles can remain trapped in the resonance if the rate of change of the distance from the resonance is sufficiently small. The condition for the trapping to occur is given by[36]

$$\left|\frac{de}{dt}\right| \leq \frac{\Delta e}{R} \frac{\beta c\, n_x^2 E_{z_o}}{n_x^2 E_{z_o} + n_z^2 E_{x_o}} \sum_{\ell=2}^{\overline{N}/2} \ell(\ell-1)\, K_{\ell,1} \qquad n_x \neq 0$$

$$\left|\frac{de}{dt}\right| \leq \frac{\Delta e}{R} \frac{\beta c\, n_z^2 E_{x_o}}{n_x^2 E_{z_o} + n_z^2 E_{x_o}} \sum_{\ell=2}^{\overline{N}/2} \ell(\ell-1)\, K_{\ell,2} \qquad n_z \neq 0 \ ,$$

Δe is the bandwidth given in Section 10.5,

$\overline{N}/2$ is the smallest integer larger or equal to N/2.

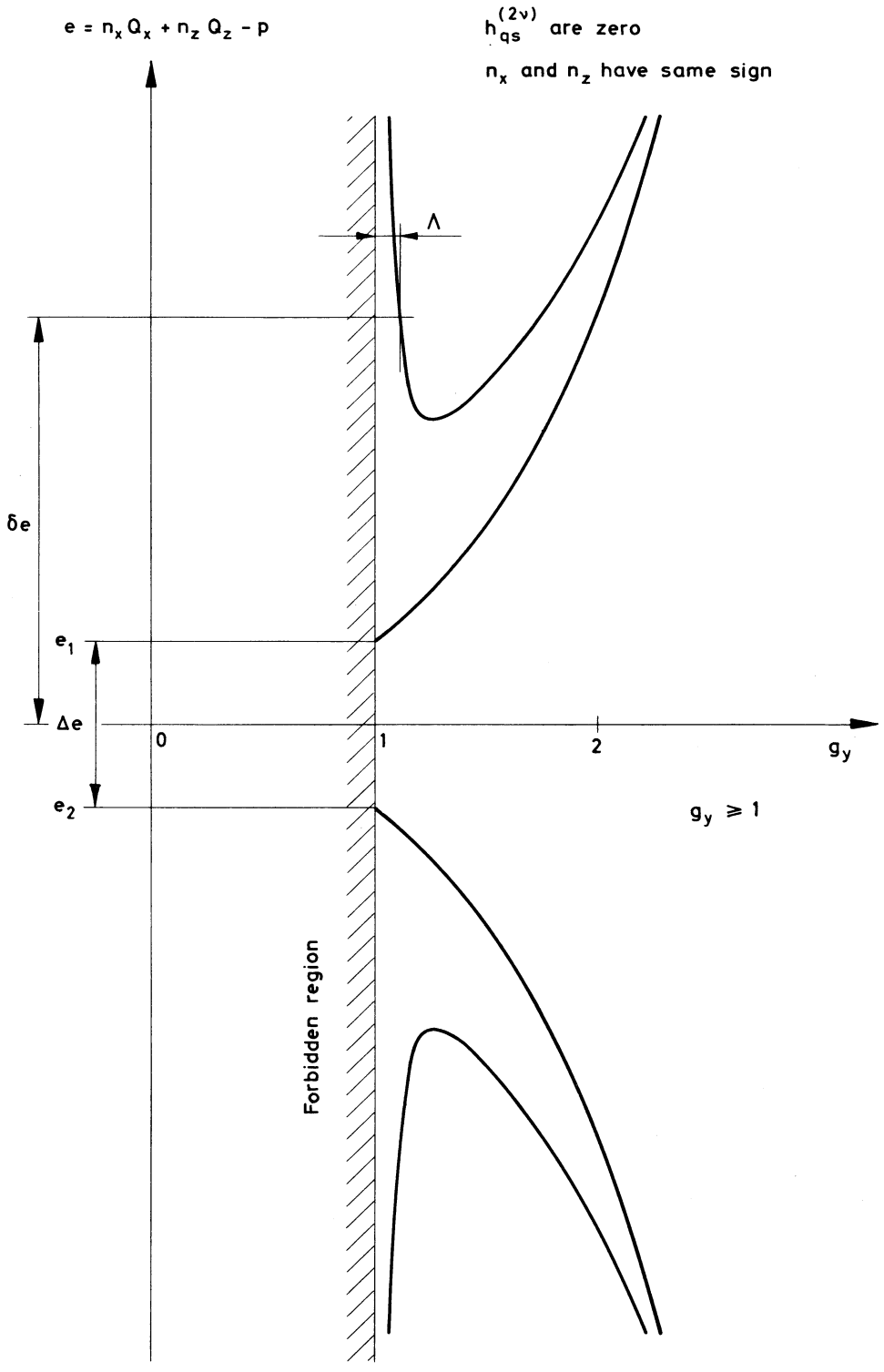

Fig. 21 Resonance curves for sum resonances

The coefficients $K_{\ell,1}$ and $K_{\ell,2}$ are given by

$$K_{\ell,1} = E_{x_o}^{(\ell-1)} \left\{ \sum_{\nu=\ell}^{\overline{N}/2} A_x^{(\nu-\ell)} \sum_{p=0}^{\ell} \left[\frac{(\nu-\ell+p)(\nu-\ell+p-1)\ldots(\nu-\ell+1)}{p!} \left(\frac{n_z}{n_x}\right)^p h_{\ell-p,\nu-\ell+p}^{(2\nu)} \right] \right\} ,$$

$$K_{\ell,2} = E_{z_o}^{(\ell-1)} \left\{ \sum_{\nu=\ell}^{\overline{N}/2} A_z^{(\nu-\ell)} \sum_{p=0}^{\ell} \left[\frac{(\nu-\ell+p)(\nu-\ell+p-1)\ldots(\nu-\ell+1)}{p!} \left(\frac{n_x}{n_z}\right)^p h_{\nu-\ell+p,\ell-p}^{(2\nu)} \right] \right\} ,$$

in which:

$$A_x = \frac{R}{n_x} (n_x E_{z_o} - n_z E_{x_o})$$

$$A_z = \frac{R}{n_z} (n_z E_{x_o} - n_x E_{z_o}) ,$$

and the coefficients $h_{qs}^{(2\nu)}$ are given in Sections 10.1 to 10.4 depending on the type of instability considered.

The form of the rate of change de/dt appearing on the left hand side of the trapping condition depends on the resonances considered:

i) Resonances in a coasting beam due to the fields of the machine magnets or of an other coasting beam (Sections 10.1 and 10.3)

$$\frac{de}{dt} = n_x \frac{dQ_x}{dt} + n_z \frac{dQ_z}{dt} - \frac{p}{f_{rev}} \frac{d f_{rev}}{dt} .$$

In the case given in Section 10.3, the same expression applies, but f_{rev}, Q_x and Q_z represent the revolution frequency and the tunes of a particle in beam 1.

ii) Betatron-synchrotron resonances (Section 10.2)

$$\frac{de}{dt} = n_x \frac{dQ_x}{dt} + n_z \frac{dQ_z}{dt} - \frac{(p + \sum_\ell b_\ell j_\ell)}{f_{rev}} \frac{d f_{rev}}{dt} - \left(m + \sum_\ell k_\ell j_\ell\right) \frac{dQ_s}{dt} ,$$

the definitions being given in Section 10.2.

iii) Resonances due to overlap knock-out (Section 10.4)

$$\frac{de}{dt} = n_x \frac{dQ_{x_1}}{dt} + n_z \frac{dQ_{z_1}}{dt} - \frac{p}{f_{rev_1}} \frac{d f_{rev_1}}{dt} - \frac{q}{f_{rev_1}} \frac{d f_{rev_2}}{dt} ,$$

the definitions being given in Section 10.4.

10.7 Maximum growth of amplitude for particles crossing a sum resonance

When the particles cross a sum resonance with a rate of change of e which is sufficient to avoid being trapped (see Section 10.6), there is still an amplitude growth. The maximum possible growth of the amplitude which may occur can be calculated for a single crossing as follows:

$$\left(\frac{n_x E_{z_o}}{n_z E_{x_o}}\right)^{n_z/2} \int_1^{g_x} \frac{dg_x}{\left(\frac{n_x E_{z_o}}{n_z E_{x_o}} - 1 + g_x^2\right)^{n_z/2} g_x^{(n_x-1)}} = \frac{\Delta e}{n_x + \frac{n_z^2 E_{x_o}}{n_x E_{z_o}}} \frac{\sqrt{\pi\beta c}}{\sqrt{2R}\sqrt{\left|\frac{de}{dt}\right|}} \quad \text{for } n_x \neq 0 \text{ only,}$$

Δe is the bandwidth defined in Section 10.5.

The relation for g_z, valid if $n_z \neq 0$ only, is simply obtained by exchanging the indices x and z in the preceding relation.

If the particle is crossing the resonance n_r times, the average growth of amplitude will be $\sqrt{n_r/2}$ times larger than for a single crossing.

The rate of change of e is given in Section 10.6 for different types of resonances.

For monodimensional resonances ($n_x = N$, $n_z = 0$) or ($n_x = 0$, $n_z = N$), this relation becomes

$$\left.\begin{array}{ll} N = 2 & \ell n\, g_y \\ N > 2 & \dfrac{1 - g_y^{(2-N)}}{N - 2} \end{array}\right\} = \frac{\Delta e}{N} \frac{\sqrt{\pi\beta c}}{\sqrt{2R}\sqrt{\left|\frac{de}{dt}\right|}} \ .$$

For bidimensional resonances ($n_x \neq 0$, $n_z \neq 0$) of order $N \leq 5$, the analytic form of the above integral is given in the Appendix.

10.8 Criterion concerning the distance of the working point from a sum resonance line

The perturbation of the oscillation amplitude of a single particle in a sum resonance decreases as the distance from the resonance increases. Assuming that the maximum tolerable blow-up for a single particle associated with the initial emittances E_{x_o} and E_{z_o} is Λ (Fig. 21), then the distance δe (Fig. 21) of the working point from the resonance must be in agreement with

$$\delta e \geq \frac{\Delta e}{2}\left(1 + \frac{1}{\Lambda}\frac{|n_x|E_{z_o} + |n_z|E_{x_o}}{n_x^2 E_{z_o} + n_z^2 E_{x_o}}\right) ,$$

Δe is the bandwidth defined in Section 10.5.

10.9 Bandwidth for a difference resonance

As in Section 10.5, e represents the distance from the resonance. Knowing the limits $e_{1,1}$ and $e_{2,1}$ on each side of the resonance between which the amplitude can become zero and the limits $e_{1,2}$ and $e_{2,2}$ on each side of the resonance between which the amplitude can become maximum, the bandwidth is defined as $\Delta e = \frac{1}{2}(|e_{1,1}| + |e_{2,1}| + |e_{1,2}| + |e_{2,2}|)$ (Fig. 22)

$$\Delta e = \frac{R}{2^{(N-2)}\, B\rho\, |n_x|!|n_z|!} E_{x_o}^{(|n_x|-2)/2} E_{z_o}^{(|n_z|-2)/2} \left(|n_x|E_{z_o} + |n_z|E_{x_o}\right) \left\{\begin{array}{l} |d_p| \\ |f_p| \end{array}\right. \begin{array}{l} \text{for } n_z \text{ even} \\ \text{for } n_z \text{ odd} \end{array}$$

$$n_x \geq 0,\ n_z \leq 0 \quad \text{or} \quad n_x \leq 0,\ n_z \geq 0.$$

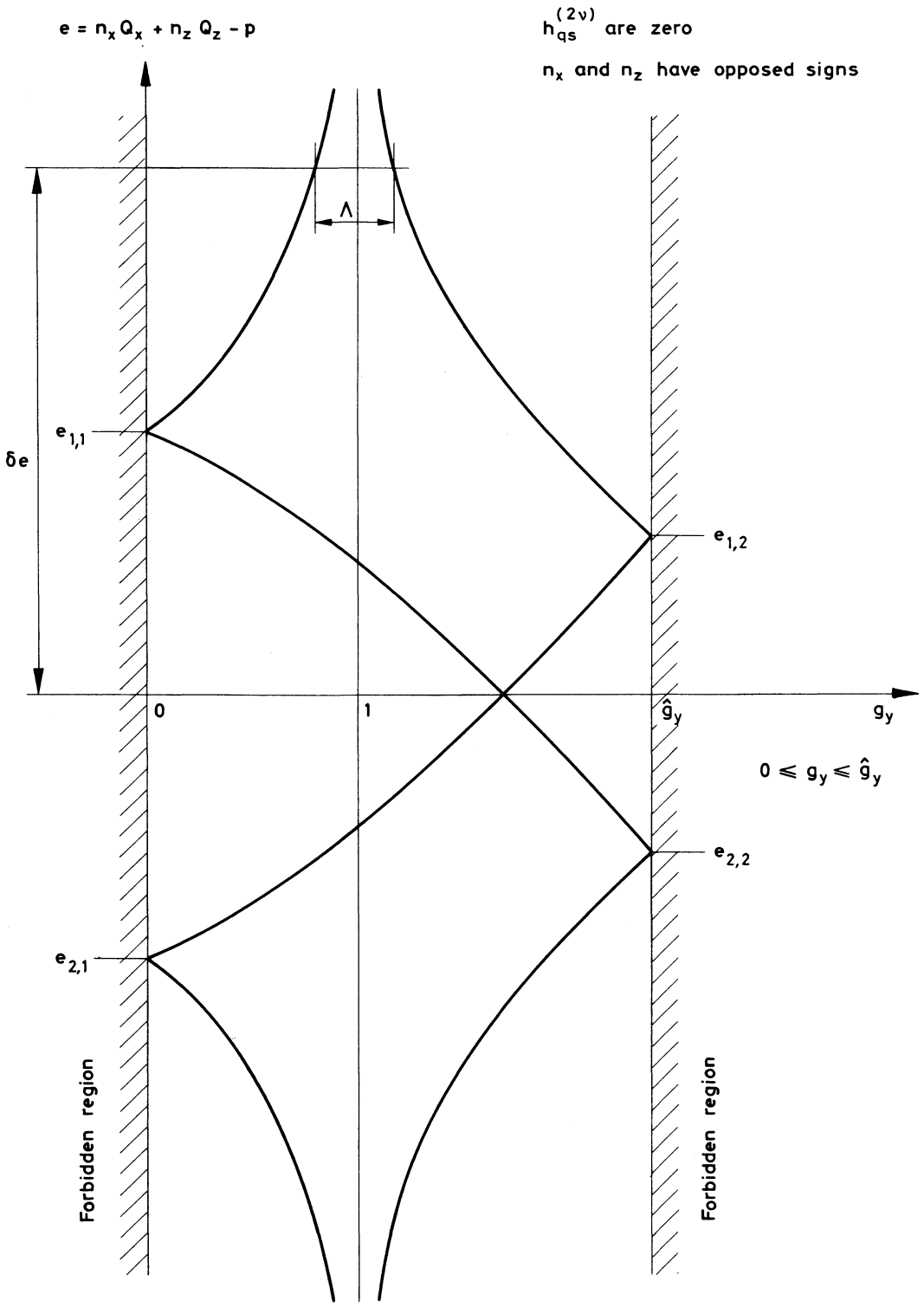

Fig. 22 Resonance curves for difference resonances

The parameters d_p and f_p are given in Sections 10.1 to 10.4, depending on the type of instability considered.

10.10 Maximum amplitude for particles on a difference resonance

Such a resonance is always stable and a particle remaining inside the band defined in Section 10.9 can oscillate between two limits (Fig. 22) given by

$$0 \leq g_x \leq \sqrt{1 + \left|\frac{n_x}{n_z}\right| \frac{E_{z_o}}{E_{x_o}}} \quad ,$$

$$0 \leq g_z \leq \sqrt{1 + \left|\frac{n_z}{n_x}\right| \frac{E_{x_o}}{E_{z_o}}} \quad .$$

10.11 Criterion concerning the distance of the working point from a difference resonance line

Since a difference resonance is stable, the amplitude of the single particle motion oscillates between two limits, but with increasing distance from the resonance these limits converge. Assuming that the maximum tolerable beating of the amplitude for a single particle associated with the initial emittances E_{x_o} and E_{z_o} is Λ (Fig. 22), then the distance δe (Fig. 22) of the working point from the resonance must be in agreement with

$$\delta e \geq \frac{1}{2} \frac{\Delta e}{\Lambda} \quad .$$

Δe is the bandwidth defined in Section 10.9.

10.12 Monodimensional resonances for coasting beams crossing at large angle

This is a particular case of the resonances mentioned in Section 10.3. The crossing angle can be either in the horizontal or in the vertical plane and it is assumed to be small as in Section 10.3, but large enough that only the monodimensional resonances $e = NQ_{y_1} - p = 0$ are excited in the perturbed beam.

It is assumed in what follows that the perturbing beam 2 has a transverse, uniform distribution in the colliding plane and a Gaussian distribution in the direction perpendicular to the colliding plane. Furthermore, the distance y_1 of the excited particle in beam 1 w.r.t. the beam 2 centre is taken as small. Under these conditions, the bandwidths of these monodimensional resonances become, using the formulae of Sections 10.3, 10.5 and 8.9

$$\Delta e = \frac{N}{2^{(N/2-2)}\,(N-1)(N/2-1)!}\,\Delta Q_{y_1}^{bb} \qquad \text{for N even}$$

$$\Delta e = \frac{N}{2^{(N-1)/2}\,(\frac{N-1}{2})!}\,\frac{y_1}{\sigma_{y_2}}\,\Delta Q_{y_1}^{bb} \qquad \text{for N odd, } \frac{y_1}{\sigma_{y_2}} \ll 1 \quad ,$$

y_1 is the distance of the particle from the beam 2 centre in the direction perpendicular to the colliding plane [m],

σ_{y_2} is the r.m.s. value of the beam 2 size in the direction perpendicular to the colliding plane [m],

$\Delta Q_{y_1}^{bb}$ is the linear beam-beam tune shift given in Section 8.9, in the direction perpendicular to the colliding plane.

Using the formula in Section 10.7 for monodimensional resonances, the transverse increase of the initial amplitude of particle 1 is given by the following equation when crossing the resonance by changing the tune and/or the revolution frequency:

$$\frac{\Delta\sigma_{y_1}}{\sigma_{y_1}} = \frac{\sqrt{\pi\beta_1 c}}{\sqrt{2R}\,N} \frac{\Delta e}{\sqrt{\left| N \frac{dQ_{y_1}}{dt} - \frac{p}{f_{rev_1}} \frac{df_{rev_1}}{dt} \right|}} ,$$

σ_{y_1} is the initial r.m.s. value of the transverse amplitude of particle 1 (Section 1.6) in the direction perpendicular to the colliding plane [m] ,
β_1 is the relative longitudinal speed of particle 1,
Q_{y_1} is the particle tune in the direction perpendicular to the colliding plane,
f_{rev_1} is the revolution frequency of particle 1 [s^{-1}] ,
Δe is the bandwidth given above.

Even if the mathematical definition used for the bandwidth does not apply to the dipole resonances, the final result concerning the transverse blow-up is still valid, using a virtual bandwidth Δe with N = 1

$$\frac{\Delta y_1}{y_1} = \frac{\sqrt{\pi\beta_1 c}}{\sqrt{2R}\,\sigma_{y_2}} \frac{\Delta Q_{y_1}^{bb}\,\sigma_{y_1}}{\sqrt{\left| \frac{dQ_{y_1}}{dt} - \frac{p}{f_{rev_1}} \frac{df_{rev_1}}{dt} \right|}} ,$$

Δy_1 is the dipole shift of particle 1 at resonance in the direction perpendicular to the colliding plane [m] .

All other parameters are defined above.

For the ISR: The crossing plane is horizontal so that $y \equiv z$. The expression for $\Delta Q_{z_1}^{bb}$ appears in Section 8.9.

10.13 Monodimensional resonances due to overlap knock-out at large colliding angle

This is a particular case of the resonances mentioned in Section 10.4. All assumptions made in Section 10.12 are also applied in the present case and y again represents the direction perpendicular to the crossing plane. The bandwidth of the monodimensional resonances (Section 10.4)

$$e = NQ_{y_1} - p - q \frac{f_{rev_2}}{f_{rev_1}} = 0$$

becomes, using the expressions in Sections 10.4, 10.5, 8.9 and 3.13,

$$\Delta e = \frac{N}{2^{(N/2-2)}\,(N-1)(N/2-1)!}\, c_q\, \Delta Q_{y_1}^{bb} \qquad \text{for N even}$$

$$\Delta e = \frac{N}{2^{(N-1)/2}\,(\frac{N-1}{2})!}\, \frac{y_1}{\sigma_{y_2}}\, c_q\, \Delta Q_{y_1}^{bb} \qquad \text{for N odd, } \frac{y_1}{\sigma_{y_2}} \ll 1 ,$$

y_1, σ_{y_2}, $\Delta Q_{y_1}^{bb}$ (Section 8.9) are defined in Section 10.12,
c_q are the harmonics amplitudes defined in Section 3.13.

Using the formula in Section 10.7 for monodimensional resonances, the transverse increase of the initial amplitude of particle 1 when crossing the resonance by tune and/or frequency changes is given by

$$\frac{\Delta\sigma_{y_1}}{\sigma_{y_1}} = \frac{\sqrt{\pi\beta_1 c}}{\sqrt{2R}\,N} \frac{\Delta e}{\sqrt{\left| N\frac{dQ_{y_1}}{dt} - \frac{p}{f_{rev_1}}\frac{df_{rev_1}}{dt} - \frac{q}{f_{rev_1}}\frac{df_{rev_2}}{dt}\right|}} ,$$

σ_{y_1}, β_1 and Q_{y_1} are defined in Section 10.12,
f_{rev_1} and f_{rev_2} are given in Section 10.4,
Δe is the bandwidth given above.

Even if the mathematical definition used for the bandwidth does not apply to the dipole resonances, the final result concerning the transverse blow-up is still valid, using a virtual bandwidth Δe with N = 1

$$\frac{\Delta y_1}{y_1} = \frac{\sqrt{\pi\beta_1 c}}{\sqrt{2R}\,\sigma_{y_2}} \frac{c_q\,\Delta Q_{y_1}^{bb}\,\sigma_{y_1}}{\sqrt{\left|\frac{dQ_{y_1}}{dt} - \frac{p}{f_{rev_1}}\frac{df_{rev_1}}{dt} - \frac{q}{f_{rev_1}}\frac{df_{rev_2}}{dt}\right|}} ,$$

Δy_1 is the dipole shift of particle 1 at resonance in the direction perpendicular to the colliding plane [m] .

All other parameters are defined above.

When the tune and the revolution frequency of particle 1 vary with momentum as given below,

$$Q_{y_1} = Q_{y_1,o} + Q'_{y_1}\left.\frac{\Delta p}{p}\right|_1$$

$$f_{rev_1} = f_{rev_1,o}\left[1 + \eta\left.\frac{\Delta p}{p}\right|_1\right] ,$$

the momenta at which the resonances appear in beam 1 are given by

$$\left.\frac{\Delta p}{p}\right|_1 = \frac{-NQ_{y_1,o} + p + q\, f_{rev_2}/f_{rev_1,o}}{q\,\eta\, f_{rev_2}/f_{rev_1,o} + NQ'_{y_1}} ,$$

$Q_{y_1,o}$ is the tune of beam 1 at centre line,
$f_{rev_1,o}$ is the revolution frequency of beam 1 at centre line [s^{-1}] ,
Q'_{y_1} is the chromaticity of beam 1,
f_{rev_2} is the revolution frequency of the bunches [s^{-1}] ,
$\left.\frac{\Delta p}{p}\right|_1$ is the relative momentum difference between the particle at resonance and the particle at the centre line.

For the ISR: The crossing plane is horizontal so that y ≡ z. The expression for $\Delta Q_{z_1}^{bb}$ appears in Section 8.9.

11. FORMULAE IN CONNECTION WITH COASTING BEAM INSTABILITIES[24,39,40,41,42,43,44,45]

Symbols frequently used in this chapter

$\Delta p/p$	momentum spread for coasting beam
$Z_o = \mu_o c$	impedance of free space (Table 1) $[\Omega]$
σ	conductivity of the chamber material $[\Omega^{-1}m^{-1}]$
E_o	rest energy of proton [eV]
n	is an integer.

11.1 Stability criterion for transverse resistive wall instabilities of coasting beams

The following stability criterion applies to a coasting beam[39]:

$$|Z_\perp| \leq kF \frac{\beta^3\gamma}{\bar{\beta}_y I} \left|(n - Q_y)\,\eta - \frac{\partial Q_y}{\partial(\Delta p/p)}\right| \frac{\Delta p}{p} \quad ,$$

where:

$k = \pi \frac{E_o}{e} = 2.947618\ 10^9$ [V],
$Z_\perp$ is the total transverse impedance in the machine $[\Omega m^{-1}]$,
n is every integer $> Q_y$,
$\partial Q_y/\partial(\Delta p/p) = Q_y'$ is the chromaticity (Section 1.1) multiplied by the tune,
$\Delta p/p$ is the full relative momentum spread at half height,
F is a form factor depending on the aspect ratio of the coasting beam.

Considering symmetric particle distributions with a central plateau and $\sin^2$ edges, the aspect ratio of the beam is defined as plateau width over sum of edge widths at half-height. The minimum form factors associated with the worst possible phase of $Z_\perp$ are given for different aspect ratios in the table below[46]:

Aspect ratio of beam	0	1	10	100
Minimum form factor F	1	0.89	0.65	0.45 .

This criterion can also be applied to a bunched beam if the rise time of the transverse instability is short compared with the period of the radio-frequency system. In this case, the current to be considered is the peak current of one bunch (Section 3.10).

For the ISR: The resistive wall instability is known under the name of "brickwall instability". Tables 3, 4, 5 and 6 give the values of $\bar{\beta}_y$, Q_y and Q_y', β and γ, and η, respectively.

11.2 Expressions for the transverse impedance

In the case of an elliptical vacuum chamber, the following expression applies[40]:

$$Z_\perp = i R \left[\frac{Z_o}{\beta^2\gamma^2}\left(\frac{1}{a^2} - \frac{1}{b^2}\right) - (1 + i)\sqrt{\frac{2RZ_o}{\beta(n-Q_y)\sigma}}\,\frac{1}{b^3}\right] \quad ,$$

a is the coasting beam height [m],
b is the half-height of the chamber [m].

In the case of cross-section variations[47], the approximation of the low frequency impedance for short circular cavities and for perfectly conducting walls gives

$$Z_{\perp} = -\frac{i Z_o}{b \varepsilon}\left(\frac{B^2 - b^2}{B^2 + b^2} - \frac{0.851}{\beta^2 \varepsilon}\right) ,$$

where:

$$\varepsilon = \pi \frac{B}{L} > 1 ,$$

while the approximation for long circular cavities and perfectly conducting walls gives

$$Z_{\perp} = \frac{i Z_o}{\beta^2 \gamma^2 b \varepsilon}\left(\frac{B^2 - b^2}{B^2 + b^2}\right) ,$$

where:

$$\varepsilon = \pi \frac{B}{L} << 1 .$$

b is the half-height of the chamber [m] ,
B is the half-height of the enlarged chamber [m] ,
L is the length of the chamber enlargement [m] .

In the case of a cylindrical resonance cavity in its lowest mode, the transverse impedance is

$$|Z_{\perp}| = 1.02 \frac{d}{r} \sqrt{\frac{Z_o^3 \beta \sigma (n-Q_y)}{2R}} \left(\frac{\sin \theta/2}{\theta/2}\right)^2$$

where:

$$\theta = \frac{d}{\beta r} j_1 ,$$

j_1 being the first zero of the Bessel function of the first order J_1[7,16].
r is the radius of the cavity [m] ,
d is the length of the cavity [m] .

For a beam surrounded by a circular metal envelope of radius r, the transverse impedance is related to the longitudinal one $Z_{//}$ by

$$Z_{\perp} = \frac{2R}{r^2 |n-Q_y|} Z_{//} .$$

For the ISR: The conductivity of stainless steel and R are given in Table 2. The values of Q_y and of the relativistic parameters are given in Tables 4 and 5, respectively.

11.3 Stability criterion for longitudinal resistive wall instabilities of coasting beams

This instability is associated with self-bunching of the beam due to the fact that the revolution frequency above transition decreases when the energy increases. The longitudinal instability above transition is also called the "negative mass instability" when it is due to space charge effects in a perfectly conducting pipe.

The following stability criterion applies to a single coasting pulse[41]:

$$\left|\frac{Z_{/\!/}}{n}\right| \leq k\, F' \frac{\beta^2 \gamma |\eta|}{I} \left(\frac{\Delta p}{p}\right)^2 ,$$

while the stability criterion for a stacked coasting beam is[42]

$$\left|\frac{Z_{/\!/}}{n}\right| \leq k\, F \frac{\beta^2 \gamma |\eta|}{I} \left(\frac{\Delta p_s}{p}\right) \left(\frac{\Delta p_F}{p}\right) ,$$

where:

$k = 4 \frac{E_o}{e} = 3.753024\ 10^9$ [V] ,

$Z_{/\!/}$ is the longitudinal impedance [Ω] ,

$\Delta p/p$ is the half relative momentum spread at half-height,

$\Delta p_s/p$ is the half relative momentum spread at half-height of the stack,

$\Delta p_F/p$ is the relative momentum width at half-height of the low energy flank,

F is the form factor depending on the aspect ratio of the coasting stack beam, given in Section 11.1,

F' is a form factor depending on the particle distribution in a single pulse. The minimum form factors F' associated with the worst possible phase of $Z_{/\!/}$ for different distributions are given in the table below[48]:

Distribution	Form factor F'
Triangular with rounded edges	0.555
Quartic	1.073
Circular limit	1.061
Very smooth	0.644

F' is very close to unity for a reasonable coasting pulse distribution where no sharp edges and infinite slopes appear in practice.

As in Section 11.1, the first criterion can be applied to a bunched beam if the rise time of the longitudinal instability is short compared with the period of the radio-frequency system. The current to be considered in this case is the peak current of one bunch (Section 3.10).

For the ISR: Table 5 gives the relativistic parameters and Table 6 gives the values of η.

11.4 Expressions for the longitudinal impedance[43,49]

In the case of a perfectly conducting circular pipe ("negative mass instability"), the following expression applies:

$$\frac{Z_{//}}{n} = \frac{i}{2} \frac{Z_o}{\beta\gamma^2} \left[1 + 2 \ln\left(\frac{b}{a}\right)\right] ,$$

b is the radius of the circular pipe [m] ,
a is the radius of a circular beam [m] .

For a resistive circular vacuum chamber, the impedance is

$$\frac{Z_{//}}{n} = \frac{1 - i}{\sqrt{2}\, b} \sqrt{\frac{R\, Z_o\, \beta}{n\, \sigma}} ,$$

b is the radius of the vacuum chamber [m] .

For a simple cylindrical cavity, the expression for the lowest mode is

$$Z_{//} = 72\, \lambda Q \frac{d}{r^2} \left[\frac{\sin(\pi d/\lambda)}{\pi d/\lambda}\right]^2 ,$$

λ is the wavelength [m] ,
Q is the quality factor of the cavity,
d is the length of the cavity [m] ,
r is the radius of the cavity [m] .

In the case of cross-section variations and bellows, the impedance can be approximated by the expression for corrugations with rectangular cross-section

$$\frac{Z_{//}}{n} = - i\, C\, \beta\, Z_o \ln\left(1 + \frac{\tau}{b}\right) ,$$

C is the fraction of the circumference occupied by these elements,
τ is the depth of the corrugations [m] ,
b is the half-height of the chamber [m] .

In the case of plates, such as those formed by clearing electrodes or pick-up stations, the impedance can be approximated by

$$\frac{Z_{//}}{n} = - i\, C\, \beta \frac{Z_o}{2\pi} \frac{w_p}{h_p} \ln \frac{b}{h_p} ,$$

C and b are defined as in the preceding expression,
w_p is the plate-width [m] ,
h_p is the distance of the plate from the chamber centre [m] .

For the ISR: The conductivity of stainless steel and R are given in Table 2. The relativistic parameters are given in Table 5.

In the special case of a cylindrical cavity in stainless steel and with R = 150 m, the following expression applies: ,

$$\frac{Z_{//}}{n} = 7.6\ 10^3\ \frac{r^{5/2}}{d+r}\ \sin^2\ (1.2\ \frac{d}{r})\ ,$$

d is the cavity length [m] ,
r is the cavity radius [m] .

11.5 Stability criterion for electron-proton oscillations without frequency spreads[45]

In coasting high energy proton beams, transverse vertical oscillations can be due to electrons moving in the potential well of the protons. These oscillations become unstable beyond a threshold in the frequency change of protons. Neglecting the effect of particles of the same species and the presence of walls, this threshold and the growth rate of the consequent instability can be approximated, in the absence of frequency spread, by

$$Q_p \leq \frac{(n-Q_e)^2 - Q_z^2}{2\sqrt{Q_e\ (n-Q_e)}}$$

$$\frac{1}{\tau} = \pi\ f_{rev}\ Q_p \sqrt{\frac{Q_e}{n-Q_e}}\ ,$$

$1/\tau$ is the growth rate of the unstable modes [s^{-1}]
n is the unstable oscillation mode, such that $n - Q_z$ is close to Q_e,
Q_e and Q_p are the vertical tune changes of electrons and protons, respectively, in the potential well of the other species

$$Q_e^2 = k_e \frac{N}{R\ b(a+b)\ f_{rev}^2}$$

$$Q_p^2 = k_p \frac{\eta_e N}{\gamma\ R\ b(a+b)\ f_{rev}^2}\ ,$$

where:

$$k_e = \frac{r_e\ c^2}{2\pi^3} = 4.08407\ [m^3 s^{-2}]\ ,$$

$$k_p = \frac{r_p\ c^2}{2\pi^3} = 2.22425\ 10^{-3}\ [m^3 s^{-2}]\ ,$$

η_e is the neutralization factor defined in Section 4.8,
N is the number of protons (Section 3.11),
a is the half-width of the beam [m] ,
b is the half-height of the beam [m] .

For the ISR: Table 2 gives the values of R and f_{rev}, while Table 5 gives γ.

11.6 Stability criterion for electron-proton oscillations with frequency spreads[45]

Considering the oscillations described in Section 11.5, it is now assumed that the frequencies of oscillation of single particles will depend both on the energy and the amplitude of the particles. Corresponding to these frequency spreads there are tune spreads which are normally assumed to have a parabolic distribution with a half-width Γ.

$$\rho(Q) = \frac{3}{4\Gamma}\left[1 - \left(\frac{Q - Q_o}{\Gamma}\right)^2\right],$$

where Q stands for Q_e, Q_p and Q_z (Section 11.5) and where Γ stands for Γ_e, Γ_p and Γ_z.

Neglecting the spread in the small quantity Q_p and assuming that the two spreads Q_e and Q_z overlap in frequency space, the stability threshold approximately corresponds to

$$Q_p \leq \frac{8}{3\pi}\sqrt{\frac{Q_z}{Q_e}}\sqrt{\Gamma_z\,\Gamma_e},$$

Q_e and Q_p are given in Section 11.5,
Γ_z and Γ_e are the widths of the distributions $\rho(Q_z)$ and $\rho(Q_e)$, respectively.

12. FORMULAE IN CONNECTION WITH BUNCHED BEAM INSTABILITIES[50,51,52,53,54,55]

Symbols frequently used in this chapter

V	cavity voltage [V]
Φ_s	phase of the synchronous particle
h	harmonic of the radio frequency system
M	number of bunches
B_f	bunching factor defined in Section 3.12
f_p	phase oscillation frequency (Section 3.3) [s^{-1}]
f_{rev}	revolution frequency (Section 3.3) [s^{-1}]
$Z_o = \mu_o c$	impedance of free space (Table 1) [Ω]
S	bunch shape factor (Section 3.12).

12.1 Growth-rate of the longitudinal motion

The motion considered here consists of rigid-bunch oscillations, i.e. dipole mode (m = 1), and of higher bunch-shape oscillations of the individual bunches, i.e. 2m-pole modes ($m \geq 2$), plus perhaps coupled motions of the different bunches, i.e. coupled-bunch modes (n). The index m specified the harmonic of the bunch-shape oscillation, while n gives the phase difference $2\pi n/M$ between adjacent bunches.

In the longitudinal phase plane, this motion corresponds to oscillations of the particle distributions with the frequency [s^{-1}]

$$f = mf_p + \Delta f_m,$$

where Δf_m is the coherent frequency shift of mode m, explicitly given below for some practical cases (Sections 12.2 to 12.4).

The growth-rate of such a motion in the absence of frequency spreads is

$$\frac{1}{\tau} = 2\pi \, \mathrm{Im}\,(\Delta f_m)$$

and the longitudinal motion is unstable when $\mathrm{Im}(\Delta f_m)$ is positive. Another stability criterion and a decoupling criterion, both valid in the presence of frequency spreads, are given in Sections 12.5 and 12.6.

12.2 Frequency shift in bunch oscillations due to perfectly conducting walls

For a bunch with approximately parabolic line density, the frequency shift of the bunch oscillations due to perfectly conducting walls is given by

$$\Delta f_m = \sqrt{m}\, \Delta f_{sc} \quad ,$$

where the space charge frequency shift is for equidistant bunches

$$\Delta f_{sc} = \frac{1}{4\pi} \frac{I\, M^2\, Z_o\, f_p}{\beta \gamma^2 (B_f S)^3\, h\, V \cos \Phi_s} \left[1 + 2\, \ell n \left(\frac{b}{a} \right) \right] ,$$

m is the mode of the oscillation (Section 12.1),
b is the radius of the round vacuum chamber [m] ,
a is the beam radius [m] .

By virtue of Section 3.12, S is roughly equal to 1.5.

For the ISR: The values of h, V and β, γ are given in Tables 2 and 5, respectively.

12.3 Frequency shift in bunch oscillations due to resistive walls

For a smooth round vacuum chamber, the frequency shift of the dipole mode (Section 12.1) is

$$\Delta f_1 = \frac{1}{24\pi} \frac{I\, M^{3/2}\, f_p}{b\, h\, V \cos \Phi_s} \sqrt{\frac{R\, \beta\, Z_o}{\sigma}}\, G\left(\frac{f_p}{M\, f_{rev}} + \frac{n}{M} \right) ,$$

n is the coupled-bunch mode (Section 12.1),
σ is the conductivity of the chamber material $[\Omega^{-1} m^{-1}]$,
b is the radius of the vacuum chamber [m] .

The bunch function G(q) is given in Fig. 23 and the motion is unstable for $q < \frac{1}{2}$ below transition and for $q > \frac{1}{2}$ above transition, by virtue of the stability criterion for the buckets (Section 3.4).

The frequency shifts for the higher modes $m \geq 2$ (Section 12.1) are estimated for equidistant bunches to be

$$\Delta f_m \cong (B_f S)^m\, \Delta f_1 \quad ,$$

Δf_1 being given above.

For the ISR: The values of σ, h, V and f_{rev} are given in Table 2. Table 5 gives the values of β.

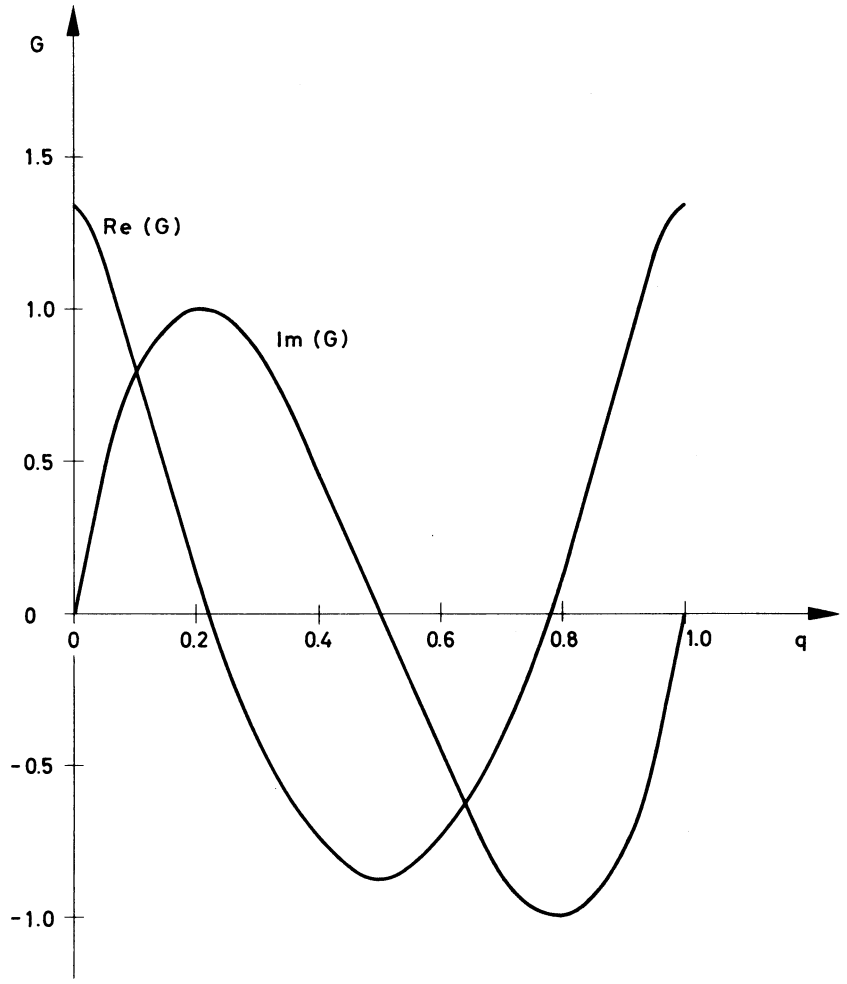

Fig. 23 The bunch function G(q)
(formula in Section 12.3)

12.4 Frequency shift in bunch oscillations due to resonant elements

A resonator is characterized by a shunt impedance and induces for equidistant bunches the following frequency shifts in the bunch oscillations described in Section 12.1:

$$\Delta f_m = \frac{1}{2\pi} \frac{R_{//} I M f_p}{B_f S h V \cos \Phi_s} D F_m (\Delta\Phi) \quad ,$$

m is the mode of the oscillation (Section 12.1),

$R_{//}$ is the shunt impedance of the resonant element $[\Omega]$,

F_m is a form factor that specifies the efficiency with which the resonator can drive a given mode. It is given in Fig. 24. The maximum values $\hat{F}_m$ are approximately $1/\sqrt{m}$.

$\Delta\Phi$ is the phase change that occurs during the passage of a bunch. It is defined by

$$\Delta\Phi = k f_{res} \frac{\ell}{\beta} \quad ,$$

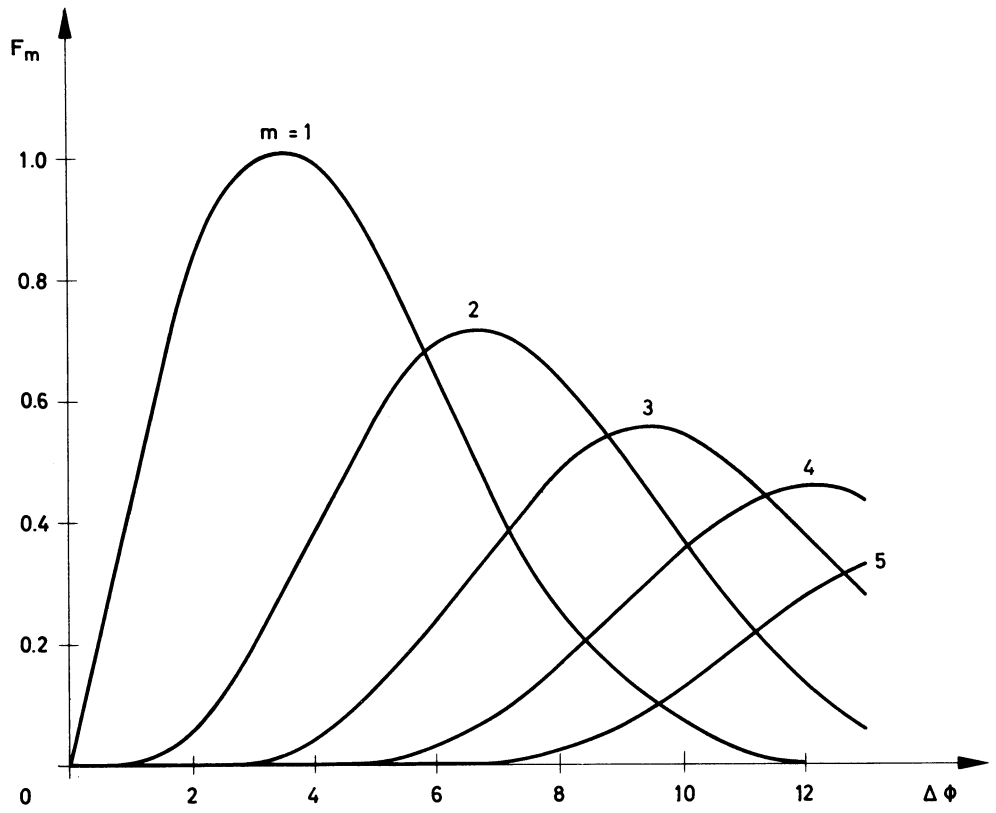

Fig. 24 Form factor for different modes
(formula in Section 12.4)

where:

$k = \frac{2\pi}{c} = 2.095845\ 10^{-8}\ [m^{-1}s]$,

f_{res} is the resonant frequency of the resonator $[s^{-1}]$,

ℓ is the full bunch length [m] .

The complex factor D is given by the following expression:

$$D = i\,\alpha \left(\frac{1}{1 - e^{a_+}} - \frac{1}{1 - e^{a_-}} \right) ,$$

where:

$$a_{\pm} = \frac{2\pi i}{M} \left(n \pm \frac{f_{res}}{f_{rev}} \right) - \alpha$$

and

$$\alpha = \pi \frac{f_{res}\ t_{bb}}{Q} ,$$

α is the attenuation factor of the induced signal between bunches,

n is the coupled bunch mode (Section 12.1). Modes n = 0 and n = M/2 for M even are not excited,

Q is the quality factor of the resonator,

t_{bb} is the time between bunch centres [s] .

The extreme modulus $|\hat{D}|$ as a function of the factor $1/\alpha$ is given in Fig. 25.

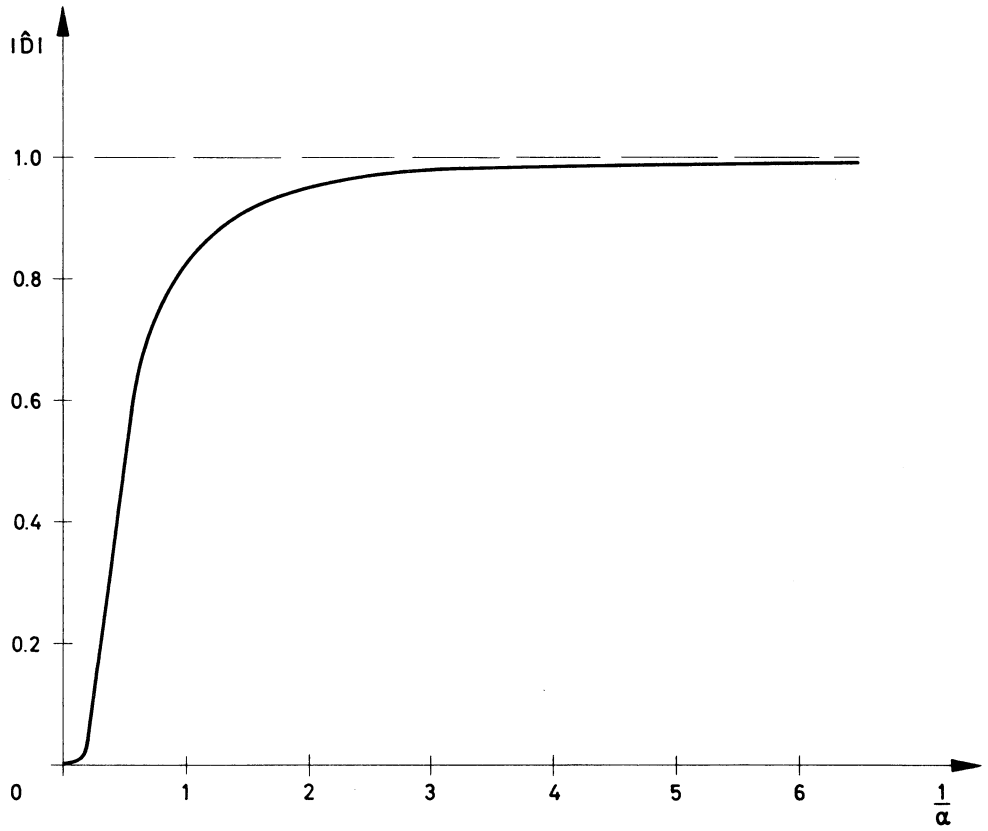

Fig. 25 Extreme modulus of the complex factor D (formula in Section 12.4)

For large values of Q, i.e. $\alpha << 1$, the expression of D simplifies to

$$D \cong \frac{f_{res}}{2Q\,(f_{res} - j\,f_{rev}) - i\,f_{res}} \quad ,$$

j being an integer. The coupled bunch mode n is excited when $f_{res} \cong j\,M\,f_{rev} \pm n\,f_{rev}$.

For small values of Q, i.e. $\alpha >> 1$, the expression of D becomes

$$D \cong -2\,\alpha\,e^{-\alpha}\,e^{i2\pi n/M}\,\sin\,(2\pi\,f_{res}/M\,f_{rev}) \quad ,$$

and coupled bunch modes near $n = \pm \frac{M}{4}$ are most strongly excited.

For the ISR: The values of h, V and f_{rev} are given in Table 2. Table 5 gives the values of β.

12.5 Decoupling criterion for longitudinal instabilities of bunched beams

A rule-of-thumb for decoupling the bunches is that the r.m.s. spread in individual bunch frequencies should exceed the frequency shift Δf_m due to the coupling force. When the spread arises naturally from a difference ΔN in bunch populations, this criterion can be written as follows:

$$|\Delta f_m| < \left(\frac{\Delta N}{N}\right)_{r.m.s.} |m\, \Delta f_{sc}| \quad ,$$

m is the oscillation mode (Section 12.1), $m > 1$,

Δf_{sc} is the space charge frequency shift (Section 12.2) $[s^{-1}]$,

N is the number of particles in a bunch,

Δf_m contains terms similar to those given in Sections 12.3 and 12.4, excluding the term in Section 12.2 which does not contribute to the coupling.

Since this rule-of-thumb is based on bunch-to-bunch differences in the incoherent motion, it does not apply to the dipole mode and is somewhat optimistic for the higher modes.

12.6 Stability criterion for longitudinal instabilities of bunched beams

The stability depends on the spread in synchrotron frequency of the bunch due to the nonlinearity of the force. For a given mode m (Section 12.1), the stability criterion becomes

$$|\Delta f_m| < \frac{\sqrt{m}}{4} F_p \quad ,$$

Δf_m is the sum of all interactions, i.e. space charge, resistive wall, resonators, etc.

F_p is the full spread in f_p (Section 3.3) between centre and edge of the bunch. It is plotted in Fig. 26 as a function of the product $B_f S$ (Section 3.12) and the parameter Γ (Section 3.1).

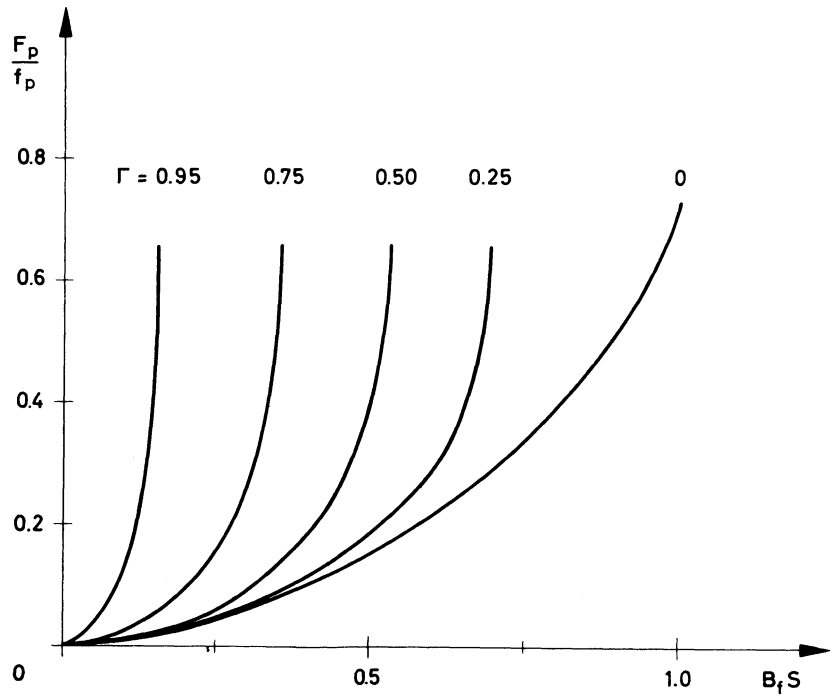

Fig. 26 Full spread in synchrotron frequency (formula in Section 12.6)

12.7 Radio-frequency voltage inside the bunches with inductive walls

For bunched beams, the space charge effects and the presence of inductive walls modify the radio-frequency voltage inside the bunches. Assuming a parabolic line density distribution λ [m^{-1}]

$$\lambda(s) = k \frac{I}{M f_{rev} \ell^3} \left(\frac{\ell^2}{4} - s^2 \right) ,$$

where:

$$k = \frac{6}{e} = 3.74508\ 10^{19} A^{-1} s^{-1} ,$$

the voltage U [V] seen by a particle at a distance s [m] from the bunch centre is:

$$U = V \left(\sin \Phi_s - s \frac{h f_p^2}{R f_{p_o}^2} \cos \Phi_s \right) ,$$

ℓ is the full bunch length [m] ,

s is the distance from the centre of the bunch [m] : $-\frac{\ell}{2} \leq s \leq \frac{\ell}{2}$,

f_{p_o} is the phase oscillation frequency in the absence of self-forces and wall inductance (Section 3.3) [s^{-1}] ,

f_p is the incoherent phase oscillation frequency in the presence of self-forces and wall inductance [s^{-1}]

$$f_p^2 = f_{p_o}^2 \left[1 - 24 \pi \frac{IR^3}{\ell^3 h M V \cos \Phi_s} \left(\frac{g Z_o}{2\beta\gamma^2} - \left| \frac{Z}{n} \right| \right) \right] .$$

Considering the coherent oscillations of the bunches described in Section 12.1, the dipole mode and quadrupole mode frequency shifts are

$$\Delta f_1 = 0$$

$$\Delta f_2 = \frac{1}{2} (f_p - f_{p_o}) .$$

The wall properties appear in the coupling coefficient g and the total inductance L. With a circular symmetry, the following formulae apply:

$$g = 1 + 2 \ell n \frac{b}{a}$$

$$\left| \frac{Z}{n} \right| = 2 \pi f_{rev} L ,$$

a is the radius of the circular beam [m] ,

b is the radius of the circular pipe [m] ,

$\left| \frac{Z}{n} \right|$ is the inductive impedance of the pipe [Ω] .

For the ISR: The values of R, h, f_{rev} and V are given in Table 2. The values of β and γ are given in Table 5.

A measurement made in the ISR[52] gives $|Z/n| \cong 26\ \Omega$ or $L \cong 13\ \mu H$.

12.8 Bunch lengthening due to inductive wall effects

The voltage perturbation mentioned in Section 12.7 provokes a bunch lengthening given by

$$\ell_o^4 = \ell^4 - 24\pi \frac{IR^3}{h\,M\,V\cos\Phi_s}\left(\frac{g\,Z_o}{2\beta\gamma^2} - \left|\frac{Z}{n}\right|\right)\ell \ ,$$

ℓ is the full bunch length in the presence of self-forces and wall inductance [m],
ℓ_o is the full bunch length in the absence of self-forces and wall inductance [m],
g and $|Z/n|$ are defined in Section 12.7.

For the ISR: The values of R, h and V are given in Table 2, while β and γ are given in Table 5. A value for $|Z/n|$ is given in Section 12.7.

12.9 Bucket area variations due to inductive wall effects

The voltage perturbation given in Section 12.7 provokes a change in the bucket area defined in Section 3.5. For $\Gamma = \sin\Phi_s = 0$, this change is given by

$$A = A_o \sqrt{1 \pm \frac{h\,I}{V}\left(\frac{g\,Z_o}{2\beta\gamma^2} - \left|\frac{Z}{n}\right|\right)} \ ,$$

A is the bucket area in the presence of self-forces and wall inductance,
A_o is the bucket area in the absence of self-forces and wall inductance (Section 3.5),
g and $|Z/n|$ are defined in Section 12.7,
the negative sign is valid below transition energy and the positive one above transition energy.

For the ISR: The values of h, V, β and γ are given in Tables 2 and 5. A value for $|Z/n|$ is given in Section 12.7.

Acknowledgements

The author is grateful to P.J. Bryant, O. Gröbner, A. Hofmann, E. Keil and B. Zotter who have checked and commented on parts of the manuscript.

REFERENCES (classified in chapters)

Chapters 1, 2 and 3

1) E.D. Courant and H.S. Snyder, Theory of the alternating gradient synchrotron, Annals of Physics, Vol. 3 (1958).

2) H. Bruck, Accélérateurs circulaires de particules, Publ. Presses Universitaires de France, Paris (1966).

3) C. Bovet et al., A selection of formulae and data useful for the design of A.G. synchrotrons, CERN MPS-SI-Int.DL/70-4 (1970).

4) E. Keil et al., AGS - The ISR computer program for synchrotron design, orbit analysis and insertion matching, CERN 75-13 (1975).

5) G. Guignard, Effets des champs magnétiques perturbateurs d'un synchrotron sur l'orbite fermée et les oscillations bétatroniques, ainsi que leur compensation, CERN 70-24 (1970).

6) P.J. Bryant, Possible skew quadrupole schemes for the ISR, CERN ISR-MA/75-51 (1975).

7) I.S. Gradshteyn and I.M. Ryzhik, Table of integrals, series and products, Publ. Academic Press, New York and London (1965).

Chapter 4

8) E. Fischer and K. Zankel, The stability of the residual gas density in the ISR in presence of high intensity beams, CERN ISR-VA/73-52(1973).

9) O. Gröbner and R.S. Calder, Beam induced gas desorption in the CERN Intersecting Storage Rings, Proc. 1973 Particle Accelerator Conf., San Francisco, p. 760 (1973).

10) O. Gröbner, The dynamic behaviour of pressure bumps in the ISR, CERN ISR-VA/76-25 (1976).

11) L. Holland, W. Steckelmacher, J. Yarwood, Vacuum Manual, Publ. E. & F.N. Spon, London(1974).

Chapter 5

12) W.C. Middelkoop and A. Schoch, Interaction rate in colliding beam systems, CERN AR-Int.SG/63-40 (1963).

13) G. Guignard, Effets sur la luminosité d'une inclinaison et d'une déformation du plan médian des faisceaux, CERN ISR-OP/73-56 (1973).

14) B.W. Montague, Calculation of luminosity and beam-beam detuning in coasting-beam interaction regions, CERN ISR-GS/75-36 (1975).

15) T. Suzuki, General formulae of luminosity for various types of colliding beam machines, KEK 76-3 (1976).

16) Jahnke - Emde - Lösch, Tables of higher functions, B.G. Teubner Verlagsgesellschaft, Stuttgart (1966).

Chapters 6 and 7

17) E. Fischer, Residual gas scattering, beam intensity and interaction rate in proton storage rings, CERN ISR-VA/67-16 (1967).

18) H.G. Hereward, Private communication (24 July 1973) .

19) A. Piwinski, Intrabeam scattering, Proc. IXth Int. Conf. on High Energy Accelerators, Stanford, p. 665-679 (1974).

20) S. van der Meer, Stochastic damping of betatron oscillations in the ISR, CERN ISR-PO/72-31 (1972).

21) H.G. Hereward, Private communication.

22) L. Thorndahl, Stochastic cooling of momentum spread and betatron oscillation for low-intensity stacks, CERN ISR-RF/75-55 (1975).

Chapter 8

23) L.J. Laslett, On intensity limitations imposed by transverse space-charge effects in circular particle accelerators, Proc. Brookhaven Summer Study, BNL 7534 (1963).

24) E. Keil, Intersecting Storage Rings, CERN 72-14 (1972).

25) B. Zotter, Q-shift due to direct space-charge field of stacked particle beams, CERN ISR-TH/75-5 (1975).

26) B. Zotter, Incoherent Q-shift of a flat, off-centred particle beam in an elliptic vacuum chamber, CERN ISR-TH/74-38 (1974).

27) B. Zotter, The Q-shift of off-centred particle beams in elliptic vacuum chambers, Nucl. Instr. and Meth. 129, p. 377-395 (1975).

28) E. Keil, C. Pellegrini, A.M. Sessler, Tune shifts for particle beams crossing at small angles in the low-β section of a storage ring, CERN ISR-TH/73-44 (1973).

29) E. Keil, Non-linear space charge effects, CERN ISR-TH/72-7 (1972).

Chapters 9 and 10

30) G. Guignard, The general theory of all sum and difference resonances in a three-dimensional magnetic field in a synchrotron, CERN 76-06 (1976).

31) P.J. Bryant and G. Guignard, Methods for measuring the complex coupling coefficient for the second order difference resonance $Q_h = Q_v$, CERN ISR-MA/75-42 (1975).

32) G. Guignard, Beam blow-up and luminosity reduction due to linear coupling (Report in preparation).

33) A. Schoch, Theory of linear and non-linear perturbations of betatron oscillations in alternating gradient synchrotrons, CERN 57-21 (1957).

34) R. Hagedorn, Stability and amplitude ranges of two-dimensional non-linear oscillations with periodical Hamiltonian, CERN 57-1 (1957).

35) P.M. Hanney and E. Keil, The width of non-linear resonances excited by beams crossing at small angles in low-β sections, CERN ISR-TH/73-55 (1973).

36) G. Guignard, Vitesse limite de traversée d'une résonance magnétique quelconque. Application aux petites perturbations et conséquence pour les accroissements maximaux d'amplitude, CERN SI-Int.DL/72-2 (1972).

37) G. Guignard, Report to be published.

38) J.P. Gourber and G. Guignard, Overlap knock-out resonances in a synchrotron, (Report to be published).

Chapter 11

39) W. Schnell and B. Zotter, A simplified criterion for transverse stability of a coasting beam,and its application to the ISR, CERN ISR-GS-RF/76-26 (1976).

40) L.J. Laslett, V.K. Neil, A.M. Sessler, Transverse resistive instabilities of intense coasting beams in particle accelerators, Rev. Sci. Instr. 36, p. 436 (1965).

41) E. Keil and W. Schnell, Concerning longitudinal stability in the ISR, CERN ISR-TH-RF/69-48 (1969).

42) K. Hübner and V.G. Vaccaro, Dispersion relations and stability of coasting particle beams, CERN ISR-TH/70-44 (1970).

43) V.K. Neil and A.M. Sessler, Longitudinal resistive instabilities of intense coasting beams in particle accelerators, Rev. Sci. Instr. 36, p. 429 (1965).

44) H.G. Hereward, Coherent instability due to electrons in coasting beams, CERN 71-15 (1971).

45) E. Keil and B. Zotter, Landau-damping of coupled electron-proton oscillations, CERN ISR-TH/71-58 (1971).

46) K. Hübner, P. Strolin, V.G. Vaccaro, B. Zotter, Concerning the stability of the ISR beam against coherent dipole oscillations, CERN ISR-RF-TH/70-2 (1970).

47) B. Zotter, The transverse coupling impedance of cross-section variations at low frequencies, CERN ISR-TH/71-13 (1971).

48) B. Zotter, Longitudinal stability diagrams for some particular distribution functions, CERN ISR-GS/76-11 (1976).

49) B. Zotter, Beam dynamical limitations of a superconducting proton storage ring, CERN ISR-LTD/76-3 (1976).

Chapter 12

50) F.J. Sacherer, A longitudinal stability criterion for bunched beams, Proc. 1973 Part. Accelerator Conf., San Francisco, p. 825 (1973).

51) F.J. Sacherer, Methods for computing bunched-beam instabilities, CERN SI-BR/72-5 (1972).

52) S. Hansen et al., Effects of space charge and reactive wall impedance on bunched beams, Proc. 1975 Particle Accelerator Conf., Washington, p. 1381 (1975).

53) V.K. Neil and R.J. Briggs, Stabilization of intense coasting beams in particle accelerators by means of inductive walls, Plasma Physics 8, p. 255 (1966).

54) V.K. Neil and R.J. Briggs, Stabilization of non-relativistic beams by means of inductive walls, Plasma Physics 9, p. 631 (1967).

55) A.M. Sessler and V.G. Vaccaro, Longitudinal instabilities of azimuthally uniform beams in circular vacuum chambers with walls of arbitrary electrical properties, CERN 67-2 (1967).

Tables

56) E. Keil, ISR Parameter List (Revision 5), CERN ISR-GS/76-4 (1976).

57) F.F. Rieke and W. Prepejchal, Ionisation cross-sections of gaseous atoms and molecules for high energy electrons and positrons, Phys. Rev. A, Vol. 6, No. 2 (1972).

58) T.A. Lasinski et al., Review of particle properties, Rev. of Modern Phys., Vol. 45, No. 2, Part II (1976).

APPENDIX

Analytic form of the integrals giving the maximum amplitude growth

The integrals in which we are interested are given in Section 10.7. Reference 5 gives the explicit expressions of these integrals for any values of n_x and n_z. Since these expressions are quite complicated, it seems judicious to give only the analytic forms for $N \leq 5$.

Let us put

$$J(n_x,n_z,\text{sign}) = \int \frac{dg_x}{(k+g_x^2)^{n_z/2}\, g_x^{(n_x-1)}} = \sqrt{|k|}^{(2-N)} \int \frac{du}{(u^2+\text{sign})^{n_z/2}\, u^{(n_x-1)}} ,$$

where:

$$k = \frac{n_x E_{z_o}}{n_z E_{x_o}} - 1 \quad ; \qquad u = \frac{g_x}{\sqrt{|k|}} ,$$

and sign = ± 1, depending on the sign of k.

Using the new variable u, the last integral on the right hand side (i.e. $J/\sqrt{|k|}^{(2-N)}$) is explicitly given below for different n_x, n_z and N ($N \leq 5$). The cases where n_x or n_z is zero do not appear, since these solutions are given in Section 10.7.

n_x,n_z / N	N - 1, 1	N - 2, 2	N - 3, 3	N - 4, 4	Sign
2	$\ell n\left[u+\sqrt{u^2+\text{sign}}\right]$				±1
3	$\frac{1}{2}\ell n \frac{\sqrt{u^2+1}-1}{\sqrt{u^2+1}+1}$	arctg u			+1
	arc cos $\left(\frac{1}{u}\right)$	-argth u			-1
4	$-\text{sign}\frac{\sqrt{u^2+\text{sign}}}{u}$	$\frac{\text{sign}}{2}\ell n \frac{u^2}{u^2+\text{sign}}$	$\text{sign}\frac{u}{\sqrt{u^2+\text{sign}}}$		±1
5	$-\frac{\sqrt{u^2+1}}{2u^2} - \frac{1}{4}\ell n \frac{\sqrt{u^2+1}-1}{\sqrt{u^2+1}+1}$	$-\frac{1}{u}$ - arctg u	$\frac{1}{\sqrt{u^2+1}} - \ell n \frac{1+\sqrt{u^2+1}}{u}$	$\frac{u}{2(1+u^2)} + \frac{1}{2}$ arctg u	+1
	$\frac{\sqrt{u^2-1}}{2u^2} + \frac{1}{2}$ arc cos $\frac{1}{u}$	$\frac{1}{u}$ - argth u	$-\frac{1}{\sqrt{u^2+1}} - \frac{1}{\cos 1/u}$	$\frac{u}{2(u^2-1)} - \frac{1}{2}$ argth u	-1

Table 1

Table of physical constants

Symbols	Meaning	Value	Units
c	velocity of light	$2.9979246\ 10^{8}$	ms^{-1}
e	electronic charge	$1.602189\ 10^{-19}$	As
N_m	number of molecules per mole	$6.022169\ 10^{23}$	-
V_m	molar volume of ideal gas at standard conditions	$2.241411\ 10^{-2}$	m^3
T_{st}	standard temperature for gas	273	K
P_{st}	standard pressure for gas	760	Torr
E_o	rest mass of proton	938.256	MeV
E_e	rest mass of electron	0.511004	MeV
r_p	classical proton radius	$1.534697\ 10^{-18}$	m
r_e	classical electron radius	$2.817938\ 10^{-15}$	m
G_H	absolute atomic gas factor for hydrogen	10.552	-
G_{He}	for helium	39.448	-
G_C	for carbon	328.64	-
G_N	for nitrogen	442.27	-
G_O	for oxygen	554.09	-
G_{Ne}	for neon	878.57	-
G_{Ar}	for argon	2709.3	-
ε_0	permittivity of free-space	$8.854188\ 10^{-12}$	$AsV^{-1}m^{-1}$
Z_0	impedance of free-space	119.917π	Ω
μ_0	permeability of free-space	$4\pi\ 10^{-7}$	$A^{-1}sVm^{-1}$
k_B	Boltzmann constant	$8.617084\ 10^{-11}$	$MeV\ K^{-1}$

Table 2

Table of parameters valid for the present ISR[56)]

Symbols	Meaning	Value	Units
ρ	bending radius	78.5895	m
R	average machine radius	150.0253	m
ℓ	machine circumference	942.6368	m
n/ρ	field index upon ρ for F unit	-3.136	m^{-1}
	for D unit	3.020	m^{-1}
n'/ρ	radial derivative of field-index upon ρ for F unit	-1.946	m^{-2}
	for D unit	1.493	m^{-2}
N	number of intersections	8	-
h	RF harmonic	30	-
τ^{ℓ}_{rev}	revolution time at $\beta = 1$	3.144298	μs
f^{ℓ}_{rev}	revolution frequency at $\beta = 1$	$3.18036\ 10^{5}$	Hz
V	cavity voltage at the beginning of the cycle	16	kV
	at the end of the cycle	700	V
ε_x	normalized horizontal emittance	13π to 18π	mm mrad
ε_z	normalized vertical emittance	8π	mm mrad
σ	stainless steel conductivity	$7.6923\ 10^{5}$	$\Omega^{-1}m^{-1}$
σ_{pp}	total proton-proton cross-section at the ISR energies	$4.09\ 10^{-30}$	m^2

Table 3

Values of some transverse parameters
for standard working conditions in the ISR

Working Line	γ_t	$\bar{\alpha}_{p,x}$	$\bar{\beta}_x$	$\bar{\beta}_z$	$\beta_{z,I}$
FP	8.8172	1.9294	20.8185	22.9348	14.56
8C	8.7977	1.9380	20.8789	22.9427	14.56
5C	8.7800	1.9458	21.0724	23.0305	14.93
TW	8.5133	2.0696	21.5626	23.8607	16.13
ELSA	9.0705	1.8232	20.2391	22.5412	12.17
Steel Low-β	9.0903	1.8152	20.5244	23.4407	2.63

Note : These values are given on the centre line.

Table 4

Values of the tunes and tune derivatives
for standard working conditions in the ISR

Working Line	H-plane			V-plane		
	Q_x central	Q_x top(+40)	Q'_x	Q_z central	Q_z top(+40)	Q'_z
FP	8.637	8.6785	2.002	8.627	8.6685	2.002
8C	8.6145	8.6475	1.599	8.6245	8.6575	1.599
5C	8.550	8.615	1.970	8.600	8.657	3.259
TW	8.637	8.6785	2.147	8.627	8.6685	2.147
ELSA	8.9015	8.955	2.439	8.8815	8.935	2.439
Steel Low-β	8.9015	8.955	2.428	8.8815	8.935	2.428

Table 5

Values of magnetic rigidity
and relativistic parameters at ISR energies

p (GeV/c)	β	γ	$B\rho$ (Tm)
11.776	0.99684	12.591	39.280
15.376	0.99814	16.418	51.288
22.505	0.99913	24.007	75.068
26.588	0.99929	28.355	88.687
31.400	0.99949	33.481	104.738

Table 6

Values of revolution frequency spread per unit of momentum spread
for different working conditions in the ISR

p (GeV/c)	η in 10^{-3} on FP	η in 10^{-3} on 8C	η in 10^{-3} on ELSA	η in 10^{-3} on Steel Low-β
11.776	- 6.55507	- 6.61215	- 5.84669	- 5.79380
15.376	- 9.15301	- 9.21010	- 8.44464	- 8.39174
22.505	-11.12779	-11.18488	-10.41941	-10.36652
26.588	-11.61912	-11.67620	-10.91074	-10.85785
31.400	-11.97081	-12.02790	-11.26243	-11.20954

Note : These values are given on the centre line.

Table 7

Factor between moving and stationary bucket area

Γ	$\alpha(\Gamma)$
0	1
0.1	0.8039
0.15	0.7294
0.2	0.6612
0.25	0.5981
0.3	0.5389
0.35	0.4833
0.4	0.4306
0.45	0.3807
0.5	0.3333
0.52	0.3151
0.54	0.2972
0.56	0.2799
0.58	0.2627
0.60	0.2461
0.62	0.2297
0.64	0.2168
0.66	0.1981
0.68	0.1828
0.70	0.1678
0.72	0.1534
0.74	0.1393
0.76	0.1255
0.78	0.1121
0.80	0.0991
0.82	0.0865
0.84	0.0744
0.85	0.0686
0.86	0.0627
0.87	0.0571
0.88	0.0515
0.89	0.0462

Table 8

Ionization cross-sections at 26 GeV/c[57] and molecular masses

Gas	Molecular mass M	Ionisation cross-section σ_+ in 10^{-23} m^2
H_2	2	1.8
He	4	1.8
CH_4	16	9.7
H_2O	18	7.5
N_2	28	8.2
CO	28	8.2
O_2	32	9.1
Ar	40	8.9
CO_2	44	13.0

Table 9

Nuclear cross-sections for protons at ISR energies[58]

Atom	Symbol	Value in mb = 10^{-31} m^2
Hydrogen	$\sigma_{n,H}$	40
Carbon	$\sigma_{n,C}$	340
Nitrogen	$\sigma_{n,N}$	390
Oxygen	$\sigma_{n,O}$	440
Argon	$\sigma_{n,Ar}$	890

Table 10

Principal beam parameters in the SFM of the ISR

SFM field T	Parameter	Central orbit momentum (GeV/c) 31.460	26.588	22.505	15.376	11.780
1.00	d_{max} [mm]	10.7	12.6	14.9		
	s_{max} [m]	3.1	3.1	3.1		
	d_{min} [mm]	68.0	80.4	95		
	s_{min} [m]	2.9	2.9	2.9		
	ℓ_I [mm]	29.3	34.7	40.9		
	ψ [degree]	17.477	17.971	18.552		
0.85	d_{max}	8.6	10.2	12.1	17.8	
	s_{max}	3.1	3.1	3.1	3.1	
	d_{min}	58.4	69.2	81.7	119.5	
	s_{min}	2.9	2.9	2.9	2.9	
	ℓ_I	25.5	30.2	35.7	52.1	
	ψ	17.080	17.503	17.998	19.494	
0.65	d_{max}	5.6	6.7	7.9	11.6	15.2
	s_{max}	3.15	3.2	3.2	3.2	3.15
	d_{min}	45.4	53.8	63.5	93.0	121.3
	s_{min}	2.9	2.9	2.9	2.9	2.9
	ℓ_I	20.5	24.3	28.7	41.9	54.7
	ψ	16.532	16.854	17.232	18.372	19.471
0.5	d_{max}	3.3	3.9	4.7	6.8	8.9
	s_{max}	3.3	3.3	3.3	3.25	3.3
	d_{min}	35.6	42.1	49.8	72.8	95.1
	s_{min}	2.9	2.9	2.9	2.9	2.9
	ℓ_I	16.8	19.85	23.4	34.3	44.8
	ψ	16.113	16.359	16.647	17.516	18.353

Notes : i) Without field in the SFM, the colliding angle ψ is 14.773^{o}.

ii) The distances s, d and ℓ given in the table are defined in fig. 27.

iii) Heavy boxes indicate standard operating conditions.

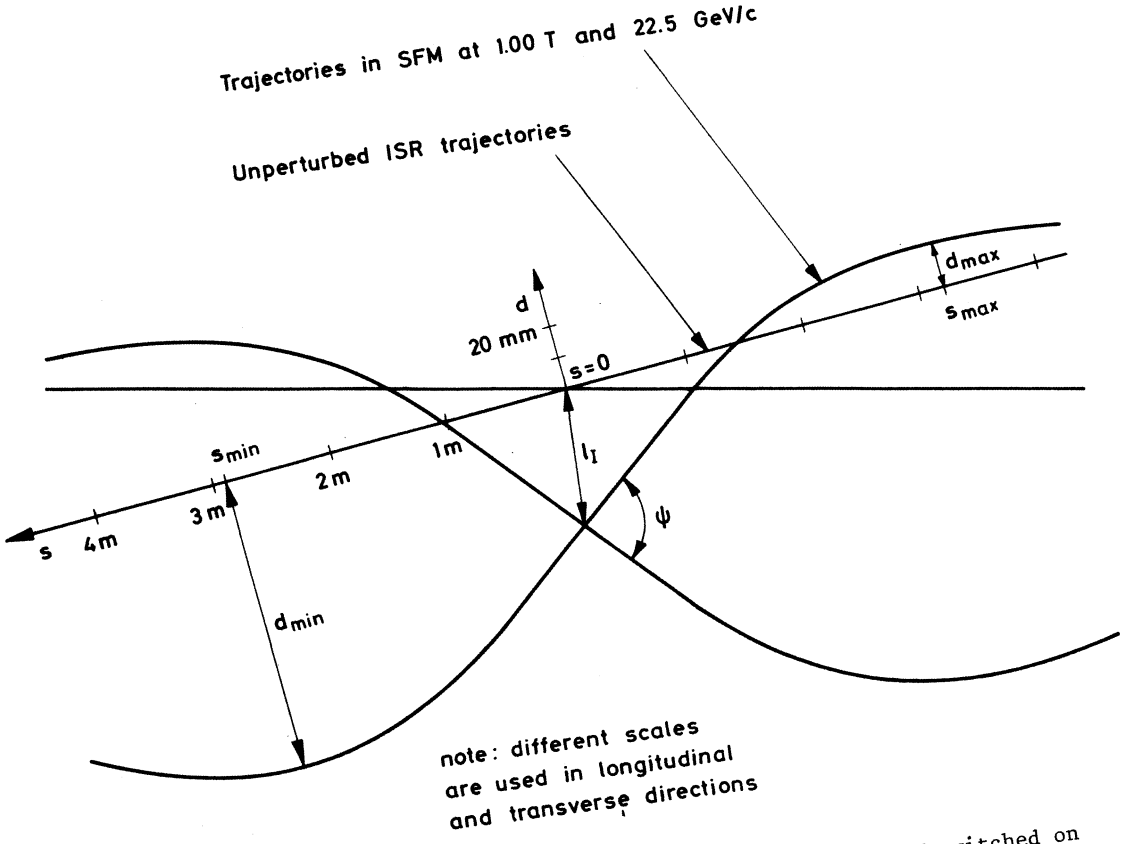

Fig. 27 Orbits in intersection 4 of the ISR with the SFM switched on

The parameters appearing on the figure are given in Table 10 for different SFM fields and beam momenta.